Graz University of Technology

Institute of Electronics

Master's Thesis

DA 621

Configuration of an EMC measuring setup for chiplevel characterisations

---

Harald Gleinser

Graz, Austria, January 2008

Thesis supervisors

Ass. Prof. Dipl.-Ing. Dr. Gunter Winkler

Dipl.-Ing. Dieter Maier

Für Oma und Opa...

Wer misst misst Mist.

Non-translatable and anonymous, german source

Deutsche Fassung:
Beschluss der Curricula-Kommission für Bachelor-, Master- und Diplomstudien vom 10.11.2008
Genehmigung des Senates am 1.12.2008

EIDESSTATTLICHE ERKLÄRUNG

Ich erkläre an Eides statt, dass ich die vorliegende Arbeit selbstständig verfasst, andere als die angegebenen Quellen/Hilfsmittel nicht benutzt, und die den benutzten Quellen wörtlich und inhaltlich entnommene Stellen als solche kenntlich gemacht habe.

Graz, am …………………………… ………………………………………………..
(Unterschrift)

Englische Fassung:

STATUTORY DECLARATION

I declare that I have authored this thesis independently, that I have not used other than the declared sources / resources, and that I have explicitly marked all material which has been quoted either literally or by content from the used sources.

…………………………… ………………………………………………..
date (signature)

Abstract

Recent developments in integrated circuit (IC) design have shown a clear trend to miniaturization and decrease of supply voltage. This implies that the packing density on a system level can be increased, however, coming at the cost of higher sensitivity to electromagnetic interference for individual chips. Therefore, it is important to consider the electromagnetic characteristics of each component for system level design.

This thesis deals with the construction of an electromagnetic immunity measurement setup based on the direct radio frequency (RF) power injection (DPI) method as described in the IEC standard 62132-4. The existing setup was further improved regarding coupling and decoupling networks. Additionally, the software was extended to enable automated measurements and more extensive monitoring of the device under test (DUT) .

Furthermore, an attenuation measurement setup was developed to verify the functionality of the above mentioned DPI testbench. This attenuation measurement setup was used to ensure if the direct power injection (DPI) testbench is compliant to the requirements in the IEC standard.

This electromagnetic immunity measurement setup was utilized for the charaterization of two test ICs. Results are presented, discussed and demonstrate the usefulness of those optimizations.

Keywords. Direct RF Power Injection (DPI), reproducibility, electromagnetic compatibility, electromagnetic immunity, electromagnetic interference, chip-level

Kurzfassung

Die fortschreitende Reduktion der Strukturgrößen und Betriebsspannungen integrierter Schaltungen ermöglicht immer komplexere kleinere Systeme. Allerdings steigt mit sinkenden Signalpegeln auch die Empfindlichkeit gegenüber Störsignalen. Gleichzeitig steigt das Störpotential durch die höheren Packungsdichten und höheren Signalfrequenzen auf Systemebene. Entsprechend werden die Eigenschaften von integrierten Schaltungen auch hinsichtlich elektromagentischer Emissionen und Störfestigkeit immer wichtiger.

Diese Arbeit beschreibt den Aufbau eines Messplatzes zur Charakterisierung von Störfestigkeit integrierter Schaltungen gegenüber leitungsgeführten Störungen entsprechend der Direct RF Power Injection (DPI) Methode, wie sie in der Norm IEC 62132 neben anderen Methoden zur EMV Charakterisierung auf Chipebene beschrieben ist. Dabei wurde ein bereits vorhandener Messplatz und dessen Automatisierungssoftware überarbeitet, sowie notwendige Baugruppen und ihr Einfluss auf Messablauf und Ergebnisse untersucht. Weiters wurde ein zweiter Messplatz für Dämpfungsmessungen mit zugehöriger Steuerungssoftware aufgebaut und entwickelt. Dieser wurde unter anderem zur Kontrolle und Spezifikation von Baugruppen für den DPI Messplatz verwendet.

Auf dem überarbeiteten Messplatz wurden zwei integrierte Schaltungen entsprechen der DPI Methode einer Untersuchung hinsichtlich ihrer Immunität gegenüber leitungsgeführten Störungen unterzogen. Die Ergebnisse dieser Messungen zeigen die Funktionalität des Messplatzes.

Schlüsselwörter. Direct RF Power Injection (DPI), Reproduzierbarkeit, elektromagnetische Verträglichkeit, Störfestigkeit, Störemissionen, Chip-Ebene

Acknowledgments

I would like to thank Ass. Prof. Dipl.-Ing. Dr. Gunter Winkler, my supervisor of Technical University Graz, for his support and help to finish this work.

Furthermore I want to thank Dipl.-Ing. Dieter Maier, Dr. Joachim Reiner and austriamicrosystemsAG for the opportunity to write my masters's thesis related to practice. Moreover, I would like to thank Andreas, Stefan and my other colleagues for their professional support and the pleasant working atmosphere.

Now my master's thesis is written and I am filled with alleviation, pride and gratefulness - therefor I want to thank my friends for awesome years of study and their help, support and friendship. Thank you to all of them! Especially I want to thank Peter, Nina and Simon.

Finally, I would like to thank my family for their mental assistance and most especially I thank my parents for their unconditional support and confidence.

Contents

1 Introduction and Motivation **1**

1.1 Contribution of this work . . . 2

1.2 Overview . . . 3

2 Electromagnetic Immunity Standard IEC 62132-4 **5**

2.1 Basic Measurement Setup . . . 6

2.2 Single and Multiple Pin Power Injection . . . 6

2.3 Test Conditions: Signal Form and Power Level . . . 8

2.4 Test Setup and Equipment . . . 8

2.5 Test Board . . . 9

2.6 Test Procedure . . . 9

3 Attenuation Measurement Setup **13**

3.1 Attenuation Measurement . . . 13

3.2 Measurement Setup . . . 14

3.3 LabVIEW Program . . . 14

3.3.1 Interface . . . 15

3.3.2 Program Structure . . . 17

3.3.3 Sub VIs . . . 23

3.4 Equipment . . . 25

3.4.1 Power Splitter . . . 25

3.4.2 Power Meter . . . 27

3.4.3 LeCroy Active Probes . . . 29

3.5 Test and Verification . . . 29

3.6 Data Analysis . . . 30

3.6.1 Comparision Power Splitter vs. Power Divider . . . 31

3.7 Calculation of impedance and attenuation . . . 32

3.7.1 Impedance Calculation for Power Splitter . . . 33

3.7.2 Impedance Calculation for Power Divider . . . 34

3.7.3 Attenuation . . . 34

3.7.4 High Impedance . . . 35

3.7.5 Low Impedance 35
3.8 Investigation in High Voltage RF Measurment 35
3.8.1 Calibration of Active Probes HFP1500 35

4 EMC Characterisation on Chiplevel **37**
4.1 Workflow of a DPI measurement 38
4.2 Existing DPI Setup 38
4.2.1 Directional Coupler 39
4.2.2 Test Board and Wiring 40
4.3 Optimisation of the DPI Setup 41
4.3.1 Coupling Network 42
4.3.2 Decoupling Network 44
4.3.2.1 Ferrite Beads 45
4.3.2.2 Inductors and SMD Ferrites 51
4.3.3 Minimalistic DPI Adapter 53
4.4 Existing Control Software 55
4.5 Optimisation of the Control Software 59
4.6 Example Measurement 63
4.6.1 Testboards 63
4.6.2 Results 66

5 Summary and Discussion **75**
5.1 Summary 75
5.2 Discussion 76

A Acronyms and Symbols **79**

Bibliography **80**

List of Figures

1.1 Overview of EMC standards at chip level. 2
1.2 Diagrammatic model of direct power injection setup 3

2.1 Block diagram DPI setup 7
2.2 Block diagram single pin power injection 7
2.3 Block diagram multi pin power injection 8
2.4 Test signal DPI method 8
2.5 Example DPI board 10
2.6 Example DPI layout 10
2.7 Flowchart DPI method 11

3.1 Block diagram of attenuation measurement principle 15
3.2 LabVIEW screenshot of configuration tab 16
3.3 LabVIEW screenshot of attenuation plot tab 17
3.4 LabVIEW block diagram of initial routines 18
3.5 LabVIEW block diagram of power meter initalisation 19
3.6 LabVIEW block diagram of main measurment loop 20
3.7 LabVIEW block diagram of final routines 21
3.8 LabVIEW block diagram of main routine - step 2 22
3.9 LabVIEW block diagram of main routine - step 3 22
3.10 LabVIEW block diagram of main routine - step 4 23
3.11 Comparison power splitter and power divider 26
3.12 Measuring results using power splitter and power divider 27
3.13 Measuring results attenuation setup (LeCroy) 30
3.14 Measuring results attenuation setup (NRVD) 31
3.15 Measuring results attenuation setup detail view (NRVD) 32
3.16 PSpice schematic of high and low impedance measurement 33
3.17 PSpice schematic for comparision of power splitter an divider 34
3.18 Calibration of active probes HFP1500 36
3.19 SMA to HFP1500 Adapter 36

4.1 DPI setup as utilized in this work. 38

4.2 Test signal generation block of the used DPI setup. . . . 40
4.3 Coupling factor directional coupler 41
4.4 Comparision DPI coupling path 43
4.5 Universal EMC test board for AMS13711 44
4.6 Comparison DPI decoupling networks 46
4.7 Ferrite Bead 1W 46
4.8 Ferrite Bead 2W 47
4.9 Ferrite Bead 2Ws 47
4.10 Ferrite Bead 3W 47
4.11 Ferrite Bead 0,5W 47
4.12 Ferrite Bead 1,5W 47
4.13 Ferrite Bead 1,75W 48
4.14 6-Hole Ferrite Bead comparison, version 1 48
4.15 6-Hole Ferrite Bead comparison, verson 1 logarithmic view 49
4.16 Ferrite Beads 3W 49
4.17 Ferrite Beads 2Ws 50
4.18 Ferrite Beads 3W 50
4.19 Ferrite Beads 1W 51
4.20 Inductor comparision 52
4.21 Adapter board probe 1 52
4.22 Adapter board probe 4 53
4.23 Adapter board probe 3 53
4.24 Adapter board probe 9 54
4.25 Adapter board probe 6 54
4.26 Adapter board probe 7 55
4.27 Minimalistic DPI adapter, version 1 55
4.28 Minimalistic DPI adapter, version 2 56
4.29 DPI adapter - coupling path characteristics 56
4.30 Minimalistic DPI adapter - coupling path characteristic 57
4.31 Existing DPI control software 58
4.32 Existing DPI control software, measurement 59
4.33 Flowchart DPI method, extended 60
4.34 Adapted DPI control software 61
4.35 DPI and TEM test board 62
4.36 EMC test PCB for DPI and TEM evaluation 64
4.42 DPI test PCB 64
4.37 EMC test PCB for TEM evaluation, bottom side 65
4.38 EMC test PCB for TEM evaluation, top side 65
4.39 DPI test PCB , version 1 66
4.40 DPI test PCB , version 2 66
4.41 DPI test PCB , version 3 66

4.43 DPI test PCB coupling path 67
4.44 DPI test PCB coupling path, 100nF 68
4.45 as5145 DPI at GND, manual reset 69
4.46 as5145 DPI at OUT, manual reset 69
4.47 as5145 DPI at VDD, manual reset 70
4.48 as5145 power supply influence 71
4.49 AS5145 DPI at GND 71
4.50 AS5145 DPI at VDD 72
4.51 AS5145 DPI at OUT 72
4.52 AS5134 DPI at GND 73
4.53 AS5134 DPI at PWM 73
4.54 AS5134 DPI at VDD 74

List of Tables

2.1 Power levels DPI method 9

3.1 Frequency step size IEC 63132-1, table 2 24
3.2 Frequency step types of *generateFrequencyTable_v004.vi* 25

4.1 Inductors 51
4.2 Performance classes 62
4.3 Used parts for DUT 1 63
4.4 Used parts for DUT 2 64

Chapter 1

Introduction and Motivation

Contents

1.1 Contribution of this work **2**
1.2 Overview **3**

This master's thesis deals with the construction of an electromagnetic immunity measurement setup. Recent developments in chip design have shown a clear trend to miniaturization in terms of structure size and decrease of supply voltage. For system designers, this means that the packing density on a system level can be increased, however, coming at the cost of higher sensitivity to electromagnetic interference for individual chips. Therefore, it is important to know about the electromagnetic characteristics of each component for system level design.

Providing electromagnetic characterization on chip level is not a trivial task since in general, they cannot be compared in a direct way (due to external circuitry, component placement and quality). To overcome these problems, the International Electrotechnical Commission (IEC) has introduced the IEC 62132 and IEC 61967 standards [6], including test procedures to obtain electromagnetic compatibility (EMC) parameters of integrated circuits (IC) (see Figure 1 for an overview). The main goal of the standard is to define an unambiguous test environment such that EMC measurements of IC can be performed in a repeatable and comparable manner. Additionally, the tests are acknowledged in several countries and companies, applicable to different types of IC and common measuring tools.

The norms IEC 61967 and IEC 62132 constitute EMC standards at chip level for electromagnetic emission and electromagnetic immunity, respectively. The focus of this master's thesis is on measuring electromagnetic immunity, which in turn is structured into

- Transverse Electromagnetic Mode Cell Method - TEM [11]
- Bulk Current Injection Method - BCI [12]
- Direct Power Injection Method - DPI [13]
- Work Bench Faraday Cage Method [14]

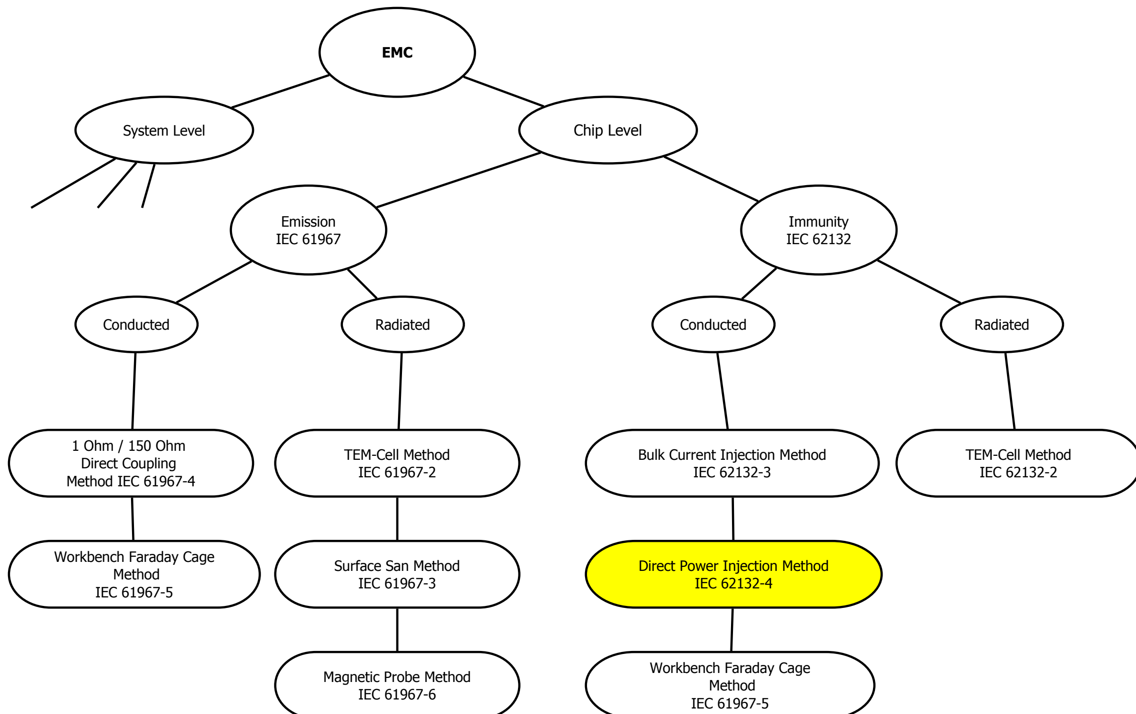

Figure 1.1: Overview of EMC standards at chip level.

1.1 Contribution of this work

The core part of this master's thesis is a measurement setup for a direct power injection-method, which has been realized in the EMC laboratory of austriamicrosystemsAG. The measurement setup consists of two components: First, an attenuation measurement setup which verifies whether the measuring environment for a DUT are compliant to the standard. Second, a Labview program has been realized that automates and monitors the frequency measurement protocol implemented in DPI . In addition, the program was extended with

a multimeter interface and controlling software for the power-supply. The resulting immunity measurement setup has been successfully evaluated on two different magnetic rotary encoder IC . In particular, electromagnetic interference (EMI) performance characteristics have been determined by DPI meausrements and transverse electromagnetic mode (TEM) cell method emission and immunity tests.

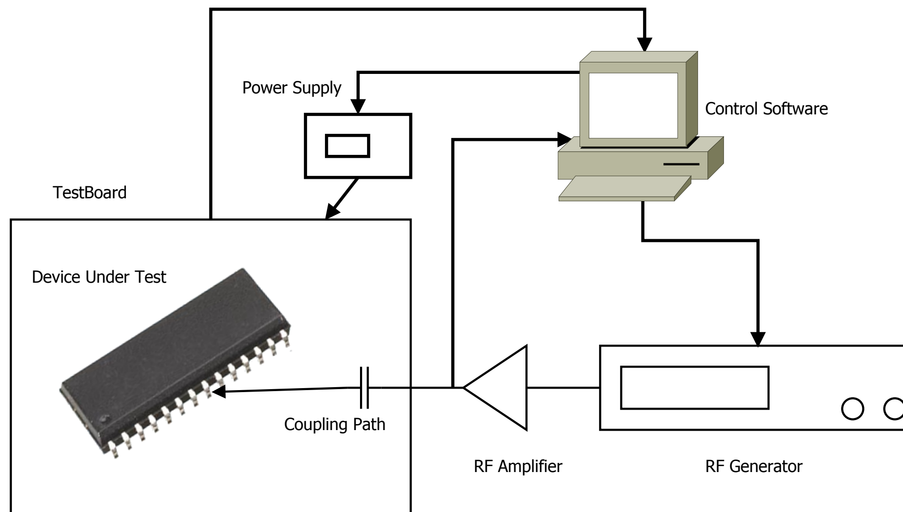

Figure 1.2: Diagrammatic model of direct power injection setup

1.2 Overview

The current chapter gives an introduction of this thesis and outlines the related literature the field of EMC . The following chapters of this master's thesis are structured as follows:

Chapter 2 describes the IEC 62132 standard for electromagnetic immunity measurements against RF disturbances. This standard defines a set of methods for chip characterization. One of this techniques, direct power injection (DPI), is covered in detail, because it is the method of choice consequently applied and investigated in the practical part of the work.

In Chapter 3 the attenuation measurement setup is described. Designed from scratch, this setup consists of a combination of dedicated hardware and is controlled by LabVIEW. The developed software is responsible for initialisation, calibration, measurement and documentation. Power splitters, power meters and active oscilloscope probes are used for the measurement and require theoretical considerations for the obtaining the correct results.

Chapter 4 describes a `DPI` measurement setup and characterisation of two test ICs. This setup was further improved regarding coupling and decoupling networks, considering in particular ferrite beads and inductors. Moreover, the software was extended to enable e.g. more reasonable frequency intervals, automated reset, and more intelligent monitoring of the `DUT` . Additionally, documentation and logging capabilities were extended.

Finally, chapter 5 summarizes and discusses the work. Aspects for further developments and improvements are presented.

Chapter 2

Electromagnetic Immunity Standard IEC 62132-4

Contents

2.1 Basic Measurement Setup 6

2.2 Single and Multiple Pin Power Injection 6

2.3 Test Conditions: Signal Form and Power Level 8

2.4 Test Setup and Equipment 8

2.5 Test Board 9

2.6 Test Procedure 9

The IEC 62132-4 standard [13] describes the Direct RF Power Injection (`DPI`) Method, i.e. the measurement protocol to determine electromagnetic immunity for `IC` in the frequency range from 150 kHz to 1 GHz against conducted disturbances. This standard defines a simple test setup and measurement procedure and guarantees a high degree of repeatability for finding the minimum electric immunity level. Moreover, the measurement reveals which pins of an `IC` need special treatment for circuitry.

The minimum electromagnetic immunity level is determined by the maximum permitted level of `RF` disturbances an electronic system can be submitted to. Knowing the immunity characteristics of an `IC` , i.e. the highest forward power not affecting its functionality, allows to design external protection circuitry in a proper way. The basic idea behind `DPI` is to provide details about the immunity level in a repeatable way, using a well-defined measurement environment.

The following sections provide a compressed summary of the norm presented in [13],

since it states the basis for this master's thesis. In particular, a review about the basic measurement setup (2.1), single and multiple pin power injection (2.2), test signal generation and signal form (2.3), power injection setup and equipment (2.4), test circuit board and electrical characteristics (2.5) and test procedure (2.6) are given.

2.1 Basic Measurement Setup

Structure and leadframe are not efficient antennas for radiated disturbancies in the frequency range below 1 GHz. However, traces of printed circuit board (PCB) or cable harnesses may be acting as antennas and provide unwanted RF energy to IC pins. The power transported by these antennas is considered to be a forward power, substantially defining the susceptibility of electromagnetic disturbances before malfunction. The goal of DPI is to determine this behavior.

The test setup is illustrated in Figure 2.1. It consists of a signal generator that provides the test signal (RF disturbance). The forward power level of the test signal after the amplifier ist measured and controlled with the help of a directional coupler and a power meter. On the test PCB the RF power is applied to the DUT through the coupling path from the injection port to the test pin. A coupling capacitor ist used as DC Block to protect the amplifier output stage. The behaviour of the DUT is monitored during the measurement. Power supply and low frequency measurement devices are connected through decoupling networks to avoid crosstalk. The optional control path allows to automate the measurement procedure and to capture the desired immunity characteristics. Malfunction can occur at any function block within the IC . So the operation mode of the IC during test procedure should use every function block. Each pin, that is expected to be exposed to disturbances in application, should be tested. The results of immunity measurments of an IC give information about the need of external protection in the application circuit.

2.2 Single and Multiple Pin Power Injection

To test an individual pin the RF power ist directly applied to the pin. As shown in Figure 2.2 a capacitor is used as DC block. A serial resistor can be used to reduce power or simulate a load as may be used in application. This network acts as highpass filter to eliminate low frequency signals. Additionally the resistor can be used to disconnect the coupling path, when other IC pins are tested.

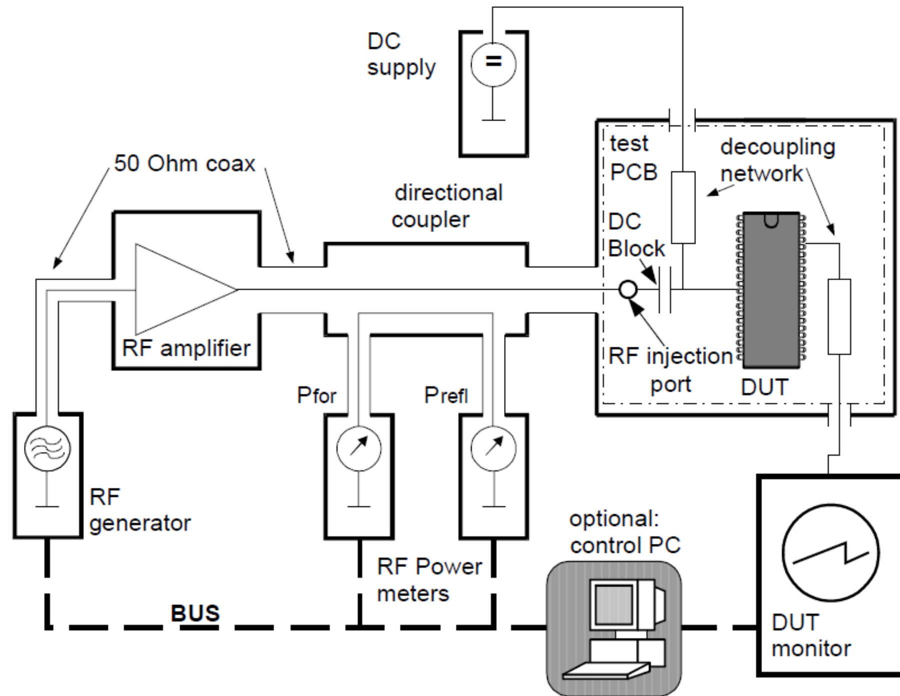

Figure 2.1: Block diagram of direct power injection setup, taken from Ref. [13].

To test differential signal ports to their common mode immuntiy or if the IC has multiple pins with the same signal, for example multiple power supply pins, multiple pin power injection ist used. Therefor the RF power is applied to the pins through multiple coupling paths. Each coupling path consist of a DC block and an optional resistor (Fig. 2.3).

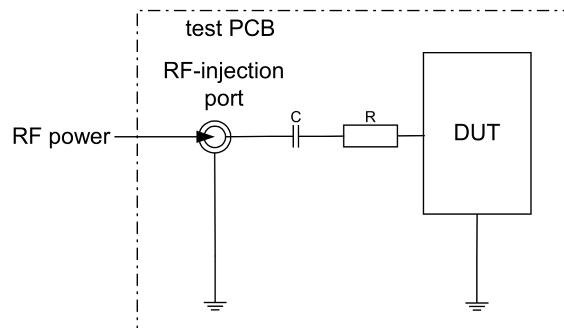

Figure 2.2: Block diagram of a single pin power injection, consisting of RF injection port, DC block capacitor (C) and serial resistor (R), taken from Ref. [13].

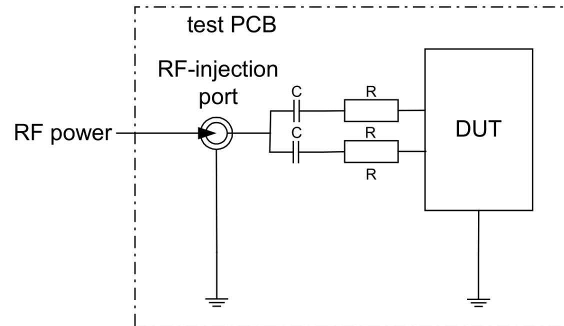

Figure 2.3: Block diagram of a multi pin power injection, consisting of RF injection port, Dc block capacitor (C) and serial resistor (R), taken from Ref. [13].

2.3 Test Conditions: Signal Form and Power Level

The powerlevel of the test signal can be up to 37 dBm or 5 W. Depending on application and tested IC the maximum powerlevel can be chosen according to Figure 2.1. The test signal can be either a continuous waveform (CW) or an amplitude modulated (AM) signal with 1 kHz 80 % modulation. The used signal form has to be documented in the test report. Both test signals use the same peak power (Fig. 2.4).

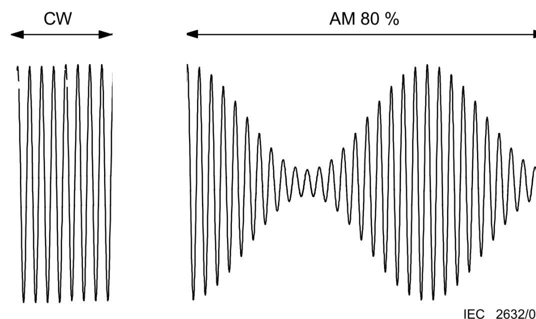

Figure 2.4: Wave form of test signals for direct power injection method, taken from Ref. [10].

2.4 Test Setup and Equipment

As shown in Figure 2.1 the setup requires a RF signal generator to provide the test signal. To achieve the appropriate forward power an amplifier with sufficient high power is needed. The impedance of the amplifier output stage has to be 50 Ω. Otherwise a matching network is necessary to prevent reflexions on the transmission line and allows proper functionality

Zone	power (Watt)	device externally protected by	example for devices
1	1 ... 5	nothing or only a small capacitor as filter	high side switches, power supply circuits, Bus-transceiver for driving wire harness (e.g. CAN, LIN)
2	0.1 ... 0.5	L-,R-,C-low pass filter	signal conditioning devices, ABS sensor circuit, communication line driver
3	0.01 ...0.05	no direct connection to the environment, decoupling by placing	Microcontroller, memories

Table 2.1: Recommended power levels for direct power injection method depending on external protection options with examples, taken from Ref. [13].

for the directional coupler. To measure the forward power a power meter with peak envelope measurment option is used.

2.5 Test Board

The DUT ist placed on a PCB without sockets to reduce inductivity in the signal line. Moreover only mandatory external components, which are necessary for IC functionality, are placed on the board close to the IC . The injection path should be a 50 Ω transmission line, or less than 1/20 of the shortest wave length. For signals up to 1 GHz trace length can be up to 1.5 cm. The coupling path is characterised by replacing the IC by a 50 Ω port and an attenuation measurement. The coupling path has to show an attenuation less than 3 dB without any resonances in the test frequency range. To prevent external equipment from the RF test signal decoupling networks are used. They should have an impedance ≥400 Ω. In Annex B of the IEC 62132 possible implemantions and concepts for building test PCB are described and pictured (Fig. 2.5-2.6).

2.6 Test Procedure

The immunity of the DUT is measured with an increasing forward power in a frequency loop, covering the frequency range from 150 kHz up to 1 GHz (see Fig. 2.7). In an automated test setup several paramters should be defined. These are the start (f_{start}) and stop frequency (f_{stop}), the frequency step size (Δf) according to IEC62132-1 (see Fig. 3.1), the maximum power level ($P_{specified}$), the power offset (x), the power step (ΔP), wait time ($dwell$) and the failure criteria. After initalisation of the measurement equipment (Start) the DUT is exposed to the test signal at the lowest frequency and power level. Therefor the signal

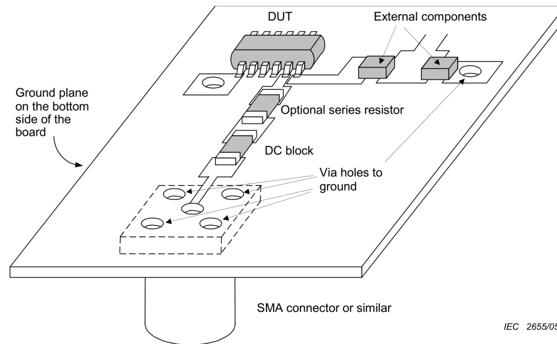

Figure 2.5: Example for a test PCB for direct power injection method, taken from Ref. [13].

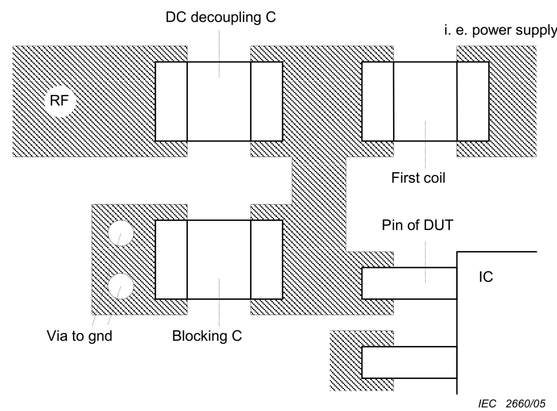

Figure 2.6: Example for the layout of coupling and decoupling path and a device pin with a mandatory blocking capacitor on a test PCB for direct power injection method, taken from Ref. [13].

frequency (f) is set to f_{start} and the power level (P) is set to $P_{specified}$ reduced by the power offset. In the power loop the power level is increased by ΔP until the DUT fail or the maximum power level is reached. Power steps of 0.5 dBm are recommended. Each forward power level should be applied for a sufficient dwell time. Until f_{stop} is reached, the test results for each frequency are stored and the test signal frequency is increased by Δf.

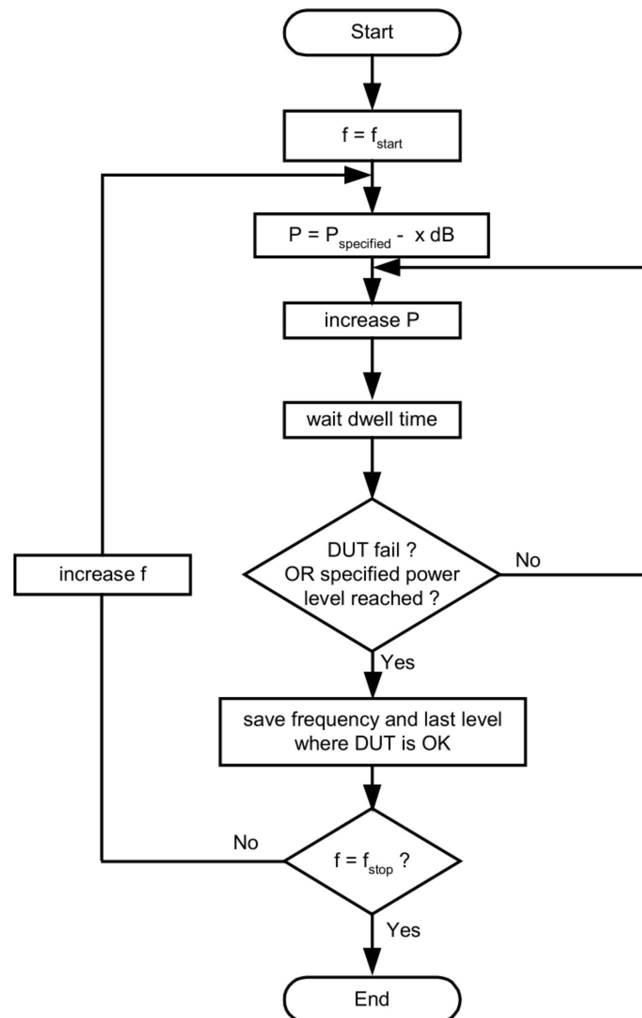

Figure 2.7: Flowchart of direct power injection method, taken from Ref. [13].

Chapter 3

Attenuation Measurement Setup

Contents

3.1 Attenuation Measurement 13

3.2 Measurement Setup 14

3.3 LabVIEW Program 14

3.4 Equipment 25

3.5 Test and Verification 29

3.6 Data Analysis 30

3.7 Calculation of impedance and attenuation 32

3.8 Investigation in High Voltage RF Measurment 35

In the field of EMC measurement the knowledge of insertion loss from different parts of the measurement setup is important. Therefore a fast and easy to use measurement setup is needed. The typical frequency range of a mentioned setup is 150 kHz up to 1 GHz. The frequency range implemented in this work is 100 kHz up to 2 GHz. To get a `DPI` measurement setup, conform to the standard, the insertion loss of the coupling path has to be less than 3 dB over the whole frequency range. The impedance of the DC biasing network has to be higher than 400 Ω. Before the `DPI` measurement, the test setup and the test board has to be specified.

3.1 Attenuation Measurement

One way to measure attenuation is the use of a network analyzer. The attenuation complies with the $s21$ or $s12$ parameters. The impedance can be calculated by the use of these

parameters. To cover the whole frequency range with available equipment, two network analyzers are needed. The network analyzers in the laboratory have different connectors, too. So the setup has to be changed during measurement and has to be calibrated twice. This requires time. A further issue was the usage of two network analyzers at the same time, because the devices are used jointly by several laboratories. To avoid this problem we decide to use a more flexible setup for attenuation measurements. It can be used with the dual channel power meter as utilised in the `DPI` setup. It also works with a high frequency Oscilloscope with 50 Ω input option. With the Oscilloscope it is possible to measure attenuation and phase. Of course this setup acquires less information than a s-parameter measurement. As the power meter is part of the special equipment of the EMC working group, this setup is always available and can be used to check the measurement setup, measure unknown impedances and the attenuation of filter circuits whenever needed.

3.2 Measurement Setup

The setup is based on a two channel relative measurement. In such a way, power level variations from the generator can be compensated. By the use of a power splitter the input signal from a generator is divided in two lines. With one channel of the power meter the actual power level which is applied to the `DUT` is measured. The other channel is used to measure the power level after the `DUT` . The attenuation and the impedance of the `DUT` can be calculated. This solution is described in the manual of the power meter R&S NRVD [20] and is shown in Figure 3.1.

Instead of the power meter, a network analyzer or a dual channel oscilloscope with 50 Ω input termination would work too. To be able to make automated measurements a control program was developed.

3.3 LabVIEW Program

The software to control the setup is written with NI LabVIEW 8.2, which is compatible to the whole 8.x series. While the measuring of attenuation is the main part of interest, the program is designed more flexible and can be used for evaluation and data acquisition in the EMC Laboratory.

The final version, named *AttMeasurement_24_06_2008_final.vi*, supports the power meter NRVD from Rohde&Schwarz and the four-channel oscilloscope LeCroy Wave pro 950 for voltage measuring. It can be either used with 50 Ω termination or with the active

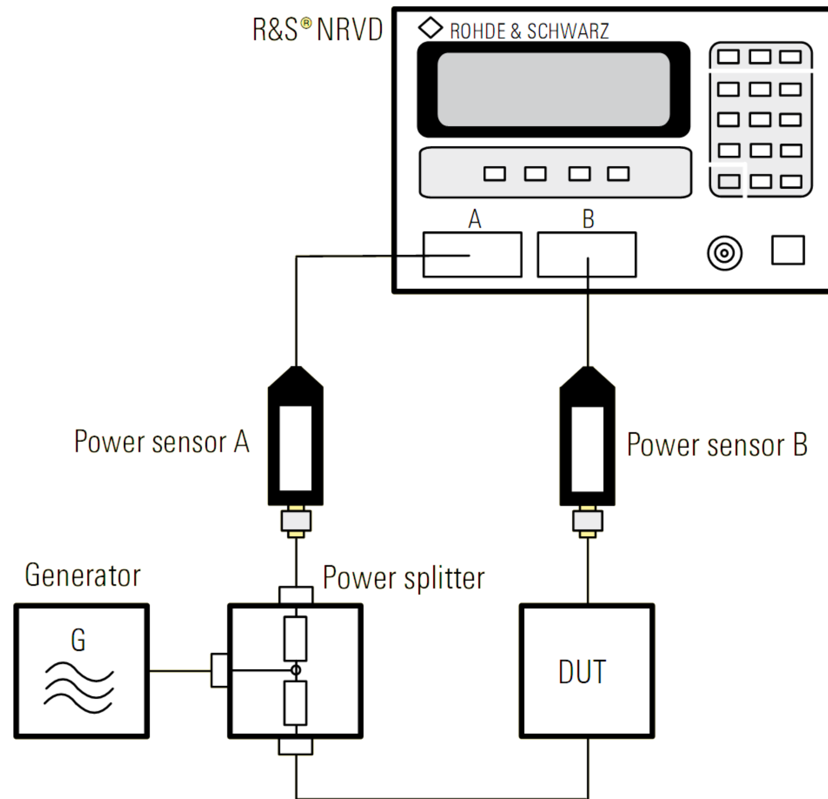

Figure 3.1: Setup for accurate attenuation measurements using two channel power meter R&S NRVD, taken from [20].

probe heads HFP1500. As signal source it supports signal generators of the HP 865xx series. For all tests and measurements a HP 8657B was used in the setup. We applied exisiting drivers for the power meter and signal generator, but the lack of drivers for the LeCroy Wave pro 950 requires us to write our own driver. As the oscilloscope is needed for signal monitoring in other test setups, these drivers can be reused in new projects and save development time in future.

The following sections describe interface, structure and possible applications of the program.

3.3.1 Interface

The control interface, seen in Figure 3.2, allows the configuration of all used devices in the setup. Project name and comments are saved in the log file header for documentation

issues. Current measurement values and debug information are displayed during operation to describe the current system status.

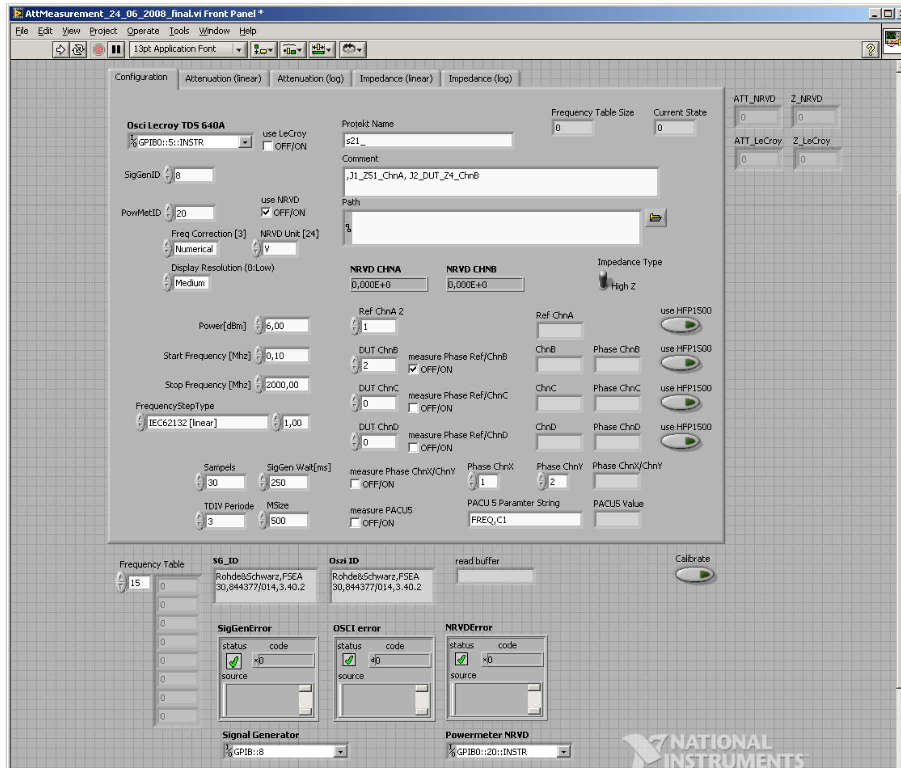

Figure 3.2: Configuration tab of the attenuation measurement control software

On the top left hand side the general purpose interface bus, IEEE-488 (GPIB) device addresses for the signal generator, power meter and oscilloscope can be configured. The default values comply with the setup in the EMC laboratory. In general the device address of a GPIB device is shown at start up, but can be changed in the device setup. The address range is from 1 to 30. Usually there is no need to change the address at the device unless two instruments in the setup have the same. The default values are restored after each restart of the system. Next to the address configuration there is a selection of the used measuring unit (1). The power meter and oscilloscope can be used alone or together. This allows monitoring and logging of up to six different voltages. At position (2) comes the configuration of the power meter, followed by the signal analyzer and the oscilloscope. At position (3) is the selection of the oscilloscope channel that should be measured. Optional phase measuring, relative to the first channel, can be activated. These values are shown in real time during operation. The oscilloscope channels are usually configured as $50\,\Omega$ input. The use of the active probe head can be selected by use of the buttons at postion

(4). The calibration button (5) can be used to force a calibration of the oscilloscope after a measuring cycle. By default the automatic calibration is deactivated during measurements. The impedance type selection switch (6) selects the calculation mode. The high impedance mode is usually used for inductors while the low impedance mode is used for capacitors.

The other four tabs seen in Figure 3.3 give graphical information about the attenuation measured between the two power meter channels ChnA and ChnB, or the oscilloscope channels Ref ChnA and DUT ChnB. The values are plotted in linear and logarithmic scaling to give a fast overview of the DUT properties. The impedance is calculated for a 50 Ω reference system.

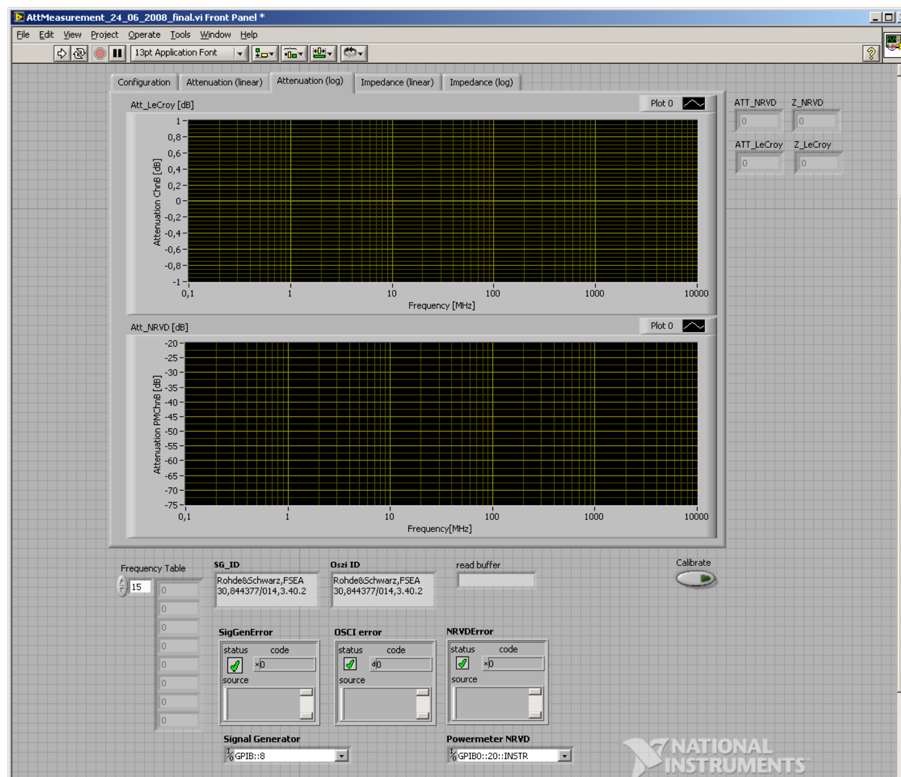

Figure 3.3: Attenuation plot tab of the attenuation measurement control software

3.3.2 Program Structure

The whole measuring process consists of three steps. It starts with the initialisation of the used equipment, followed by the measuring at each specified frequency and ends with resetting the equipment to the default configuration. The main control sequence consist of a four stage stacked sequence. For documentation more detailed information about the

program structure is given below. In the first stage the log file header with the setup configuration is written (1) and the initialisation of the signal generator (2) and the four-channel oscilloscope (3) is done, as shown in Figure 3.4.

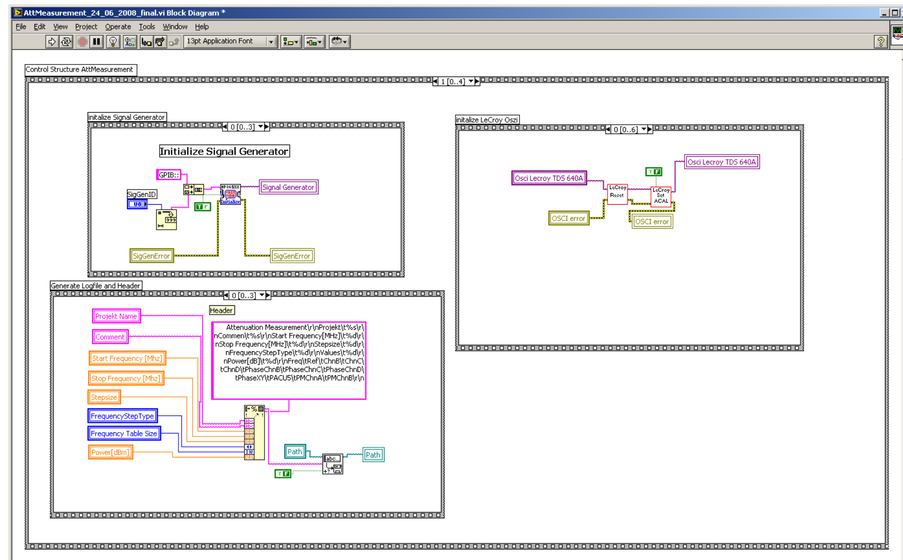

Figure 3.4: Initialisation of the attenuation measurement control software

The log file header starts with the project name, the comment string, the measured frequency range, the number of measured data points and the used signal generator output power. It includes a table with the mapping of the oscilloscope channels. Because of easier post processing, the channels in the log file have the names ChnA to ChnD. ChnA is used as reference for attenuation calculation and phase measurement. It is often not possible to use the oscilloscope channels in a fixed order. The mapping between the input channels and the log file channel names are parallelized used as shown in Figure 3.2. The channel mapping table is followed by a list, that specifies, if and for which channel a phase measuring is selected. If there is the need of phase measuring between two other channels, the two channels ChnX and ChnY can be selected optionally. This option can also be used to check causality of the measurement. The phase differences relative to ChnA have to be the same as the direct measured phase if the setup is working properly. As the program offers the option to specify a custom parameter measurement like signal frequency, root mean square (`RMS`) or peak to peak (`PkPk`) value or any other available signal parameter supported by the oscilloscope firmware. This information is stored in the log file, too. The whole list can be found in the LeCroy Wave pro manual [17]. In the last line of the header the measurement data table row names are saved.

The initialisation of the signal generator is simply done by using the available drivers. After calling the routines for the `GPIB` communication, the signal generator is configured with respect to frequency and output power.

For the oscilloscope new developed virtual instruments (`VIs`) are used. The sequence starts with a reset, and if enabled, a forced calibration. Then the `GPIB` communication is tested by an ID query. If the device works properly an initial auto set is carried out. Further on the selected measurement options are programmed. Finally, the trigger options are set.

In the next step, the power meter is initialised and configured, as illustrated in Figure 3.5. The original drivers were updated considering frequency correction, display settings and resolution. First, the signal generator is switched off to allow calibration of the power meter probe heads to zero power. This calibration is always done at start up but can be forced either manually by using the front panel or remotely by using `GPIB` commands. After initialisation the built-in test generator output is disabled. For each channel zero correction is enabled and frequency correction is switched off. Then resolution and measuring units are set as selected. Both channels are set to average measuring mode. To use the power meter in dual mode, each channel has to be configured before dual mode is enabled. Otherwise the power meter does not work properly. Finally the power meter is switched to dual mode and the signal generator output is enabled.

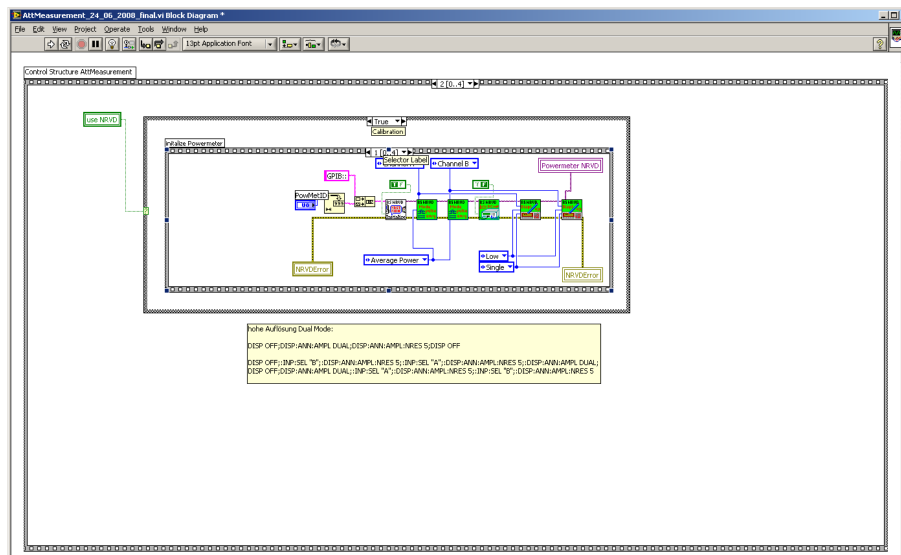

Figure 3.5: Initialisation and calibration of the power meter

Figure 3.6 shows the main measurement loop. For each frequency a measuring cycle

is performed. The results are written to the log file immediately. This solution can cause problems when data is written to remote hardware. The measurement visualisation is updated and displayed in the corresponding tabs (Figure 3.3).

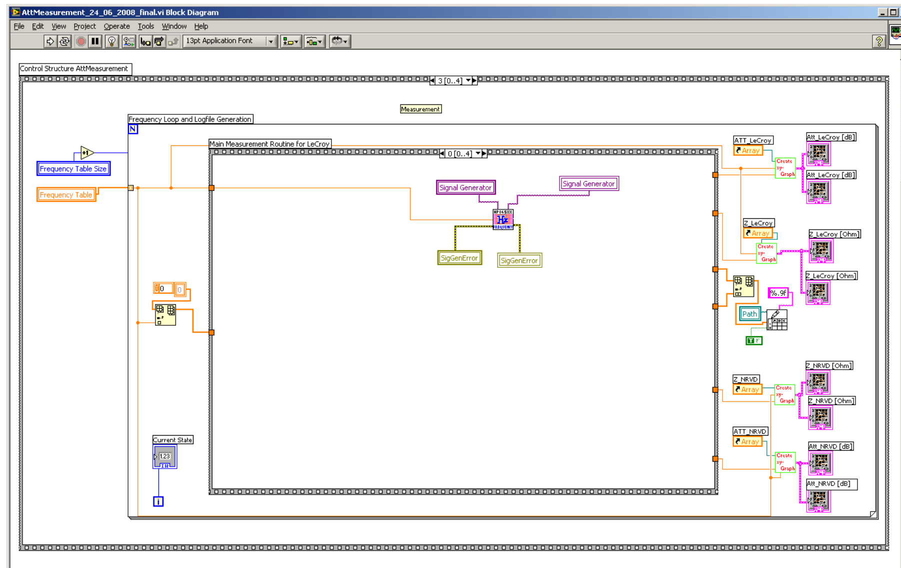

Figure 3.6: Frequency loop of attenuation measurement control software

In the final step, shown in Figure 3.7, the used equipment is set to its default configuration. This guarantees proper functionality if the measuring instruments are used in other setups. It also allows manual measurements to reproduce results.

To complete the documentation of the attenuation measurement software the main measuring routine and some sub `VIs` that can be reused and adapted in other projects, are described and discussed.

Each measurement cycle starts with setting up the signal generator to the new frequency, given the frequency table calculated at program start. This follows a delay time defined by the SigGen Wait[ms] value. It is important to use a high enough value to guarantee a stable voltage level and oscillation. Values in the range from 100 ms to 250 ms leeds to acceptable results. Because this delay occurs in each iteration it is significant for the overall measurement duration. After that, if selected, the calibration of the oscilloscope is done. Due to the fact, that the automatic calibration is deactivated, this should be done a few times per day if the setup is used intensively. In the third sequence the main measuring routine starts with two independent actions. If the oscilloscope is used, for each active channel an automated voltage division selection is done, based on a single test measurement. It is important to distinguish between direct connected coaxial wires

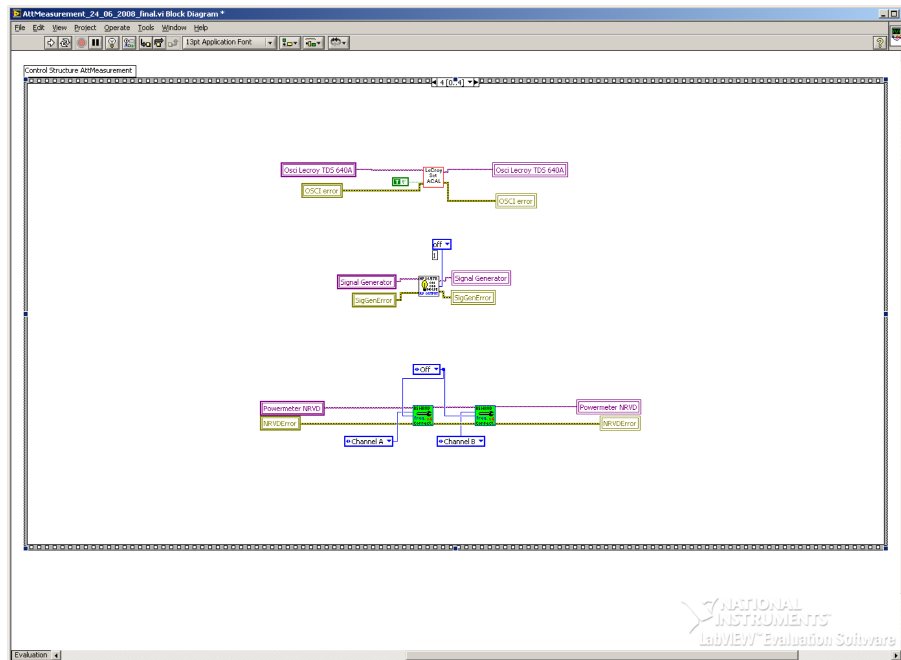

Figure 3.7: Termination of the attenuation measurement control software

and 50 Ω termination and the very high resistive active probe heads that use the DC termination. After each channel setup the time division is configured. Depending on the time division period value and the current frequency a suitable time division is selected and programmed to the LeCroy Wave pro. Simultaneously the correct frequency correction for the two power meter channels is configured. This can be seen in Figure 3.8.

Figure 3.9 shows the next step. For each oscilloscope channel multiple measurements are performed and the mean value is written to the logfile. The quantity is defined by the sampling parameter. The impedance and attenuation assuming a 50 Ω system is calculated according to the selected impedance type. High impedance type typically stands for an inductive load within the signal line, whereas low impedance stands for capacitive loads connected to the probe head. The loads are connected between the signal line and ground, respectively. Because the power meter adjusts the integration time of its sensors automatically, there is no need to sample more values and calculate the average. So simply the measure command is triggered and the values for both channels are read out.

In the last sequence (Figure 3.10) the phase measuring is done. The five configurable custom parameters, offered by the oscilloscope firmware, are read out. In the initialisation of the oscilloscope these parameters were configured to measure the phase between the reference signal and the respective channels. It is important to know, that this functionality

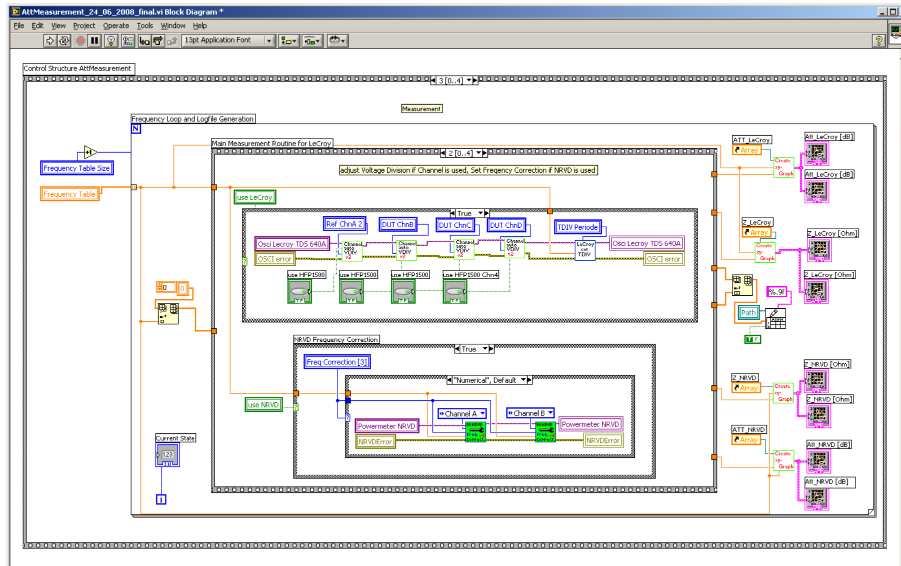

Figure 3.8: Voltage devision selection of oscilloscope channels and fequency correction of power meter channels

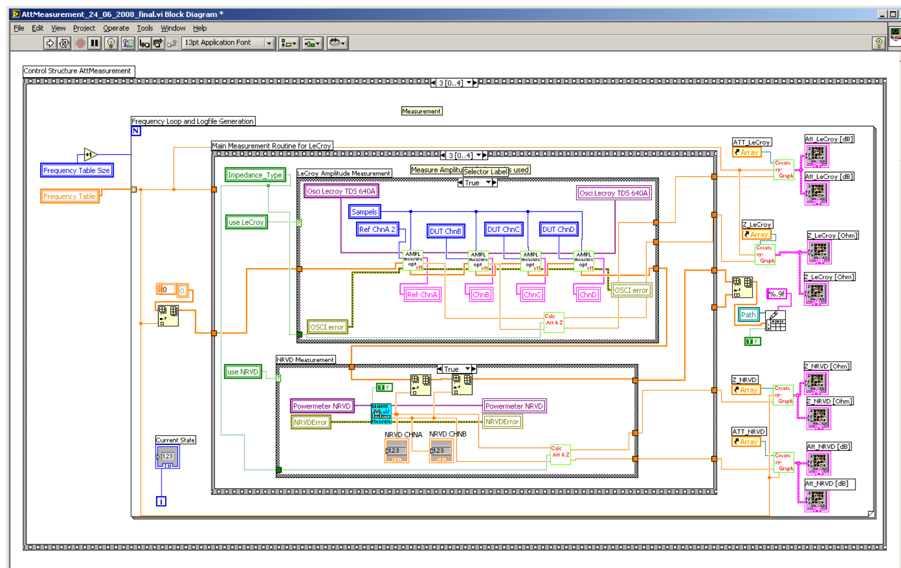

Figure 3.9: Amplitude measuring and calculation

is only given for an adequate signal quality and amplitude. As described above, the fifth parameter can be defined individually. Of course it has to be a command string supported by the oscilloscope firmware.

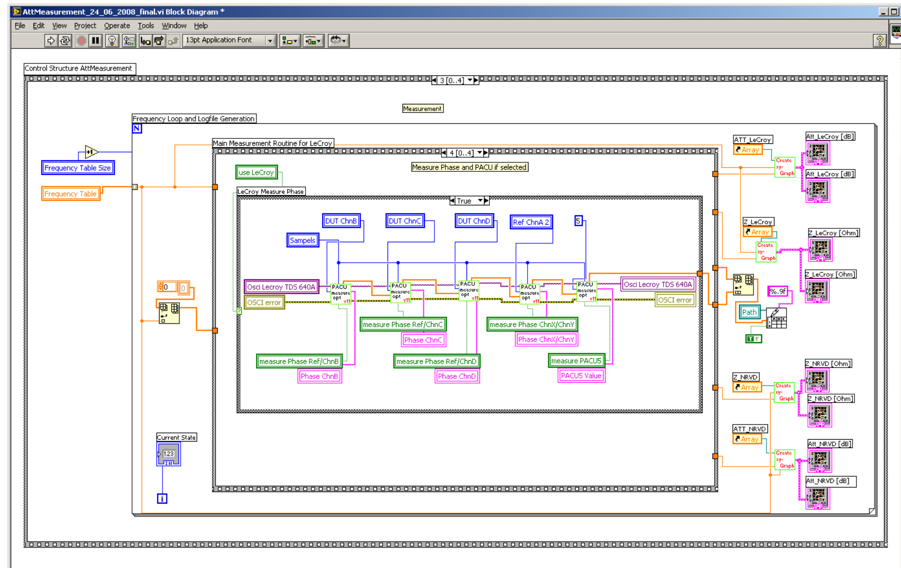

Figure 3.10: Phase and custom parameter measuring

3.3.3 Sub VIs

The `VIs` developed in the attenuation measurement control software to interact with the LeCroy Wave pro oscilloscope can be found in the corresponding sub VI folder. As already described in Section 3.3, the idea was to create a basic driver system that can be easily reused and extended. In addition to the basic initialisation commands a set of tested functions for data acquisition is provided. These Sub`VIs` are listed below:

- LeCroy_Reset.vi
- LeCroy_IDN.vi
- LeCroy_AutoSet.vi
- LeCroy_SetACAL_v001.vi
- LeCroy_SetTDIV.vi
- LeCroy_SetVDIV_v011.vi
- LeCroy_SetPACU.vi
- LeCroy_ReadAmplitude.vi
- LeCroy_ReadPACU.vi

Frequency range [MHz]	0.1 – 1	1 – 100	100 – 1000
linear step	≤ 0.1 MHz	≤ 1 MHz	≤ 10 MHz
logarithmic step	**≤ 5% increment**		

Table 3.1: Recommended frequency step sizes according to IEC 62132, taken from Ref. [10].

- LeCroy_MeasureAmplitude_v004.vi
- LeCroy_MeasurePACU_v002.vi
- RSNRVD Display Settings_v2.vi
- RSNRVD Frequency Correction_v4.vi
- generateFrequencyTable_v004.vi

To use the whole functionality of the available power meter, two functions of the existing driver library are changed to support high resolution, dual measuring and frequency correction. To activate the dual channel measuring, the command string *DISP OFF;:INP:SEL "B";:DISP:ANN:AMPL:NRES 5;:INP:SEL "A";:DISP:ANN:AMPL:NRES 5;:DISP:ANN:AMPL DUAL;* can be used. The changes made in the driver and this command were added to the printed power meter manual, too.

Doing frequency sweeps over a wide range, it is difficult to choose an efficient and accurate step size. Using a percentage increment in the measurement, generate results with very small steps at the beginning of the measuring cycle, but gives a low resolution at higher frequencies. A linear step size is practicable for small ranges, or it has to be adjusted for different decades. Based on the recommended frequency step sizes in IEC 62132-1 [10], as shown in Figure 3.1, the following functionality was implemented. To achieve a high resolution with an acceptable number of data points we recommend to use linear iteration according to the IEC 62132-1. While the 5% relative step size results in 189 data points and steps greater 50 MHz the default linear step size results in 198 data points but guarantees a resolution of 10 MHz even in the higher frequency range.

The SubVI *generateFrequencyTable_v004.vi* supports the following modes of operation:

- Step size is interpreted as fixed Step size in MHz
- Step size is interpreted as %-Value based on the actual Frequency
- Step size is interpreted as the amount of Measurement Points
- Step size is interpreted as a Quality Level of IEC62132 compatible Frequency Steps default 1 → fast, 0.1-1MHz: 0.1MHz, 1-100MHz: 1MHz, 0.1-1GHz: 10MHz Steps other Value → Step size = default/Value

Table 3.2: Supported frequency step sizes of SubVI *generateFrequencyTable_v004.vi*, according to Ref. [10].

3.4 Equipment

Devices such as power splitters, power meters and active oscilloscope probes were incorporated in the measurement setup. The following chapter gives an overview of the used measurement equipment and its features.

3.4.1 Power Splitter

As shown in Figure 3.1 the setup needs a broadband power splitter to work correctly. In practical usage there is the risk to interchange the splitter with another three port device, the power divider. Even in literature the two devices are used concurrently. But they have different properties and can be used for different applications. Using the wrong device tends to result in measuring errors, but is hardly detectable. The devices can often only be identified by their serial number and a corresponding datasheet. Depending on manufacturer and design looking at the shape of the device can't identify them. A good comparison of power splitters and dividers can be found in [2] and [3]. Figure 3.11 gives a brief overview abut the differences between power splitters and power dividers.

The broadband power splitter consists of two high quality resistors. In contrast to the power divider it has a $50\,\Omega$ input port and two output ports. To its signal rationing effect it improves the source match and reduces reflected and re-reflected signals. So it can be used for gain or attenuation measurements at different power levels. It has a insertion loss between input and output ports of 6 dB.

The broadband power divider is symmetric in its properties. It consists of three matched resistors. Each port has $16\ 2/3\,\Omega$. If it works in a $50\,\Omega$ system it can be used to divide or combine a signal. It has a standing wave ratio (SWR) of 3:1 and an insertion loss between any ports of 6 dB.

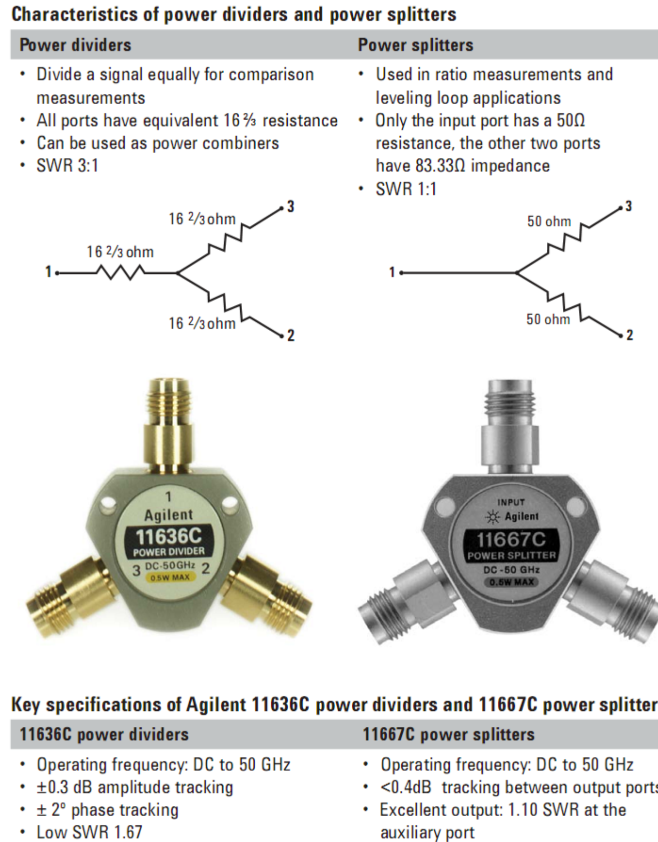

Characteristics of power dividers and power splitters

Power dividers	Power splitters
• Divide a signal equally for comparison measurements • All ports have equivalent 16⅔ resistance • Can be used as power combiners • SWR 3:1	• Used in ratio measurements and leveling loop applications • Only the input port has a 50Ω resistance, the other two ports have 83.33Ω impedance • SWR 1:1

Key specifications of Agilent 11636C power dividers and 11667C power splitter

11636C power dividers	11667C power splitters
• Operating frequency: DC to 50 GHz • ±0.3 dB amplitude tracking • ± 2° phase tracking • Low SWR 1.67	• Operating frequency: DC to 50 GHz • <0.4dB tracking between output ports • Excellent output: 1.10 SWR at the auxiliary port

Figure 3.11: Most important differences between broadband power splitters and power dividers on the example of the agilent 11636C and 11667C, taken from [3]

Because of the high insertion loss of the broadband resistive devices, they have a maximum operation power from typically around 0.5 W or 1 W.

As shown in the schematic of power splitter and divider (Fig. 3.11), usage in the same setup would cause different measuring results. At higher frequencies the `SWR` of the power divider causes measuring errors. However, for software development, testing and improving the measurement setup, the available power divider HP 11636A was used. To show the functionality of the setup and the need of a power splitter for valid measuring data, a comparison between the two devices was done. For this purpose the power divider was used in the measuring setup at the IFE. The results match with the calculated difference and simulation results. The measured curves are shown in Figure 3.12

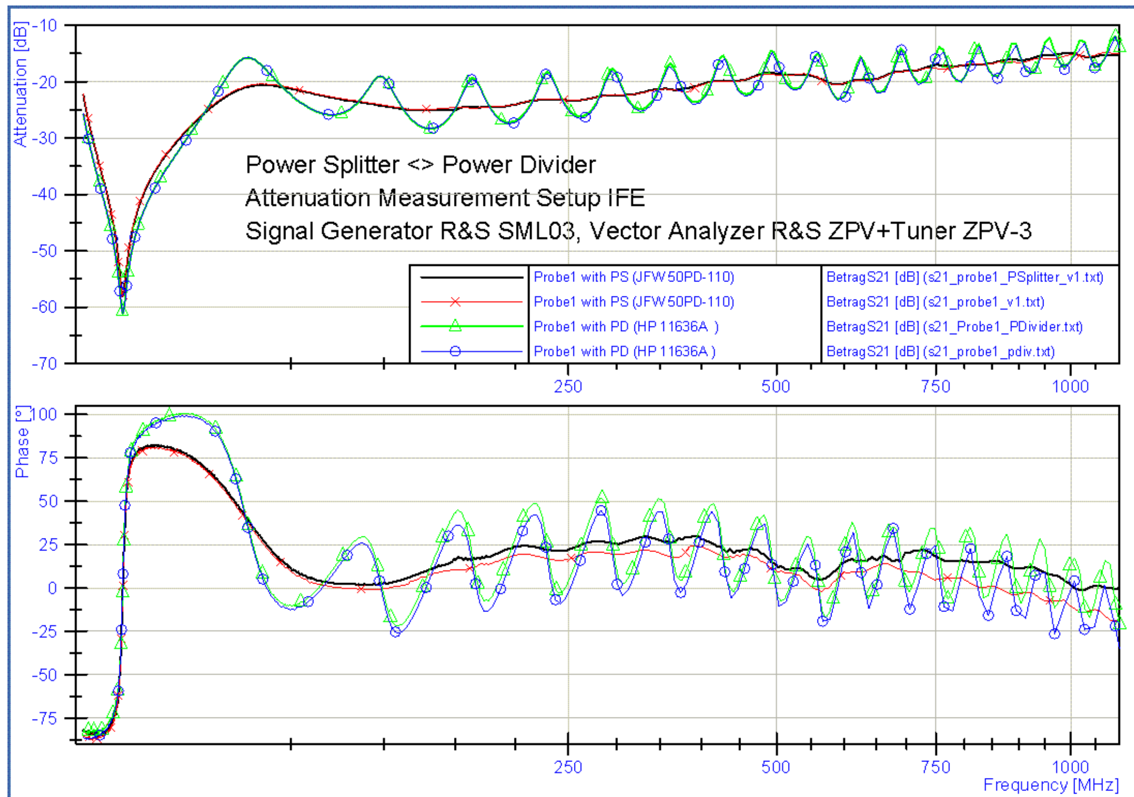

Figure 3.12: Measuring results using power splitter and power divider in the same setup. The results show that a power splitter is needed for valid measuring data.

3.4.2 Power Meter

The power meter from NRVD (R&S) is based on the milli-voltmeter series URV (R&S) and provides the same functionality. The new NRV series support the DC capable thermal power sensors while the URV only support the diode power sensors. With little changes in driver libraries, both devices can be interchanged. The different sensor types came up with some limitations. The thermal power sensors are capable of measuring modulated signals as well as `CW` signals by `RMS` weighting of all spectral components within the specified frequency range. The diode sensors are more sensitive and faster in application. Up to a specific power level they are also able to measure the average power of modulated signals. Above this power level they do not work reliably with `AM` signals. For the attenuation setup this difference is not that important, because the test signal is always `CW` . To the fact, that the power meter is also used in the `DPI` setup and it could be used for voltage

measurements, a brief summary of the available sensors and their properties is given below.

NRV-Z51 The NRV-Z51 is a 50 Ω terminating thermal power sensor. So it is capable of measuring `CW` signals and the average power of any type of modulated signals.
Power range: 1 μW to 100 mW (-30 dBm to 20 dBm)

NRV-Z4 The NRV-Z4 is a 50 Ω terminating diode power sensor. It is capable of measuring `CW` signals up to its maximum range. Its true `RMS` measuring range is significantly lower compared to a thermal power sensor.
Power range: 100 pW to 20 mW (-70 dBm to 13 dBm)
RMS range: up to 10 μW (-20 dBm)

NRV-Z5 The NRV-Z4 is a 50 Ω terminating diode power sensor. It is capable of measuring `CW` signals up to its maximum range. Its true `RMS` measuring range is significantly lower compared to a thermal power sensor.
Power range: 10 nW to 500 mW (-50 dBm to 27 dBm)
RMS range: up to 1 mW (0 dBm)

URV5-Z2 The URV5-Z2 is an insertion unit that uses the same technology as the diode sensors. So it also has a limited true `RMS` range.
Power range: 200 μV to 10 V (-60 dBm to 33 dBm)
RMS range: up to 22 mV (-20 dBm)

URV5-Z4 The URV5-Z4 is a URV5-Z2 with an integrated capacitive voltage divider with 20dB. So it has a very high decoupling and a low insertion loss. But it also has a limited true `RMS` range.
Power range: 2 mV to 100 V (-40 dBm to 53 dBm)
RMS range: up to 2 mV (0 dBm)

URV5-Z7 The URV5-Z7 is a RF probe with a low input capacitance and high DC voltage tolerance. Compared to active, high impedance probes it has a higher dynamic range. It came with two plug-on dividers that allow a measuring range up to 1 kV and an input impedance of 0.5 pF || 10 MΩ
Power range: 200 μV to 10 V (-60 dBm to 33 dBm)
RMS range: up to 22 mV (-20 dBm)

3.4.3 LeCroy Active Probes

While the 50 Ω inputs of the LeCroy Wave Pro work very accurate even at high frequencies, the performance of the two available active probes is not as desired. As they are optimized to measure in fast logic circuits, the input range is limited to $\pm 8\,V$ and $\pm 12\,V$ offset voltage. For investigation on signal quality, voltage levels during EMC measurements this limitation can be exceeded. In worst case like a shortcut caused by a damaged IC, the applied voltages are higher than the absolute maximum ratings of the HFP1500 [18] active probes. The default accessories to connect the probe to the DUT are not suitable for higher frequencies. The available wires for ground connection are too long and come with high resistive clip terminals. For good signal quality it is important to use soldered connectors and minimum wire lengths for ground connection. With these simple modifications the signal quality and frequency range can be increased. In addition the influence of arrangement of measuring equipment to the achieved measuring results is reduced. By connecting the probes directly to a soldered connector a good reproducibility is guaranteed.

3.5 Test and Verification

Each software module was tested during development to guarantee proper functionality of the whole setup. Special attention was turned on minimizing data communication and waiting loops to optimize the duration of the entire measurement. After those improvements, the average measuring time for 200 data points could be reduced from over 35 min down to 15 min. The simple impedance or attenuation measurement, done by the NRVD only, needs negligible time. Depending on the used accuracy, a cycle takes less than three min. This allows quick and efficient system tests of measurement equipment and test setups. The used samples are different kinds of ferrite beads, inductors, capacitors, simple connectors and typical equipment like attenuation elements and DC-blocks. The following figures show the performance of the test setup.

Figure 3.13 show results achieved by the usage of the oscilloscope LeCroy Wave Pro 950 compared to the reference test bench. Both, phase and attenuation values, match very well. So it is shown, that for simple attenuation measurements the oscilloscope could be used as replacement for a network analyzer.

In a next step the support of the power meter was improved. Figure 3.14 shows the smooth curve that can be achieved at very low signal strength. The measuring sweep takes

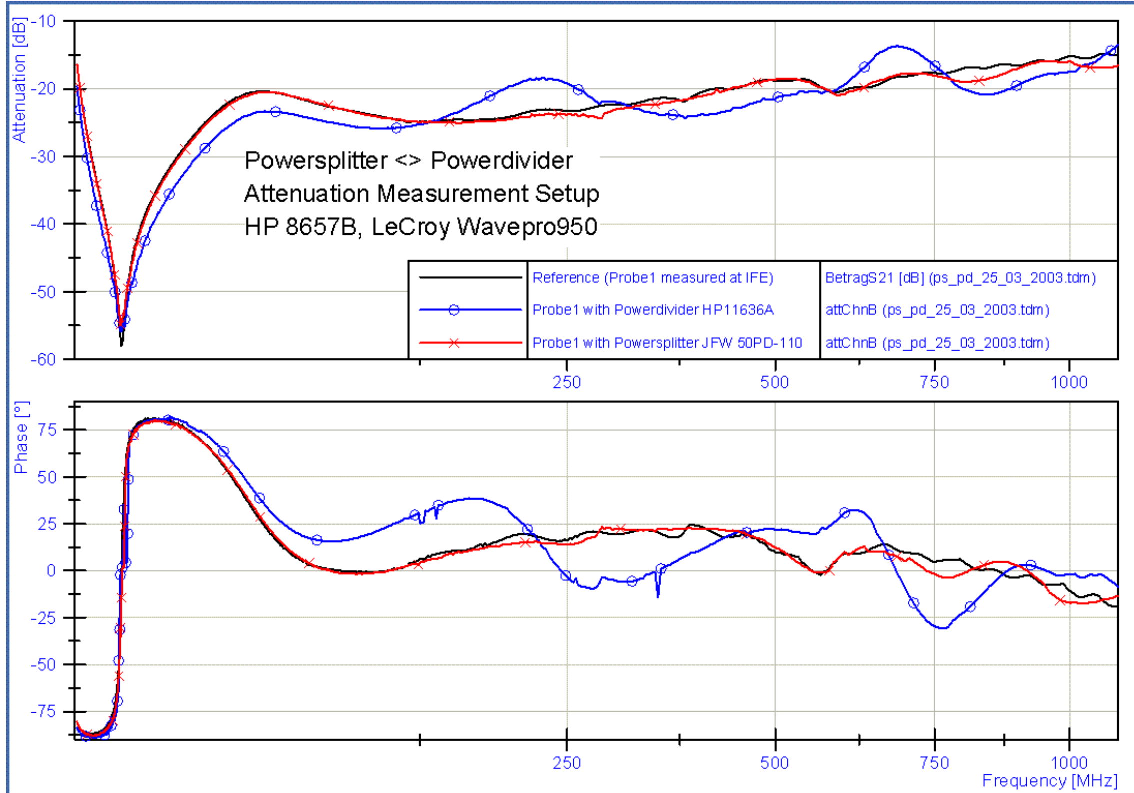

Figure 3.13: Measuring results using power splitter and power divider with LeCroy Wavepro. As reference a measuring result, done at the IFE, is shown.

less than 3 min at high resolution. Compared to the reference setup, or the setup using the oscilloscope, this is a significant speed up. To show the high reproducibility, a detailed plot of the high attenuation region of the sample filter at 3 MHz is given in Figure 3.15.

3.6 Data Analysis

During development of the measurement setup there was the need to have a tool for evaluating first results and compare them with reference test results. This calculation and visualization was done with NI DIAdem. It offers some features, MS Excel can not support. However, data export functions and scripting support give full compatibility to the group internally used software products.

The schematic of the test setup is shown in Figure 3.16. With respect to the setup calibration measurement, the measured voltages can be used to calculate the attenuation of the sample. Depending on the measuring method, high impedance with the sample

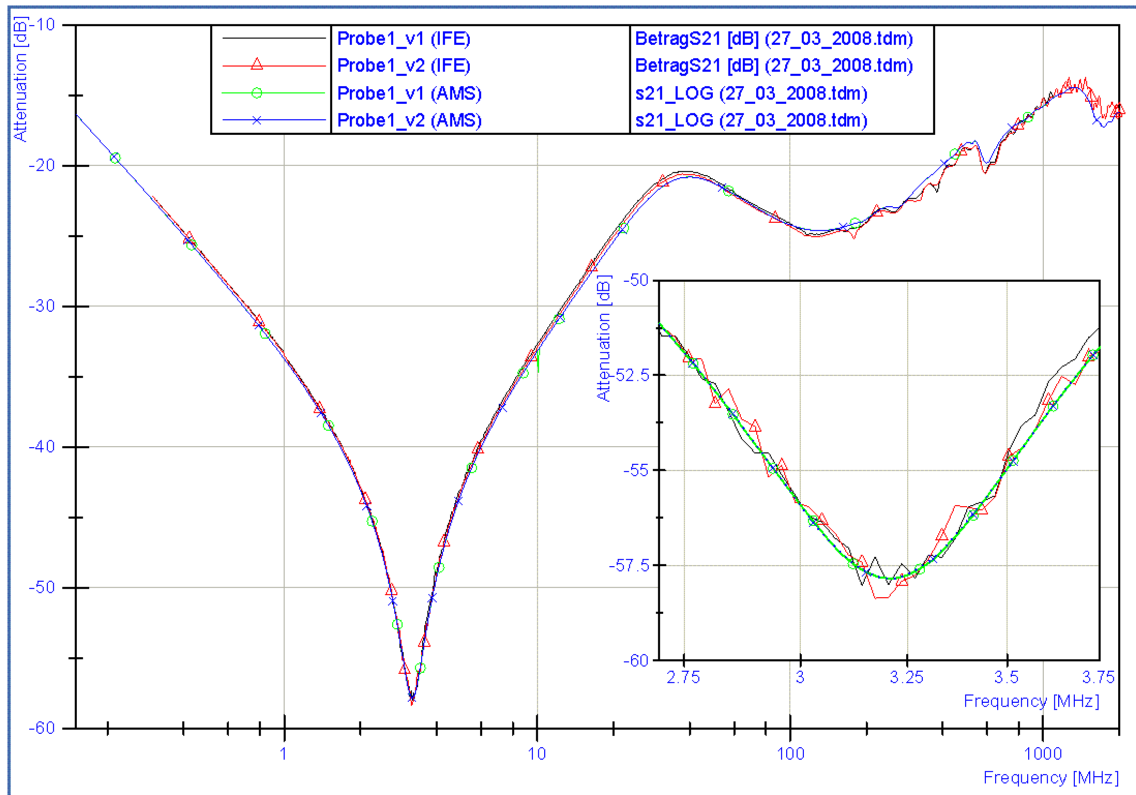

Figure 3.14: Measuring results using power meter and sample "Probe1" compared to two reference measurements.

in series to the detector and low impedance with the sample in parallel to the detector, the impedance of the DUT can be calculated with the equations given in section 3.7. First they were implemented and evaluated in DIAdem only. In the final version some calculations are also included in the control and data acquisition software, developed with NI LabVIEW.

3.6.1 Comparision Power Splitter vs. Power Divider

As shown in Figure 3.11 the devices came with different internal structure. Doing measurements in the same test setup with the same DUT , resulting in a systematic mismatch. Of course the usage of a power divider would lead to more unwanted reflections and should not be used. However, the difference between both setups was calculated and proved by simulation and measuring. As the schematic in Figure 3.17 shows, the equations in section 3.7 can be used to calculate the impedance of a DUT in an attenuation measurement setup

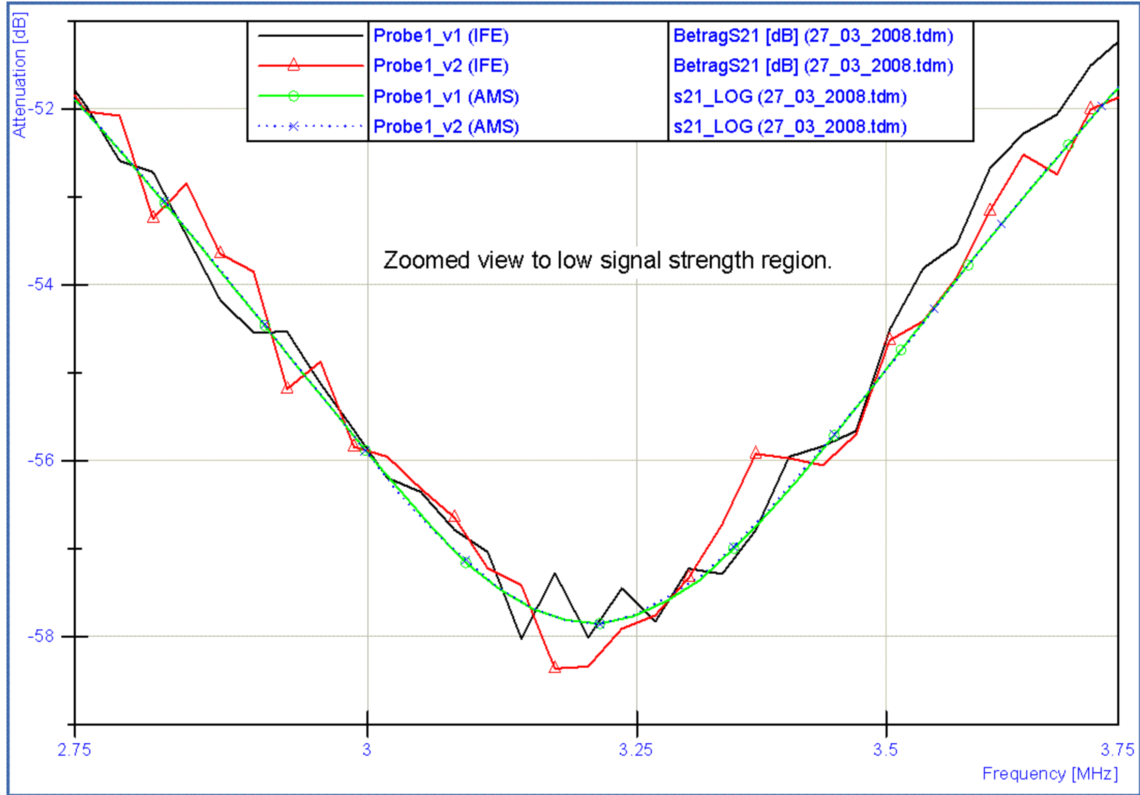

Figure 3.15: Zoomed view at low signal strength region, showing the high sensitivity of the power meter and the good reproducibility of the test bench.

as shown in Figure 3.1.

3.7 Calculation of impedance and attenuation

In this section A (also entitled as *Chn1* in the figure) is the voltage at the first acquisition channel, which is usually used as the reference voltage, and B (or *Chn2*) represents the voltage measured at the channel connected to the DUT .

U_{PS} denotes the voltage and Z_{PS} the impedance of the DUT in the given test setup with a power splitter. Subsequently, U_{PD} denotes the voltage and Z_{PD} the impedance of the DUT , if a power divider is used.

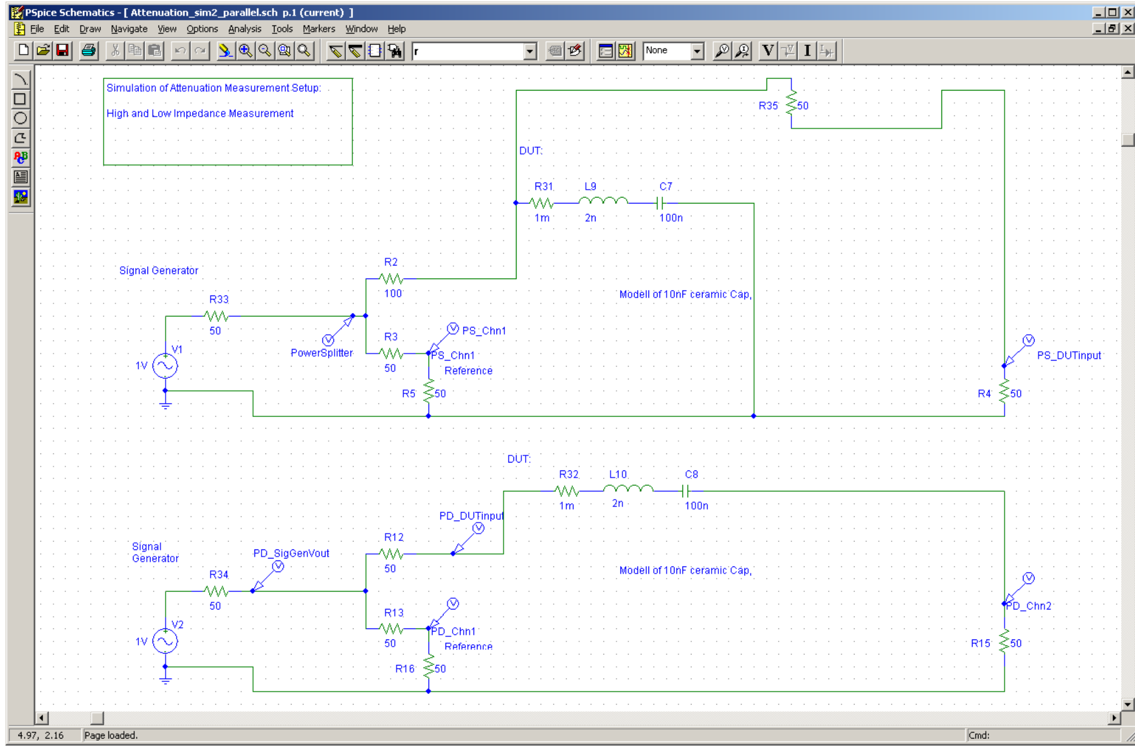

Figure 3.16: PSpice Simulation of Attenuation Measurement with a simple model of a 10 nF capacitor for comparision between high and low impedance setup type.

3.7.1 Impedance Calculation for Power Splitter

$$
\begin{aligned}
U_{PS} &= A \times \frac{50+50}{50} \\
U_{PS} &= B \times \frac{50+Z_{PS}+50}{50} \\
\frac{A}{B} \times 100 &= Z_{PS} + 100 \\
Z_{PS} &= \left(\frac{A}{B} - 1\right) \times 100
\end{aligned}
\tag{3.1}
$$

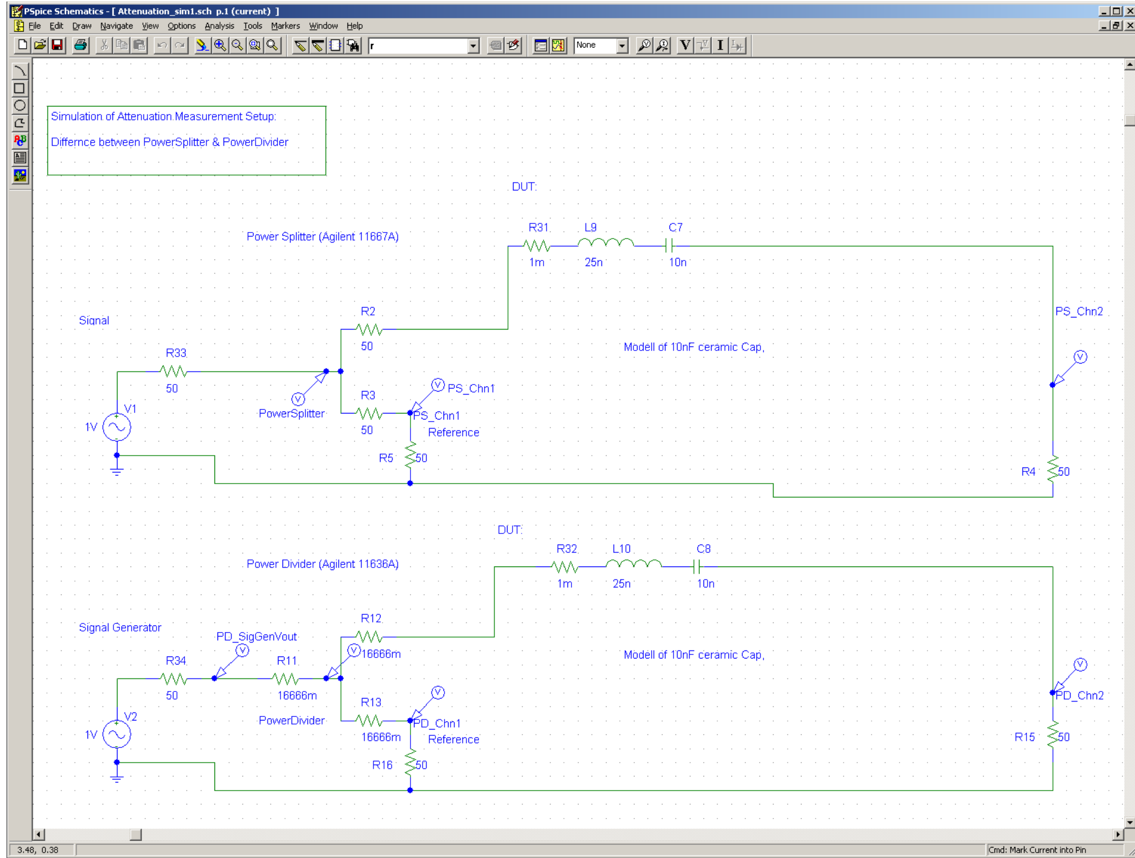

Figure 3.17: PSpice Simulation of Attenuation Measurement with a simple model of a 10 nF capacitor for comparision between the usage of a Power Splitter and a Power Divider in the same setup.

3.7.2 Impedance Calculation for Power Divider

$$
\begin{aligned}
U_{PD} &= A \times \frac{16\frac{2}{3} + 50}{50} \\
U_{PD} &= B \times \frac{16\frac{2}{3} + Z_{PD} + 50}{50} \\
\frac{A}{B} \times 66\frac{2}{3} &= Z_{PD} + 66\frac{2}{3} \\
Z_{PD} &= \left(\frac{A}{B} - 1\right) \times 66\frac{2}{3}
\end{aligned}
\tag{3.2}
$$

3.7.3 Attenuation

$$
att[dB] = 20 \times \log \frac{B}{A} \tag{3.3}
$$

3.7.4 High Impedance

$$Z_{high} = \left(\frac{A}{B} - 1\right) \times 100 \tag{3.4}$$

3.7.5 Low Impedance

$$Z_{low} = \frac{25}{\frac{A}{B} - 1} \tag{3.5}$$

3.8 Investigation in High Voltage RF Measurment

A project investigated `EMI` susceptibility of high voltage ESD protection structures. In this context the question arised, whether the voltage applied to the device under test can be measured with available equipment. The problems of such an experiment are the unmatched circuitry and a very broad frequency range. The frequency range of interest was above 200 MHz. In theory it is possible to use active probes for low influence of the signal path. Due to DC bias voltages up to 40 V and the AC test voltages up to 22 V the available active probes HFP1500 can not be used. The results of investigation on different voltage divider explained the invalid measurement results. However, it was not possible to find an alternative voltage divider, that covers the region of interest, regarding voltage and frequency. However, an alternative solution would be the usage of the URV5-Z7 voltage probe and the appropriate measurement device (NRVD or URV5). Due to its DC tolerance and input voltage range this probe would fulfil the requirements mentioned above. Unfortuntely, a limitation is, that the time response of the signal can not be analysed with this measurement hardware.

3.8.1 Calibration of Active Probes HFP1500

In a first step the two active probes were tested. The achieved results showed significant differences depending on signal strength, frequency of the test signal and the probe used. With the help of a self made adapter as shown in Figure 3.19 it is possible to calibrate the two active probes. The adapter is mounted in the described attenuation test bench. As a result it is possible to get the attenuation caused by the probe. In addition the voltage measured from the probe and the reference signal voltage measured by the power meter or by a 50 Ω port of the oscilloscope is available. This allows the calculation of the relative measuring error and thus enables a calibration.

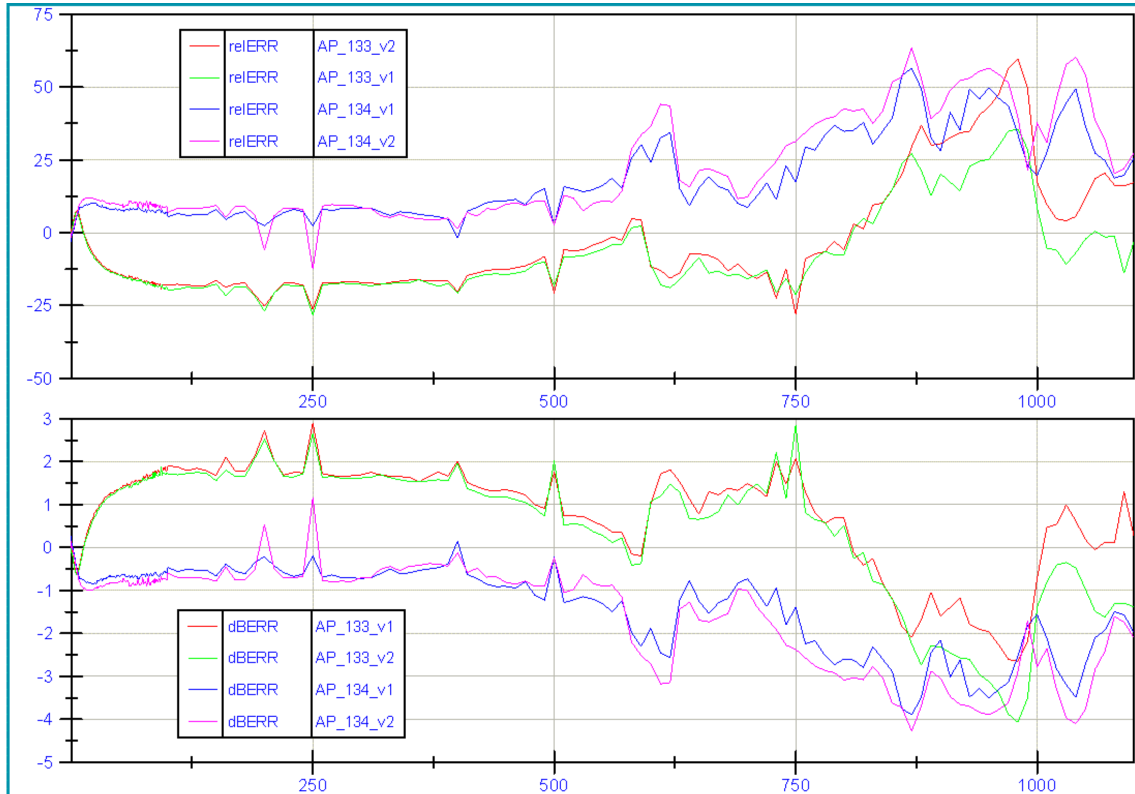

Figure 3.18: Calibration of Active Probe Heads HFP1500, SN00133 and SN00134 for the LeCroy WavePro 950 oscilloscope.

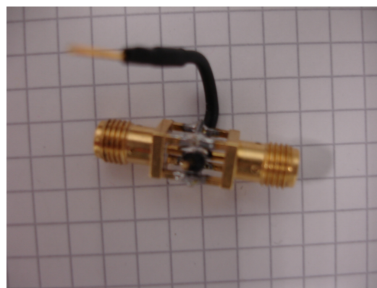

Figure 3.19: `SMA` to HFP1500 Adapter

Chapter 4

EMC Characterisation on Chiplevel

Contents

4.1 Workflow of a DPI measurement 38

4.2 Existing DPI Setup 38

4.3 Optimisation of the DPI Setup 41

4.4 Existing Control Software 55

4.5 Optimisation of the Control Software 59

4.6 Example Measurement 63

In the previous chapter an attenuation measurement setup was developed and tested. Based on this work, the DPI measurement setup can be verified according to the IEC standard. The current chapter summarizes the equipment which has been used and introduces further improvements regarding coupling and decoupling networks. The software of the `DPI` measurement process is described and modifications to enable e.g. more reasonable frequency intervals, automated reset, and more extensive monitoring of the DUT are mentioned. The functionality of the modified setup is shown by presenting the results of `DPI` measurments at two magnetic rotary encoder `IC` .

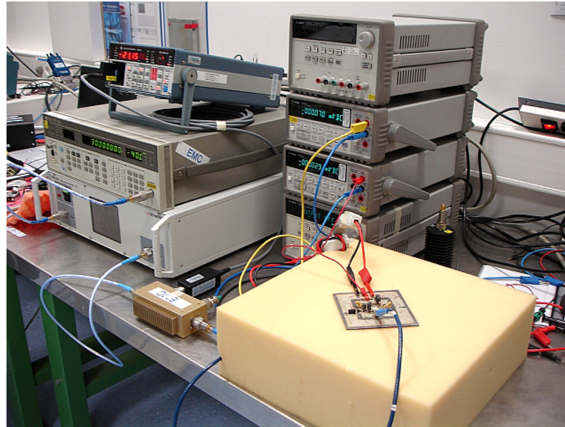

Figure 4.1: DPI Setup as utilized in this work. Please refer to the text for an comprehensive description of the hardware.

4.1 Workflow of a DPI measurement

Typical DPI software starts at the lower end of the frequency range (in this work 150kHz) and increases the power applied to the device under test until a pre-specified threshold has been reached. Subsequently, after exceeding this threshold, the frequency is increased and the test is restarted beginning at the lowest power level.

As a result, the immunity level, which is the maximal forward power level without failure of the IC is determined. The information of this test is used to check, whether the defined failure criteria is meet. However, the definition of the failure criteria is non-trivial and subject to device specifications as well as tolerance definitions.

4.2 Existing DPI Setup

This section contains the measurements hardware/equipment (Fig. 4.1).

- HP Signal Generator 8657B 0.1 - 2060MHz
- Schaffner Power Amplifier CBA 9479
- Power Meter NRVD, NRV-Z51, NRV-Z4
- Millivoltmeter URV5, NRV-Z5
- Agilent E3631A Power Supply

- Weier Electronics W30 Power Supply
- Agilent Digital Multimeter 34401A
- Werlatone 30dB Dual Directional Coupler
- Set of sub miniature version A (SMA) cables and adapters
- Individual Test Board

The DPI setup utilized in this work uses a forward power regulation to compensate the output characteristic of the signal generator, the amplifier and the insertion loss of the used SMA cables. The measurement hardware for the test signal generation involved in the power regulation loop is shown in Figure 4.2.

The power sensors used with the power meter, measure the mean power at the directional coupler. Using diode power sensors in the setup with AM test, the RMS range has to be respected as listed in chapter 3.4.2. To achive the same peak voltage level for CW and AM the DPI test power has to be reduced by -3.9 dB. If a spectrum analyzer ist used to measure the forward power of the AM signal, the measured power level is reduced by -5.1 dB because of the energy transmitted in the sidebands of the AM signal. In a setup without power regulation loop, but with a calibrated signal path, the signal strength of the signal generator should be reduced by -5.1 dB, too [19], [16]. The same holds true for manual measurements, if the test signal is changed from CW to AM at the signal generator [7],[22]. Given the same peak voltage level for CW und AM this can be summarized as shown in (4.1-4.2).

$$\begin{aligned} V_{AM_{peak}} &= V_{CW_{peak}} \\ V_{AM} &= 20 \times \log(1+m) = 20 \times \log(1+0.8) = 5.1dB \\ V_{AM} &= V_{CW} - 5.1dB \end{aligned} \tag{4.1}$$

$$P_{AM} = P_{CW} \times \frac{2+m^2}{2(1+m)^2} = P_{CW} \times 0.407 = P_{CW} - 3.9dB \tag{4.2}$$

4.2.1 Directional Coupler

The measurement parts in the setup allow EMI tests even above 1 GHz. The frequency range oft the signal generator limitate test signals up to 2 GHz. The behavior of the directional coupler gives a limit at 1.8 GHz. However, as the device is specified for a frequency range of 0.01-1000 MHz only, degradation of SWR and coupling characteristic

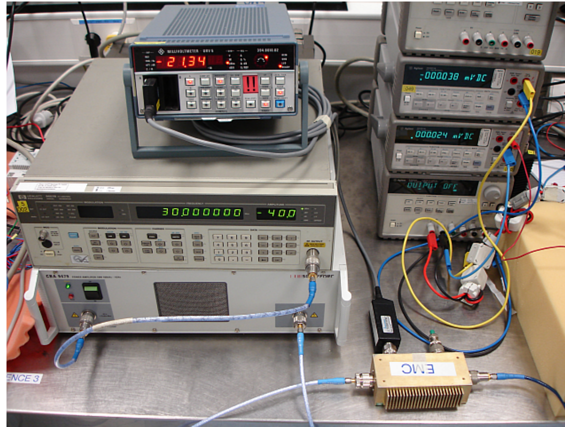

Figure 4.2: Test signal generation block of DPIshort setup, showing the signal generator, the amplifier, the directional coupler with connected power sensor and URV5.

above the nominal frequency range has to be observed. The real insertion loss and coupling behavior was determined and is shown in Figure 4.3.

4.2.2 Test Board and Wiring

The disturbance forward power from the output of the directional coupler is injected to the DUT through a further SMA cable, the injection port and the coupling path on the test board. The allowed insertion loss of the coupling path ist given in the IEC 62132 with at most -3 dB. However, even the SMA cable used to interconnect the disturbance power source and the test PCB causes an attenuation. Thus, the cable length and quality influence the real disturbance power applied to the DUT . SMA connectors are sensitive to tightening torque. Weak fastening causes higher insertion loss and reflection. However, too high fastening torque can damage the SMA connector. For reproducibility an adequate torque wrench should be used for the cable connections in the setup, especially for the connection between testboard and the directional coupler.

To achive reproducibility and full documentation each part of the equipment was labeled clearly. The insertion loss of the used SMA cables was determined.

While in house knowledge for electromagnetic emission (EME) methods (TEM cell, Surface scan,...) is well established, the DPI setup for EMI susceptibility characterisation is fairly new [16][5]. However, influence of test PCB and test equipment to test results are known [19].

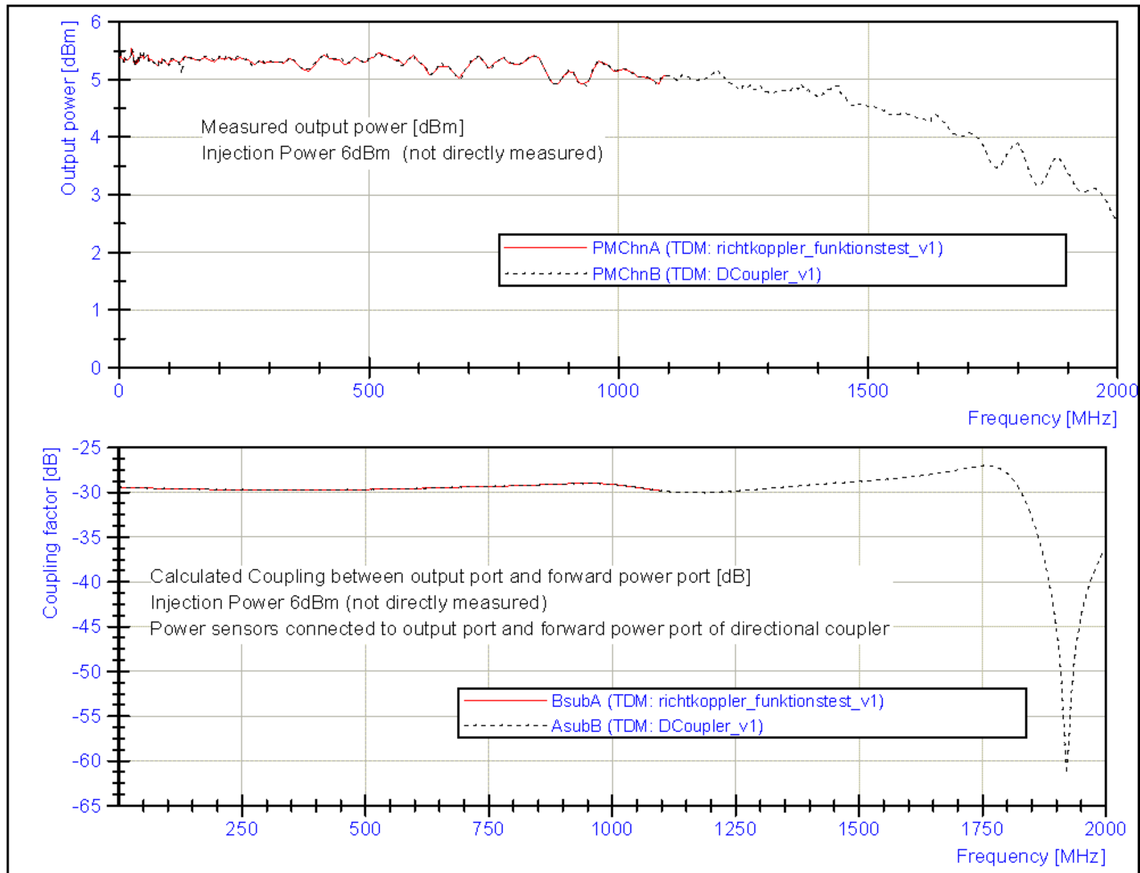

Figure 4.3: Coupling factor and insertion loss characteristic of Werlatone 30 dB Dual Directional Coupler 0.01-1000 MHz, measured with the attenuation measurement setup show the possibility of higher frequency measurements.

4.3 Optimisation of the DPI Setup

Based on the recommendation of the IEC standard, first test measurements on ICs showed that the dimensioning of the coupling capacitors were not adequately to achieve sufficient power at the DUT . Therefore, several coupling capacitors as well as the impact of the PCB design were evaluated. Different ferrite beads and power inductors were tested and measured regarding their capability to decouple the power supply from the RF circuit. However, the standard defines a minimum impedance of 400 Ω, but the DC impedance is requested to be as low as possible.

4.3.1 Coupling Network

The choice of the coupling capacitor for the DPI test setup has significant influence to the test results. If a supply pin is tested, the applied power is reduced by the frequency depending voltage divider formed by the decoupling network. If a single pin is tested, the same problem arises because of parasitic capacitances of the PCB . To avoid too high influences on the test results, the standard allows a deviation between disturbance input port and IC pin of -3 dB over the whole frequency range. This verification shows test board design failures like resonances caused by bad ground planes or too long signal traces. The coupling path is tested in a 50 Ω measurement system like the described attenuation measurement setup, vector network analyzers or equivalent setups. In a simplified view the coupling capacitor acts as DC block and forms a high pass filter with the 50 Ω measuring resistor. This high pass should have a cut off frequency of 150 kHz. Otherwise even low frequency distortion signals can be applied to the test setup and may cause failures not induced by the high frequency disturbances. Using coupling capacitors with higher capacitances would lead to more stress for the DUT . Calculating the smallest capacitance that fulfils the requirements, follows in the usage of a 22 nF coupling capacitor.

At old test boards different coupling capacitors were found. Used configurations are 2.2 nF || 100 nF, 6.8 nF, 4.7 nF and for a project with very sensitive test object in the lower frequency range 4.7 pF. In the IEC 62132-4 from 2006 a default capacitor value of 6.8 nF and a default resistor value of 0 Ω is mentioned in Chapter 4.2. In addition, the IEC 61967-4 and Annex A is referenced. This chapter describes coupling and matching networks for the 150 Ω method. In the corresponding table a coupling capacitor of 6.8 nF for a cut off frequency of 174 kHz is given. However, this value is given for the 150 Ω measuring circuit.

Measurements on coupling paths showed an attenuation of -1 dB at 500 kHz and -2.4 dB at 300 kHz for a 6.8 nF capacitor. Nevertheless the attenuation is lower than it should be. Without parasitics the simulation and calculation result in -2.7 dB at 500 kHz and -10 dB at 150kHz. Later done investigation on appropriate parts for the coupling path gave nearly the same results. Thanks to the possibility to start the frequency sweep at 100 kHz it could be shown, that the approximations of the results, achieved with an other setup starting at 300 kHz, were wrong. Using a 6.8 nF capacitor is not practicable because it cause a attenuation of more than the allowed -3 dB at 150k Hz. Considering this results, the recommanded default capacitor value of 6.8 nF as mentioned in the IEC 62132 part 4 (direct RF power injection method) chapter 4.2 should not be used for common test

setups.

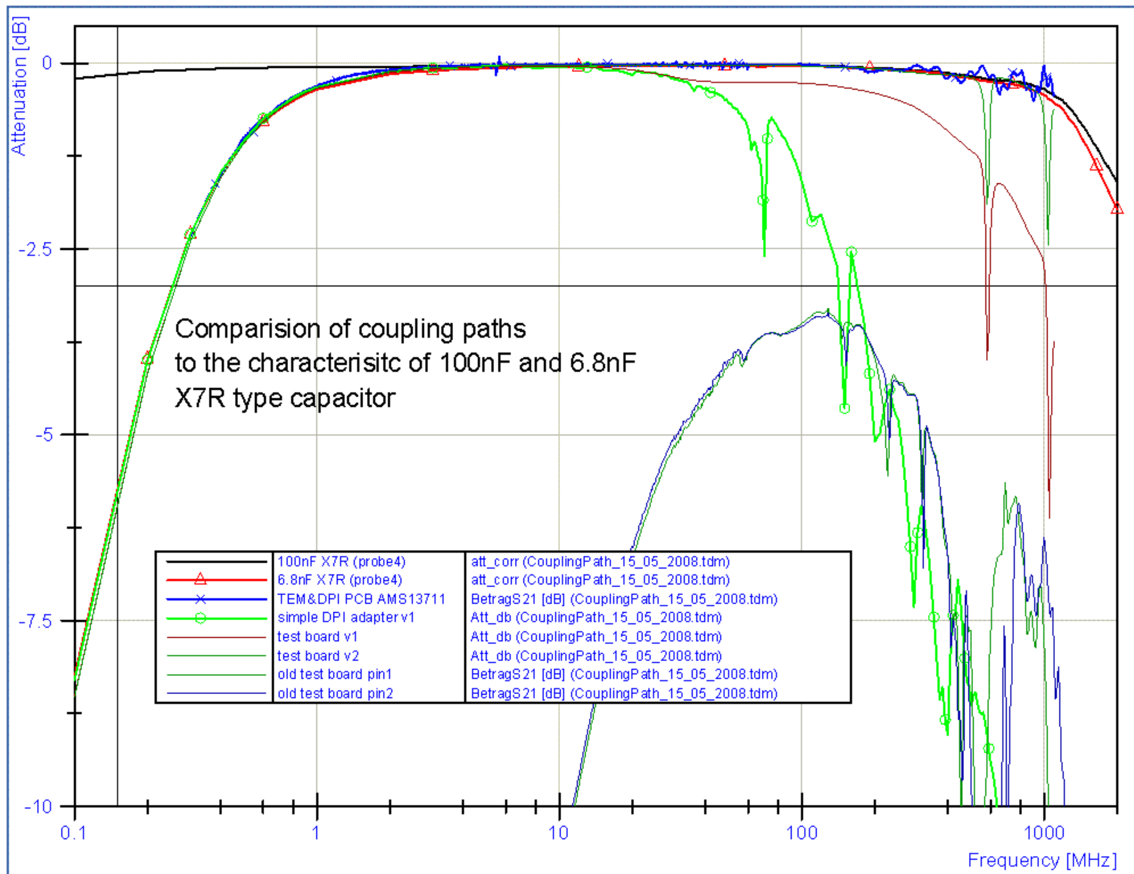

Figure 4.4: Insertion loss of existing test board coupling paths compared to coupling capacitors mounted in ”Probe4”

Another question is about the design of the coupling path. In the current version of the corresponding standard layout examples are shown. They show the RF connector on the bottom side. The parts of the coupling network should be placed as close to the test pins as possible. The coupling path length should be less than 1/20 of the shortest wave length. For test setups up to 1 GHz this is only about 15 mm. The signal traces from the injection port to the DC block capacitor should be 50 Ω traces. Otherwise it has to be as short as possible too. In the end, the whole signal path form injection port to test pin has to fulfil the requirement of less than 3 dB attenuation. To save space it is possible to use one injection path and coupling capacitor for multiple pins by using a 0 Ω resistor to select the pin to test. To change the test setup there is the need of soldering the resistor, acting as a jumper, to other positions. This solution is used to cover more IC pins at the

universal test board (Fig. 4.5).

The used RF-connector type should match to the available equipment. In this case most equipments use N-type or SMA connectors. The SMA connector is a good compromise between used board space, stability and handling. However, in some cases the smaller SMB connector are needed. It is necessary to resume sufficient space on the board layout, since the SMA cable need a torque wrench to be fastened to the connector. This and the cable junction needs more space than the footprint only.

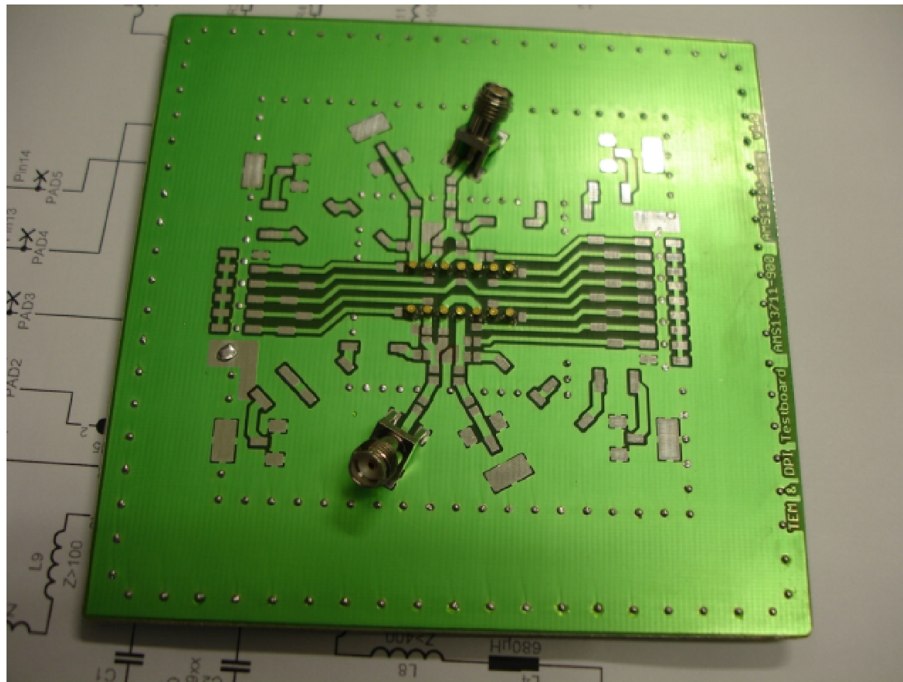

Figure 4.5: The images show a unassembled test board for DPI and TEM method. Two SMA connectors are mounted in 45° technique. The coupling path show footprints to select between two input pins.

4.3.2 Decoupling Network

The decoupling network is responsible for two things. First it has to guarantee that the injected power is really applied to the IC pin. Using a decoupling filter with less impedance, most energy is deflected by the cable harness and power supply but not injected to the DUT . The IEC 62132-4 specifies an impedance of 400 Ω as minimum. Second, it shields power supply or measurement devices against high frequency disturbances. This is essential for proper operation of the automated error detection. In some cases there would be the need of a second filter stage to protect the instruments and guarantee signal analysis without

influences from the test signal. The influence of the filter to the test results depends on the impedance ratio of test pin and decoupling network. We require a well defined decoupling network with a smooth and constant impedance curve. Anyway, it is up to the operator to use a higher impedance decoupling network, probably to achieve more stress for the DUT or to obtain a better decoupling of power supply or measuring device.

The decoupling network used so far occupies a high amount of space on the test board and does not perform that well, which is why an investigation on alternative solutions was started. The main goal was to improve decoupling at higher frequencies, achieve a smoother characteristic and to shrink space. As known from developing and testing of the attenuation setup, the decoupling filter presented in [8] comes with a better performance. A comparison is shown in Figure 4.6. In the 50 Ω measurement setup a 400 Ω impedance cause an attenuation of -13.9 dB.

$$\begin{aligned} Z_{high} &= \left(\frac{A}{B} - 1\right) \times 100 \\ att[dB] &= 20 \times \log \frac{B}{A} \\ \frac{Z[\Omega]}{100} + 1 &= 10^{\frac{|att[dB]|}{20}} \\ att[dB] &= 20 \times \log \left(\frac{Z[\Omega]}{100} + 1\right) \end{aligned} \tag{4.3}$$

4.3.2.1 Ferrite Beads

The used decoupling network consists of three 6-hole ferrite beads. Each one came with different windings that result in different filter characteristics. Together they cover the hole frequency range from 150 kHz up to 1 GHz. For other projects there was the need to cover the frequency range up to 2 GHz and higher. To find other filter solutions a survey on SMD ferrite beads and existing 6-hole beads with different windings and materials was started.

In the following diagrams (Fig. 4.14-4.19) the naming convention count of windings and material type or product number of manufacturer is used. For example 3W_1200 stands for a 6-hole ferrite bead of material type 1200 with 3 windings as mentioned as 3 turns vertical in the product catalogue from *Würth Elektronik* or in [9]. However, the 2x1 turn vertical type is used as two parallel turns in this work and called 0.5W. The winding patterns are illustrated in Figures 4.7 to 4.13.

The first measurement series should be based on the *Würth Elektronik* 742750-4 ferrite

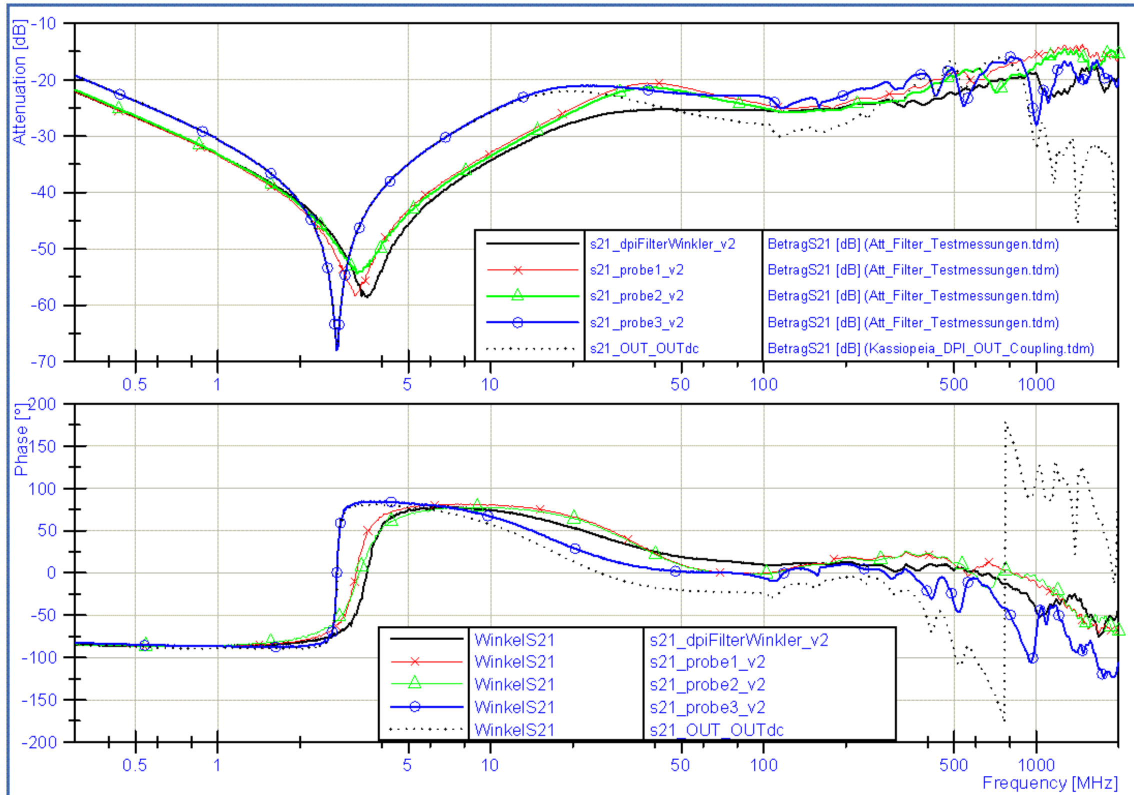

Figure 4.6: Comparision between known decoupling networks.

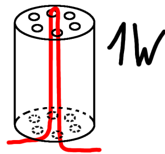

Figure 4.7: Ferrite Bead with 1 Winding

with core material type 1200, but the results show characteristics of different material types. However, the results show the functionality of the new built up measurement setup. It also gives an overview of the possible filter characteristics that can be achieved by adjusting winding count or changing the core material.

Corresponding to the values given in the data sheet, the highest filter impedance is achieved in the frequency range near 100 MHz. With less winding the filter can be used at higher frequencies. At lower frequencies the different material types shows significant different characteristics. For frequencies below 10 MHz the filter impedance become very

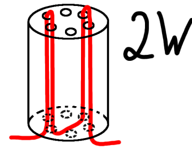

Figure 4.8: Ferrite Bead with 2 Windings

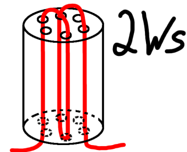

Figure 4.9: Ferrite Bead with 2 Windings, old Edition

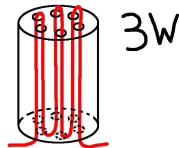

Figure 4.10: Ferrite Bead with 3 Windings

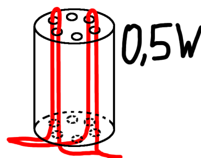

Figure 4.11: Ferrite Bead with 2 parallel Windings

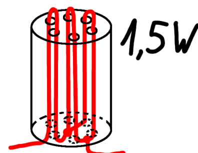

Figure 4.12: Ferrite Bead with 1 + 2 parallel Windings

small.

Figure 4.14 shows that some 6-hole ferrite configurations can achieve the wanted 400 Ω impedance up to 1 GHz. Figure 4.15 shows that the same ferrites perform well, down to 30 MHz. So it should be possible to find a filter configuration that works above 1 GHz or to reduce the amount of components for the current filter. Since the material type of

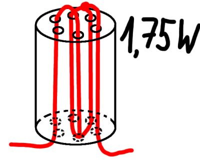

Figure 4.13: Ferrite Bead with 1 + 2 half parallel + 1 half Windings

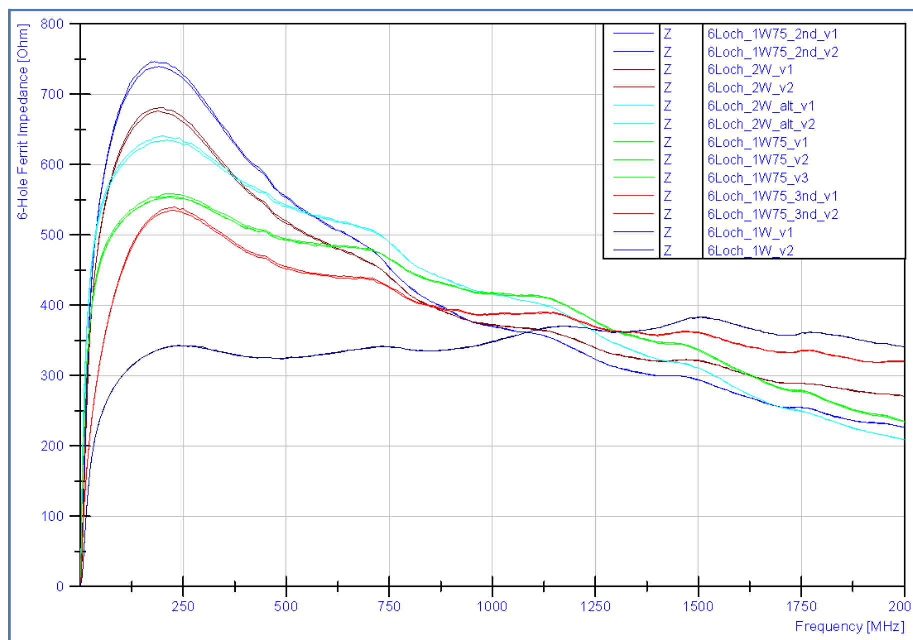

Figure 4.14: 6-Hole Ferrite Bead Comparison 1, with different winding patterns and material types in linear view

some ferrite cores was not known correctly, a second measurement series with new samples was done. Each measurement was done with at least two samples of each material and winding type. This results are shown in Figure 4.16- 4.19

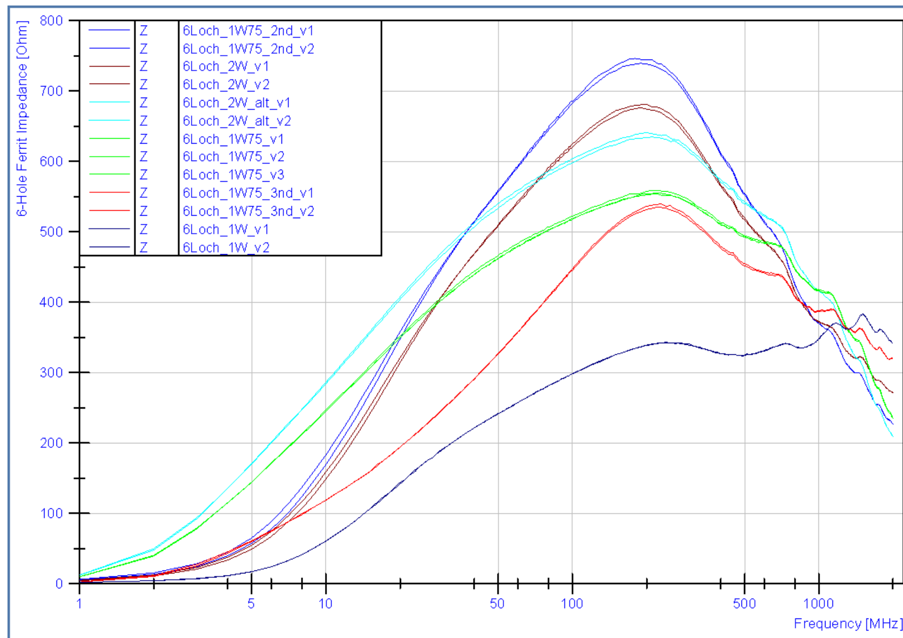

Figure 4.15: 6-Hole Ferrite Bead Comparison 1, with different winding patterns and material types in logarithmic view

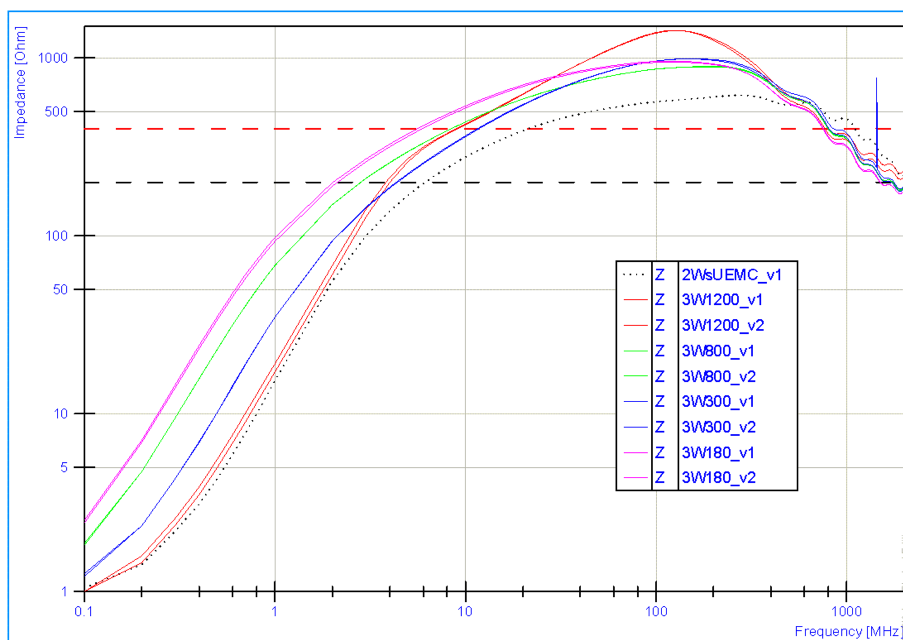

Figure 4.16: Ferrite Bead Comparision with 3W winding and different core materials.

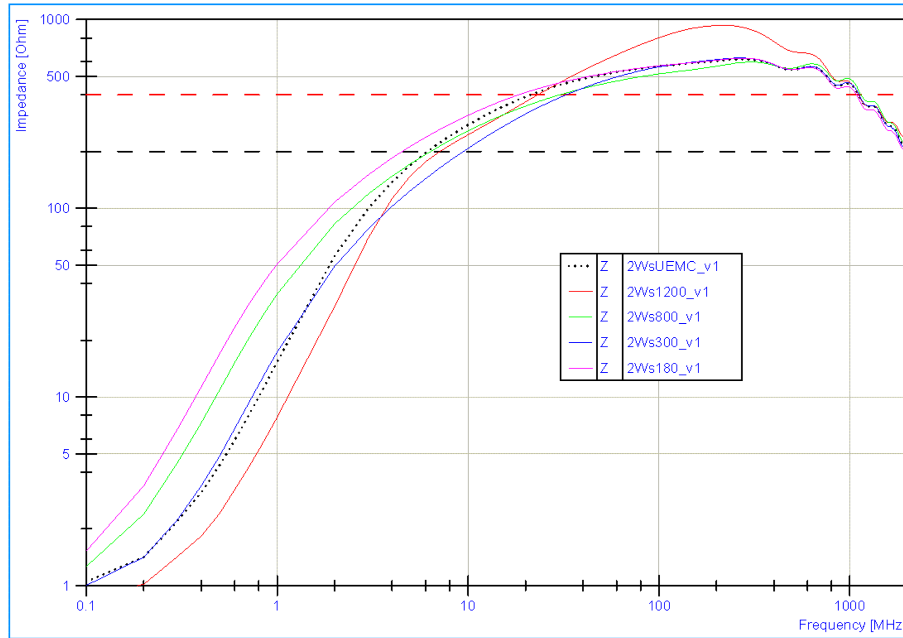

Figure 4.17: Ferrite Bead Comparision with 2Ws winding and different core materials.

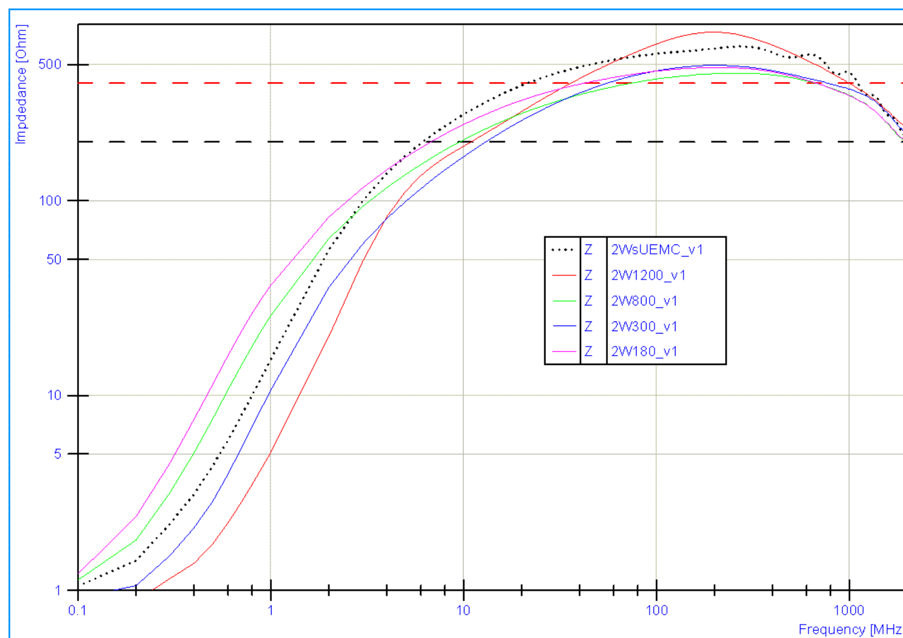

Figure 4.18: Ferrite Bead Comparision with 2W winding and different core materials.

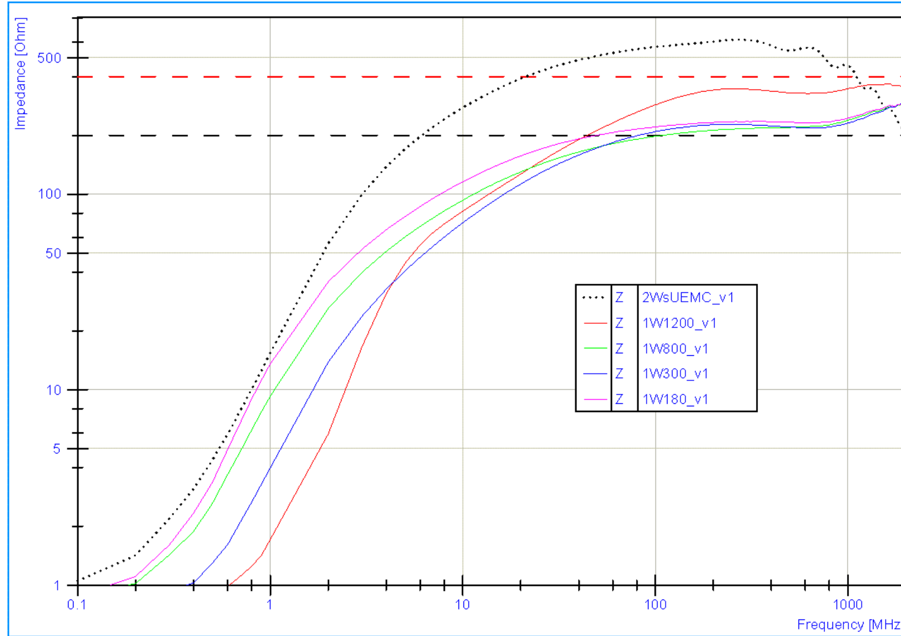

Figure 4.19: Ferrite Bead Comparision with 1W winding and different core materials.

4.3.2.2 Inductors and SMD Ferrites

As known from existing setups, power inductors in the range of 400 μH can achive the required decoupling impedance. These inductors can cause problems because of the high inductivity. So we investigate for other appropriate parts. Available SMD ferrites came with the same limitation as the 6-hole ferrites. However, both types can be used for decoupling networks above approximately 20 MHz. For the lower frequency range no alternatives for the power chokes were found.

Farnell 1636097	Würth Elektronik	74454268	WE-PD3	680 μH
Sample	Würth Elektronik	74451268	WE-PD3	680 μH
Farnell 1636107	Würth Elektronik	74459247	WE-PD3	470 μH
RS 432-4401	Würth Elektronik	744772101	WE-TI	100 μH
RS 432-4546	Würth Elektronik	744772221	WE-TI	220 μH
RS 489-0087	Würth Elektronik	744743221	WE-TI	220 μH
RS 488-9958	Würth Elektronik	744741471	WE-TI	470 μH

Table 4.1: Inductors

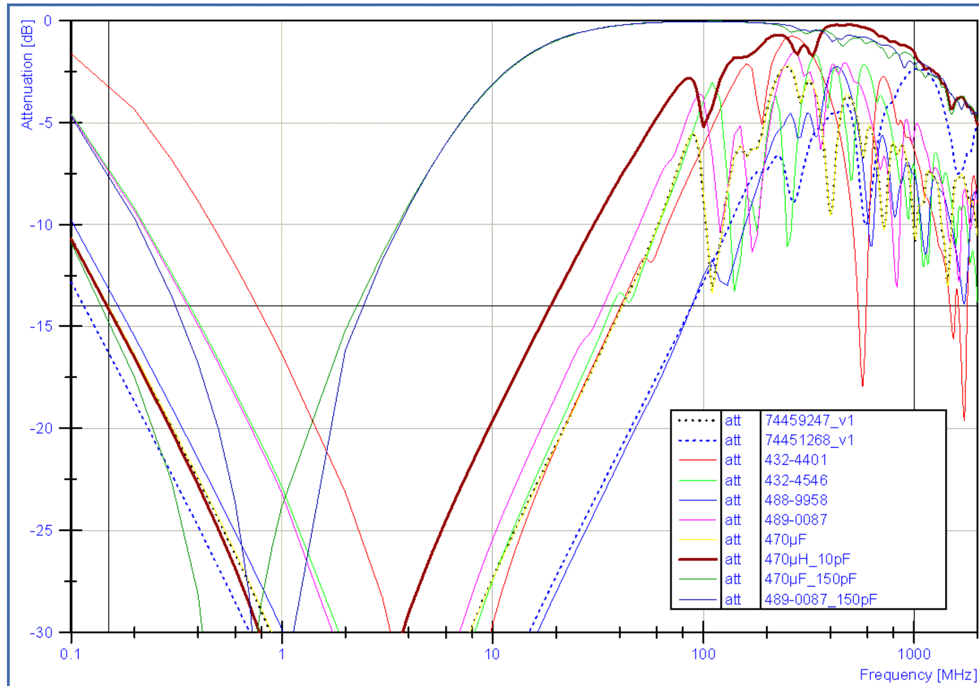

Figure 4.20: Inductor Comparision to find parts for decoupling in the low frequency range.

The parts were mounted on small adapter boards or between two `SMA` connectors, as shown in Figures 4.21, 4.22, 4.23, 4.24.

Figure 4.21: Decoupling Network (Fig. 4.6) mounted in a simple Adapter Board, called Probe 1 or Probe 2.

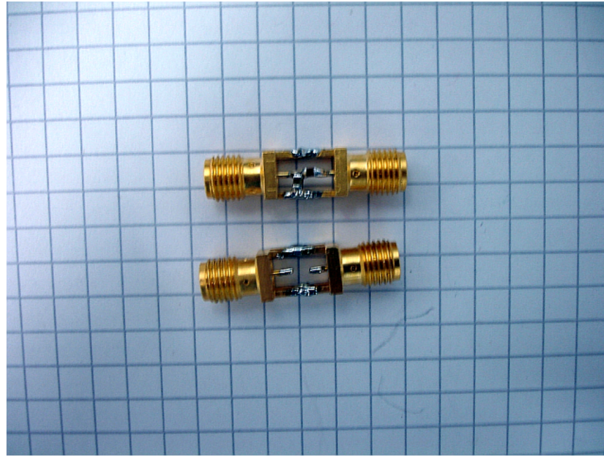

Figure 4.22: Coupling Capacitance mounted a in Adapter consisting of two SMA connectors, called Probe 4.

Figure 4.23: Decoupling Network mounted in a simple Adapter Board, called Probe 3.

4.3.3 Minimalistic DPI Adapter

In some cases it is helpful to have measuring equipment, which allows investigation on EMC weakness at a common PCB , like evaluation boards or prototypes. The measurement setup for standard DPI testing can be used to inject disturbances into nearly any kind of electric circuit. In combination with other methods, a critical group of components can be identified. To achieve a good reproducibility and avoid problems with the mechanical interface, an adapter board was developed. Main function of the board is to allow thin and elastic connection to the circuit board or DUT , but offer default and mechanical robust connection options for high frequency injection and power supply. To achieve this,

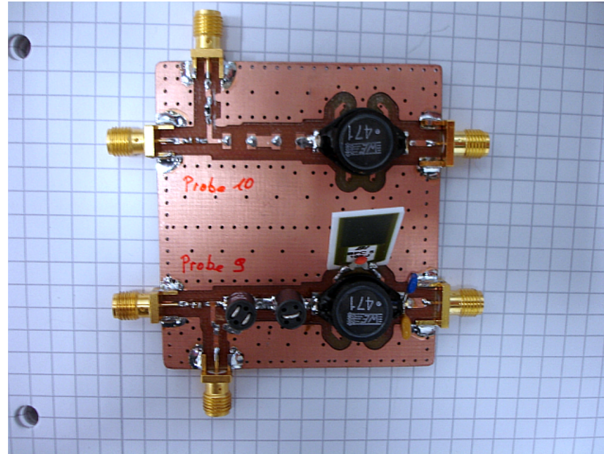

Figure 4.24: Coupling and Decoupling Networks on Adapter Boards, called Probe 9 and Probe 10.

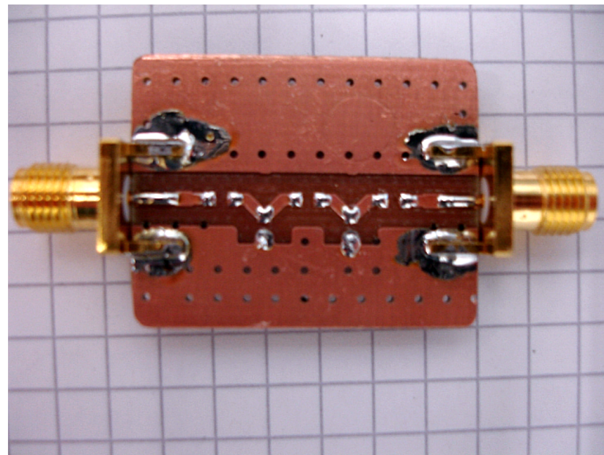

Figure 4.25: Adapter Board for SMD filter parts testing, called Probe 6.

footprints for coupling capacitor, decoupling filters, banana plugs and SMA connectors are combined to a small adapter board and optimized in several iterations with respect to the guidelines, given in the IEC 62132. The adapters were used for evalution of input output (IO) structures, bondet to ceramic prototype packages. The characteristic of the coupling path ist shown in Figure 4.29. The finally used version had a well defined coupling path up to 1 GHz (Koppelstrecke_Adapter3).

The evalution of the two adapter boards (Fig. 4.27, 4.28) show an influence of the coupling path caused by parasitics of the decoupling path. While each testet configuration have an attenuation less than 3 dB up to 2 GHz, different characteristics can be measured. They depend on the used filter parts. The prefered parts are a 3W1200 ferrite, followed

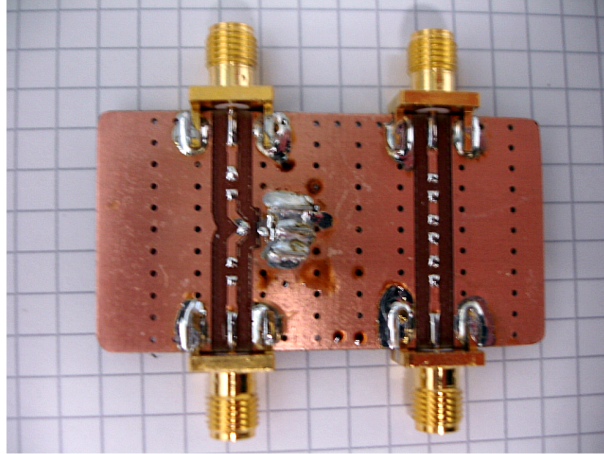

Figure 4.26: Adapter Board for SMD filter parts testing, called Probe 7 and Probe 8.

by a 0.5W1200 ferrite and the 470 μH, optionally bypassed with a 1 kΩ resistor. However, also the combination of a 2W180 and a 1W180 ferrite show a good performance. If there is no need to use the decoupling network, it should be disconnected to reduce parasitic effects. The coupling path characteristic is shown in Figure 4.30.

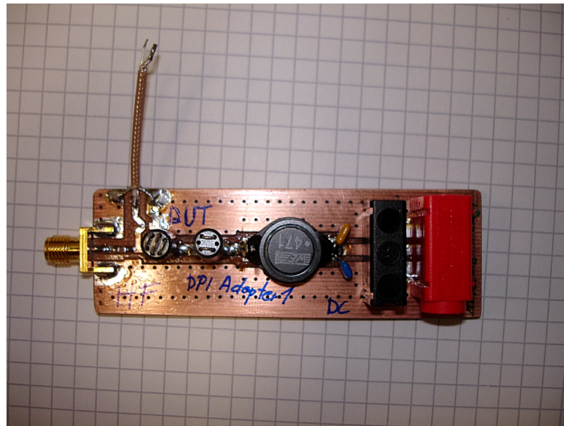

Figure 4.27: DPI Adapter with decoupling network and a standard conform coupling path characteristic.

4.4 Existing Control Software

The existing control software (Fig. 4.31) was developed in-house [16][19] and was already adapted to further projects. The control software support the power meter NRVD to achieve a power regulation. The mentioned measuring algorithm for DPI testing (2.6) is

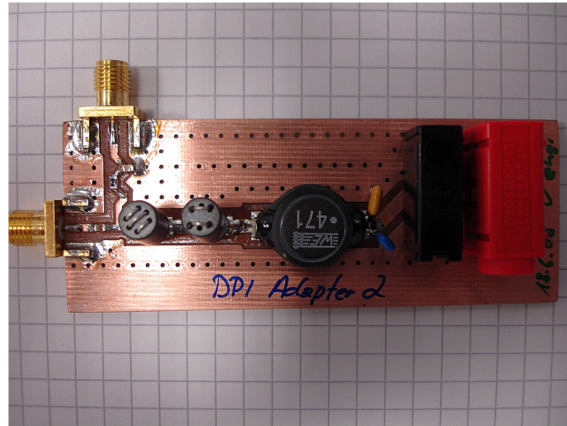

Figure 4.28: DPI Adapter with decoupling network, optional footprints for the purpose of filter parts testing and a standard conform coupling path characteristic.

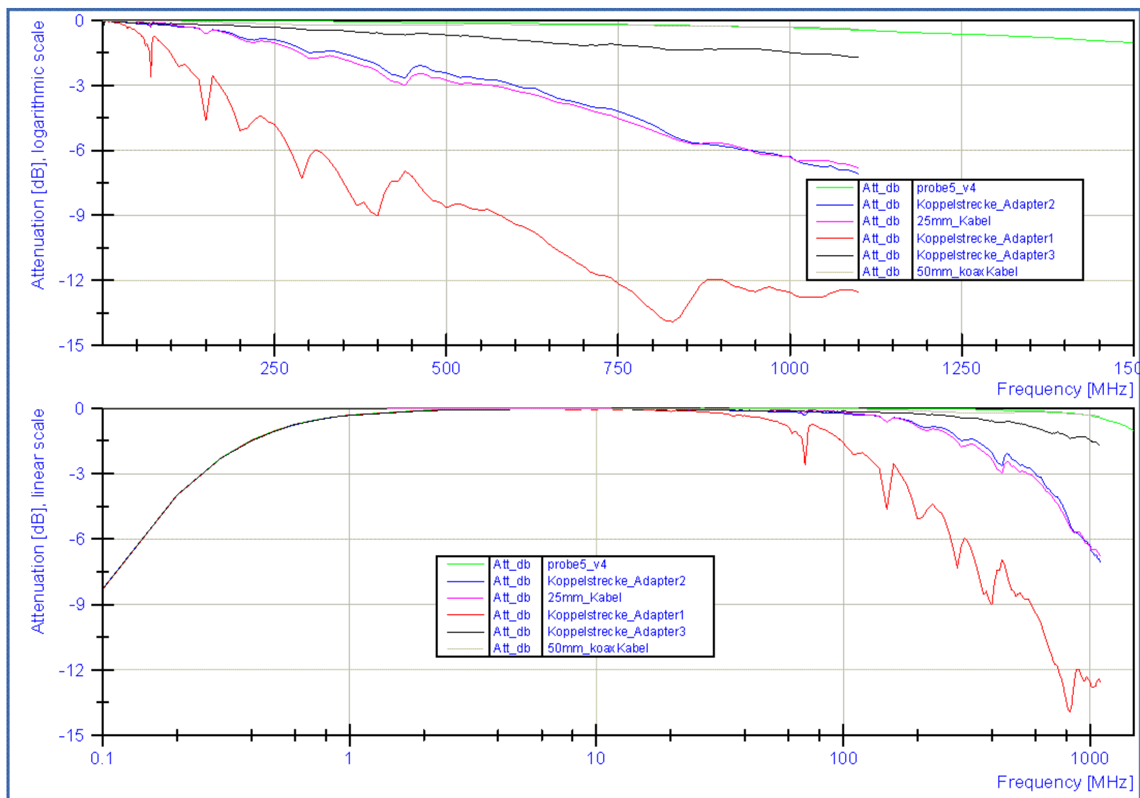

Figure 4.29: Comparison of the coupling path attenuation of different DPI Adapters, compared to the insertion loss, caused by a piece of twisted pair wires with a length of 2.5 cm, a piece of coax wire with the length of 5 cm and a 6.8 nF capacitance mounted in two SMA connectors.

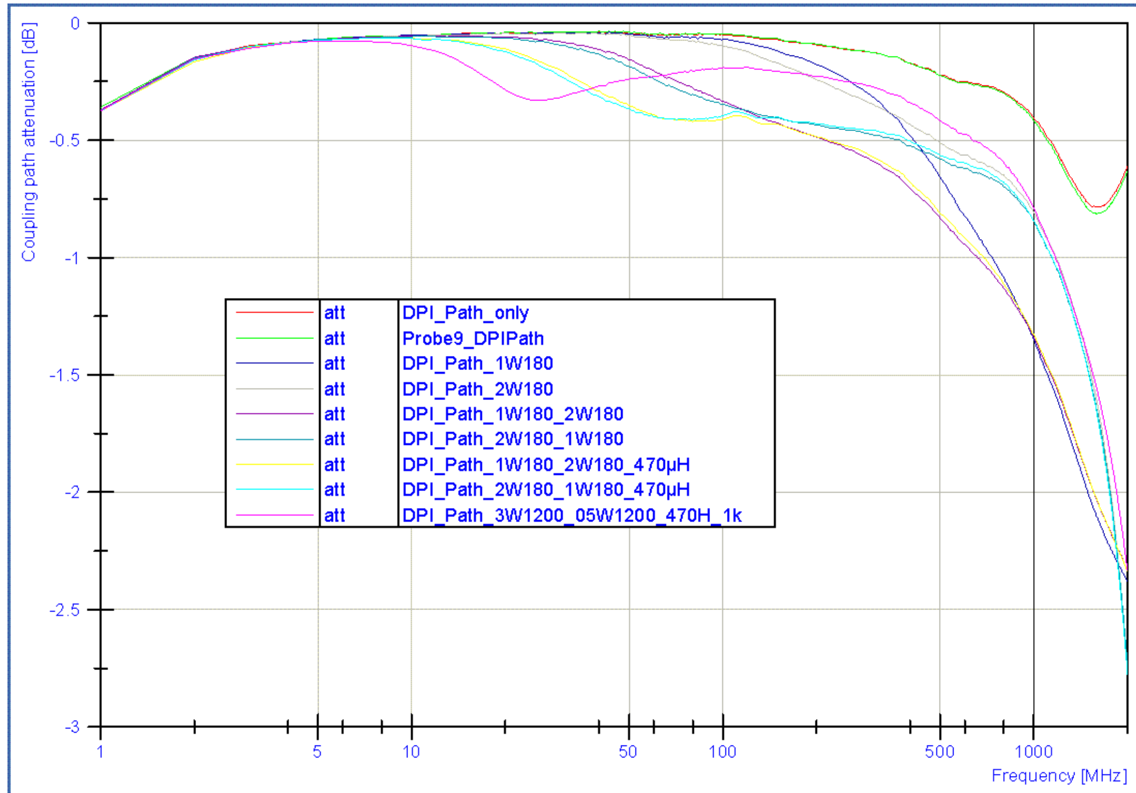

Figure 4.30: Comparison of the coupling path attenuation of the Minimalistic DPI Adapter Bords depending on the used decoupling networks.

implemented. It support voltage reading by a GPIB compatible multimeter to monitor a failure criteria. The test results are written to a log file and visualized during measurement.

In the configuration tab the test power range is spezified by the input fields *Upper Power Limit [dBm]* and *Zero Power [dBm]*. The parameter *Delta Start Power [dBm]* defines the amount the disturbance power is reducued by, after reaching the power limit or failure criteria. *Power Tolerance [dBm]* defines the accuracy of the power regulation loop. The amount of the forward power is increased during each frequency is defined in *Stepsize Power [dBm]*. The power levels given, comply with the reading of the power meter. Thus, the coupling characteristic of the directional coupler (-30 dB), has to be considered. *Start Frequency [MHz]*, *Stop Frquency [MHz]*, *Stepsize Frequence [MHz]* set the frequency range oft the measurment. The dwell time is configured by the paramter *Wait [ms]*. The tool can be used to do IC characterisation according to the DPI or the TEM cell method.

The graphic representation (Fig. 4.32) of the measuring results show two plots. The

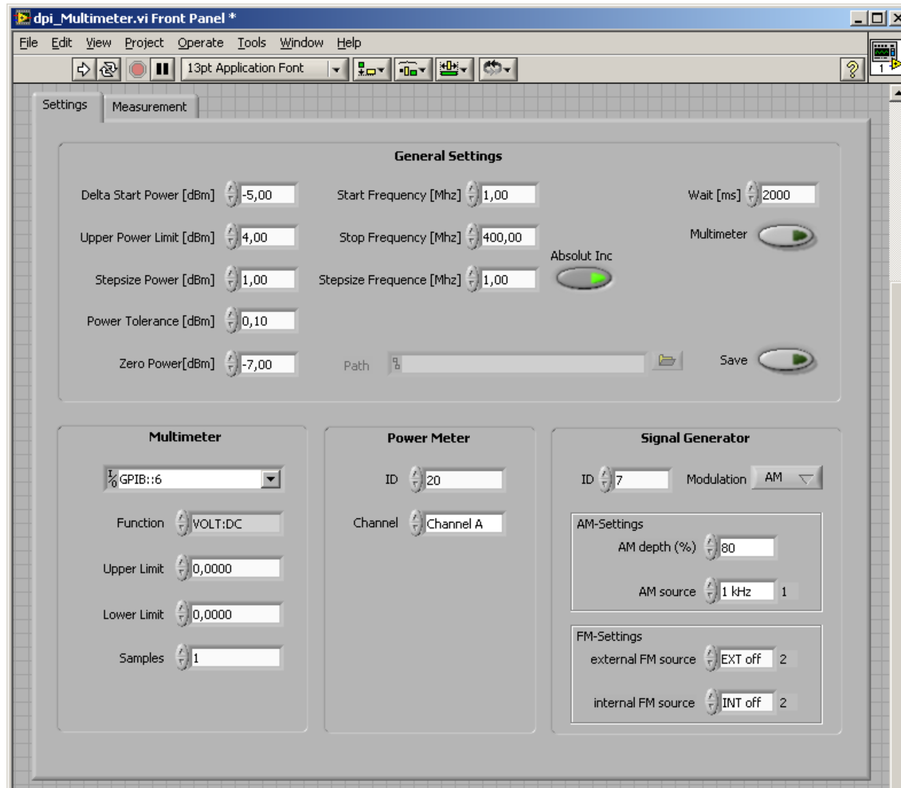

Figure 4.31: Screenshot of the existing DPI LabVIEW control software, showing the test configuration tab.

red histogram shows the highest power level of the disturbance signal, the DUT was still working within the specified tolerance. The white line represents the failure criteria. In this case it is a DC output voltage of the DUT with a value of 2.15 V. The power level of the test signal is shown without correction of the -30 dB offset, caused by the directional coupler. The value of 7 dBm correspond with the maximum value of 5 W (Fig. 2.1). The diagramm show that the DUT ist sensitive to EMI at frequencies higher than 100 MHz and fail above 250 MHz, even at the lowest configurated test power, in this case -20 dBm.

However, this result does not show the real behavior of the DUT . The setup was not able to recognize the device malfunction that remain after reducing the disturbance signal. So the diagram contains the information, that the DUT has a good immunity against EMI in the frequency range lower than 100 MHz, showing the performance of a class A device. For frequencies up to 250 MHz, the DUT show a class B or class C performance. Above 250 MHz the DUT show a class D performance and does not recover from malfunction until a reset. Thus the limits for the failure criteria are exceeded even with the minimum test

power applied to the DUT . To determine the behavior oft the DUT further measurement, restarting at the frequency the first class D malfunction has occured first, has to be done. The configurated power step size, the frequency step size and the defined tolerances of the failure criteria influence the apperance of such a broken measurement cycle. Nevertheless, it shows a weakness of the DUT and the need of further investigation.

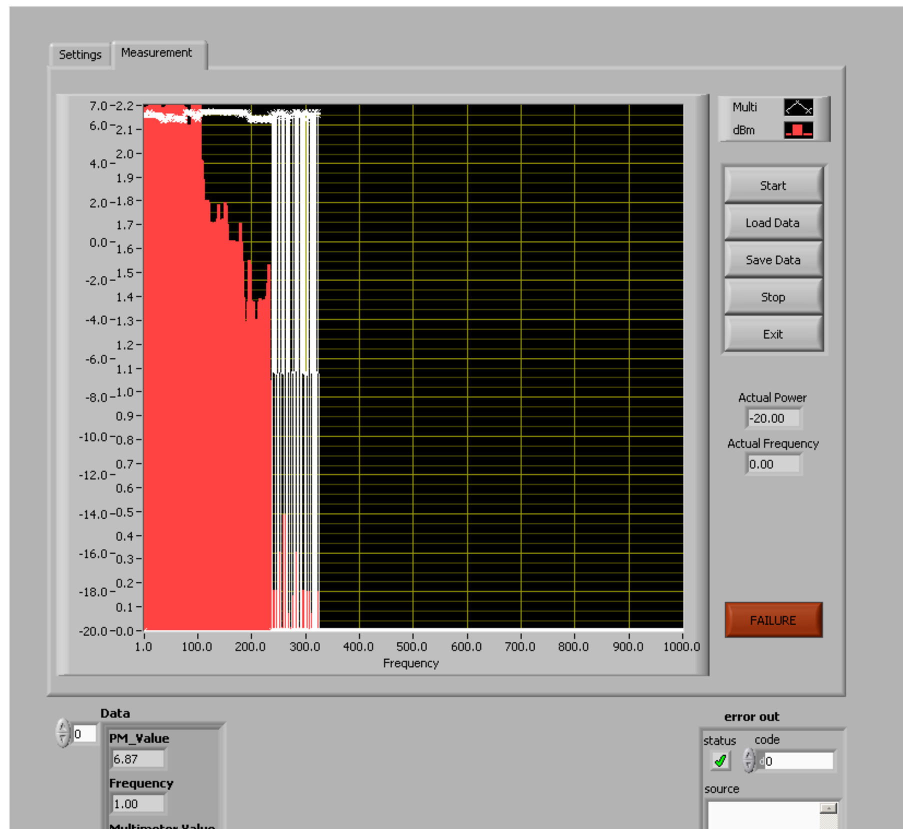

Figure 4.32: Screenshot of the existing DPI LabVIEW control software, showing the test result of an aborted test run.

4.5 Optimisation of the Control Software

The existing software was extended to enable e.g. more reasonable frequency intervals (Table 3.1, 3.2), automated reset, and more intelligent monitoring of the DUT . Additionally, documentation and logging capabilities were added. The existing software was extended by the following features:

- automated reset

- frequency steps and range
- log file structure
- power supply suport
- URV5 support
- zero power correction

The main changes on the measurement routine, done to support this features, are shown in Figure 4.33.

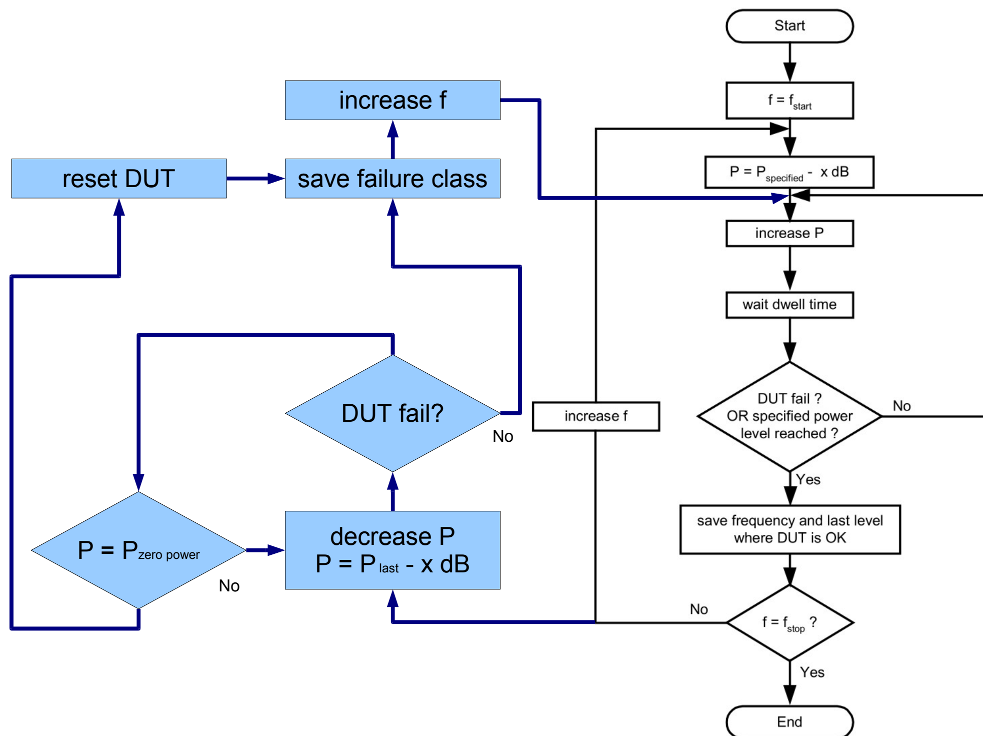

Figure 4.33: Flowchart of the modified direct power injection method control software, based on the recommended flowchart (Fig. 2.7), given in [13].

The configuration tab as shown in Figure 4.34 allows the selection of the frequency steps used for the investigation as described in chapter 3 and shown in Table 3.2. To monitor more than one signal, the support for a secound GPIB compatible multimeter was

added. This version allow to select between the power meter NRVD or the milli-voltmeter URV5 to work in the power regulation loop.

The automated reset allows to cycle the power at the DUT by using a GPIB compatible power supply unit. After reaching the failure criteria the DUT functionality ist tested while no disturbance power is applied. So it can be distinguished between failure class C and failure class D. In addition, the automated measurement setup is able to recover from failures classified as performance class D (Table 4.2) without the need of operator interaction. Therefor the existing control loop was modified.

In additon the initalisation process of the power meter and the signal generator was changed to support zero correction of the power sensors to consider the no load noise of the ampliefer. Due to the functionality of the power meter, using adaptive measuring modes, the noise floor influences metering and response time [21]. The log file structure was modified to document all configuration parameters. For data evalution of the ASCII based log files, import scripts for usage with NI Diadem were developed.

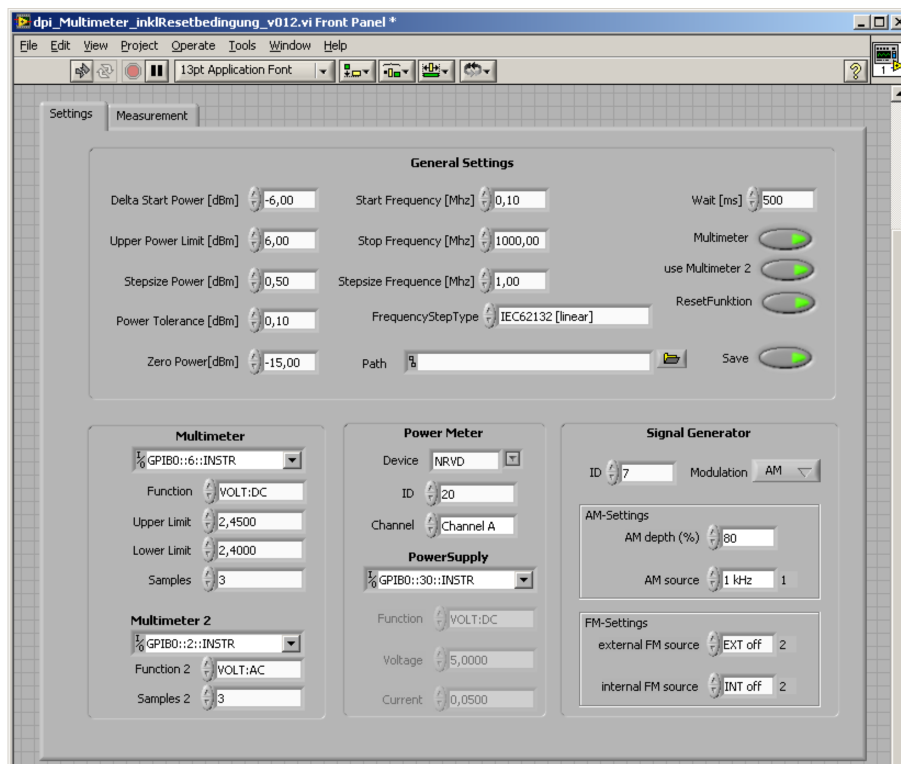

Figure 4.34: Screenshot of the adapted LabVIEW DPI control software.

Class A: all functions of the IC perform as designed during and after exposure to a disturbance.

Class B: all functions of the IC perform as designed during exposure; however, one or more of them may go beyond the specified tolerance. All functions return automatically to within normal limits after exposure is removed. Memory functions shall remain in class A.

Class C: a function of the IC doesn't perform as designed during exposure but returns automatically to normal operation after exposure is removed.

Class D: a function of the IC doesn't perform as designed during exposure and doesn't return to normal operation until exposure is removed and the IC is reset by simple operator action (e.g. switch off supply).

Class E: one or more functions of an integrated circuit does not perform as designed during and after exposure and cannot be returned to proper operation.

Table 4.2: Performance grades according to IEC 62132, taken from [10].

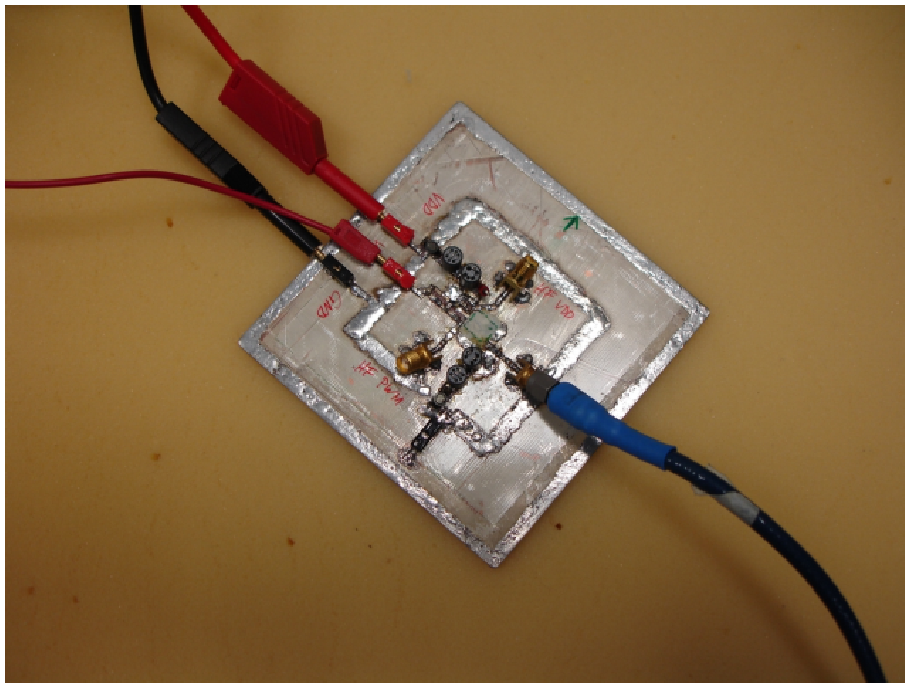

Figure 4.35: EMC Testboard for `DPI` and `TEM` chracterisations, shown during `DPI` testing (4.1).

4.6 Example Measurement

During this work several test PCB were built. Changes of the measurement setup and its influence to measuring results were evaluted. During measurement setup development two rotary encoder IC were evaluated. The used test PCB are made in-house. The existing sample designs for TEM cell test PCB were adapted and libraries for Eagle and Orcad PCB were developed, including drawings with TEM cell dimensions, SMA connector footprints for 45° usage and parts for decoupling and coupling networks. The following section show a selection of used test PCB for IC evaluation. The tested IC is connected to its minimum circuitry, as given in the corresponding datasheet.

4.6.1 Testboards

DUT 1 (AS5145) was tested on a multi purpose PCB supporting the DPI and the TEM method (see Fig. 4.36). It is very important that only the DUT is on the bottom side of the TEM -cell test PCB , so that no feed line can influence the EMC measurement result. All the other components to run the IC in its normal operation mode have to be placed at the opposite side of the TEM -cell test PCB . These are the parts for the external passive lowpass filter of the PWM output, the buffer capacitor for VDD3V3, the buffer capacitor for VDD5V. The other parts are needed to do measurements according to the DPI method as defined in IEC 62132-4. These are RF decoupling networks for VDD5V, VSS and Vout after the lowpass filter. The lowpass filter consists of the same parts as shown in the datasheet.

Lowpass filter:	2x 4.7 kΩ SMD resistor 0804
	2x 1 μF ceramic capacitance 0804
Buffer capacitance VDD3V3:	1 μF ceramic capacitance 0804, X7R
Buffer capacitance VDD5V:	100 nF ceramic capacitance 0804, X7R
RF decoupling network:	3x Würth Elektronik, Art.Nr. 742750421
	3x Würth Elektronik, Art.Nr. 74275043
	3x Würth Elektronik, Art.Nr. 74451268
DPI coupling capacitance:	6,8 nF ceramic capacitance 0804, X7R

Table 4.3: Used parts for DUT 1

DUT 2 (AS5134) was tested, using separate PCB for the TEM (see Fig. 4.37-4.38) and the DPI (see Fig. 4.42) method. The test PCB consists of DUT with its minimum operation circuit. For normal operation the AS5134 need a $100nF$ capacitance between VDD and VSS. The PCB also includes the parts for the external passive lowpass filter of the PWM output, and the RF decoupling networks for VDD, VSS and Vout after the lowpass filter

to protect the DC power supply an the multimeter used for monitoring the DC output voltage. The lowpass filter consists of the same parts as shown in the datasheet.

Lowpass filter:	2x 4.7 kΩ SMD resistor 0804
	2x 1 μF ceramic capacitance 0804, X7R
Buffer capacitance VDD5V:	100 nF ceramic capacitance 0804, X7R
RF decoupling network:	3x Würth Elektronik, Art.Nr. 742750421
	3x Würth Elektronik, Art.Nr. 74275043
	3x Würth Elektronik, Art.Nr. 74451268
DPI coupling capacitance:	6,8 nF ceramic capacitance 0804, X7R

Table 4.4: Used parts for DUT 2

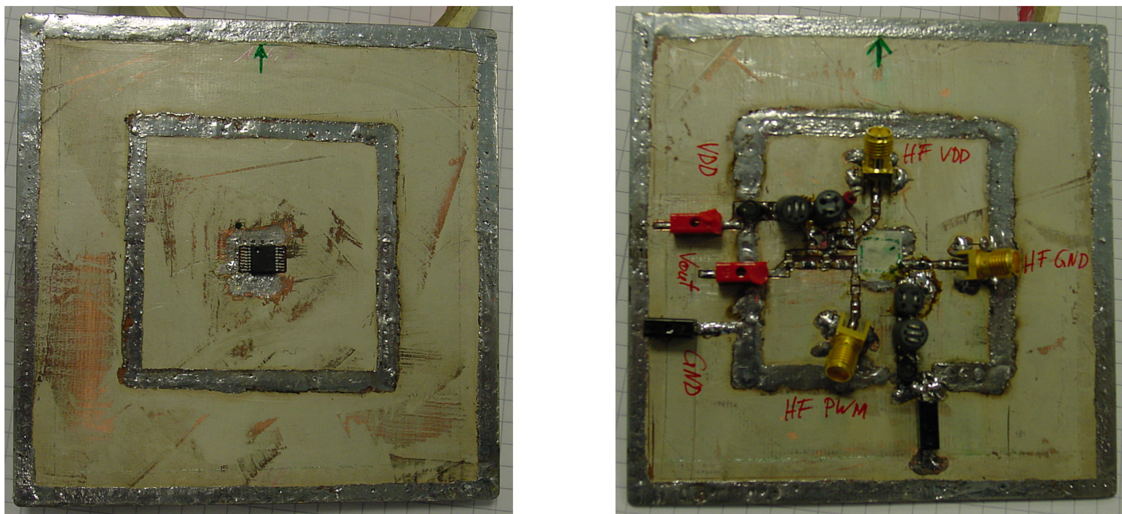

(a) Bottom side (b) Top side

Figure 4.36: Assembled EMC test PCB for evaluation according to the DPI and TEM method (AS5145).

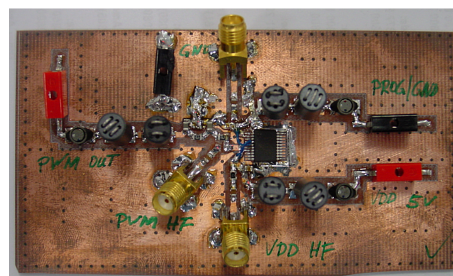

Figure 4.42: DPI test PCB (rev.4) including coupling and decoupling networks and the DUT for DPI charactersisation of three IO pins.

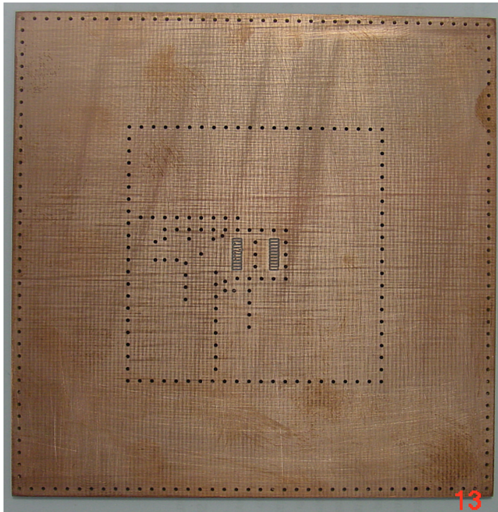

(a) Bottom side

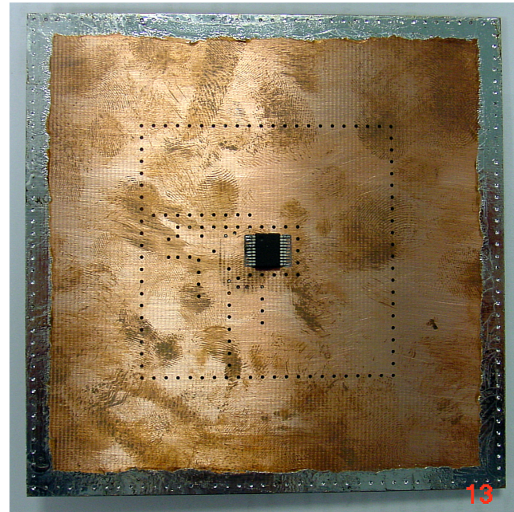

(b) Bottom side, assembled

Figure 4.37: EMC test PCB for evaluation according to the TEM method, bottom view (AS5134).

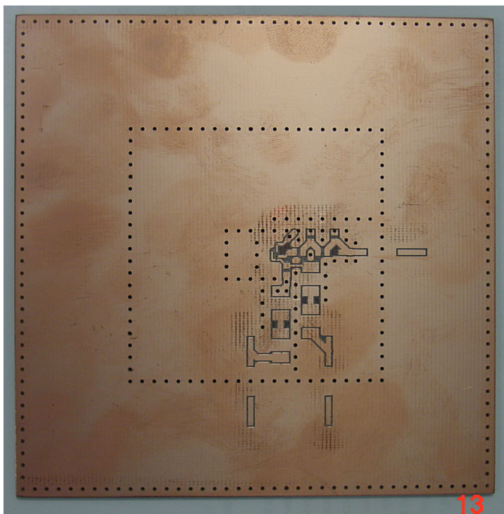

(a) Top side

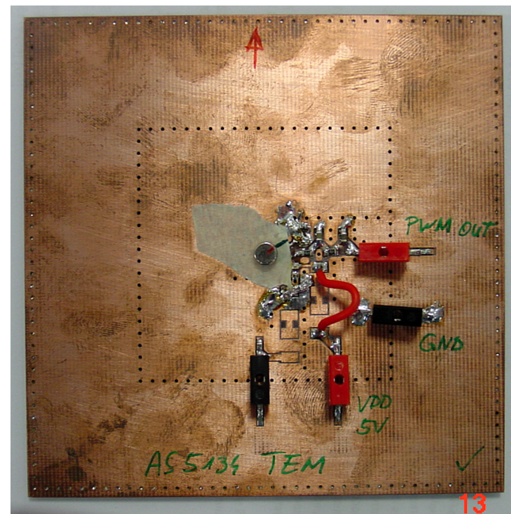

(b) Top side, assembled

Figure 4.38: EMC test PCB for evaluation according to the TEM method, top view (AS5134).

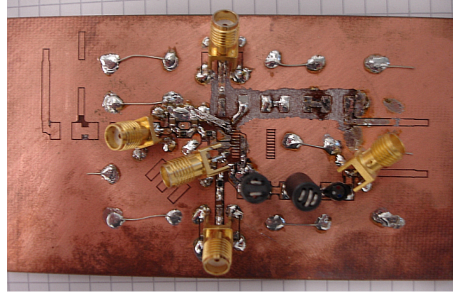

Figure 4.39: DPI test PCB including one coupling and decoupling network, ready to measure the characteristics of this coupling path.

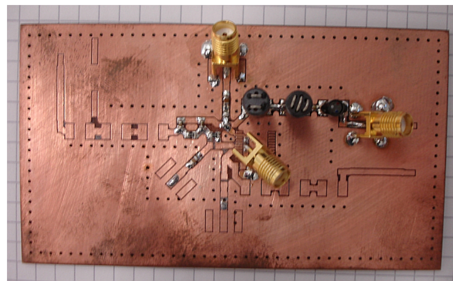

Figure 4.40: DPI test PCB including one coupling and decoupling network, ready to measure the characteristics of this coupling path.

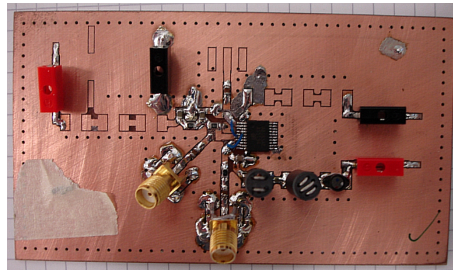

Figure 4.41: DPI test PCB (rev.3) including two coupling and one decoupling networks and the DUT , ready to do a DPI measurement.

4.6.2 Results

The following plots show electromagnetic immunity results when testing two magnetic rotary encoder IC against conducted RF disturbances. Each diagram consists of two curves, the DPI disturbance levels and the corresponding values of the failure criteria. Figures 4.45-4.47 show test results of several measurements. In particular, the plots show DPI disturbance measurements with injections on the GND pin (Fig. 4.45), output pin (Fig. 4.46) and VDD pin (Fig. 4.47) in color-coded ways, respectively. As can be seen,

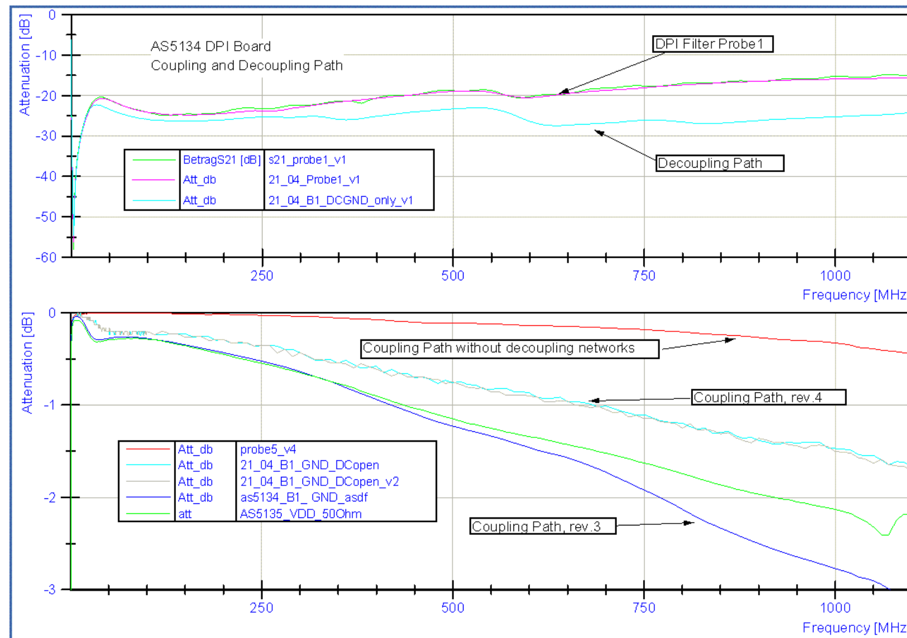

Figure 4.43: Coupling path characteristics of test PCB (Fig. 4.42, Fig 4.41) with and without connected decoupling networks, compared to the behavior of the coupling capacitor.

several measurements had to be acquired since the software adaptations as described in Section 4.5 were not available at this time. Additional measurements (depicted in Figures 4.48 and 4.49) illustrate inadequate failure class detections when testing the same rotary encoder IC . The failure cases were caused by the influence of the power supply and the decoupling network, respectively.

In what follows, we demonstrate measurement results conducted with the proposed adaptations of the measurement control software.

The AS5145 is tested to its immunity against conducted disturbances at three pins. To detect a failure, the PWM output voltage after the lowpass filter was monitored by a digital multimeter. Additionally, the PWM signal was monitored by a digital oscilloscope. Three different measurements were performed:

- Direct power injection to pin VDD5V (Fig. 4.50)
- Direct power injection to pin PWM (Fig. 4.51)
- Direct power injection to pin VSS (including the lowpass filter) (Fig. 4.49)

Figure 4.50 show the maximal disturbance power and the resulting output voltage after lowpass filtering of the PWM output signal. Because of the good EMC performance

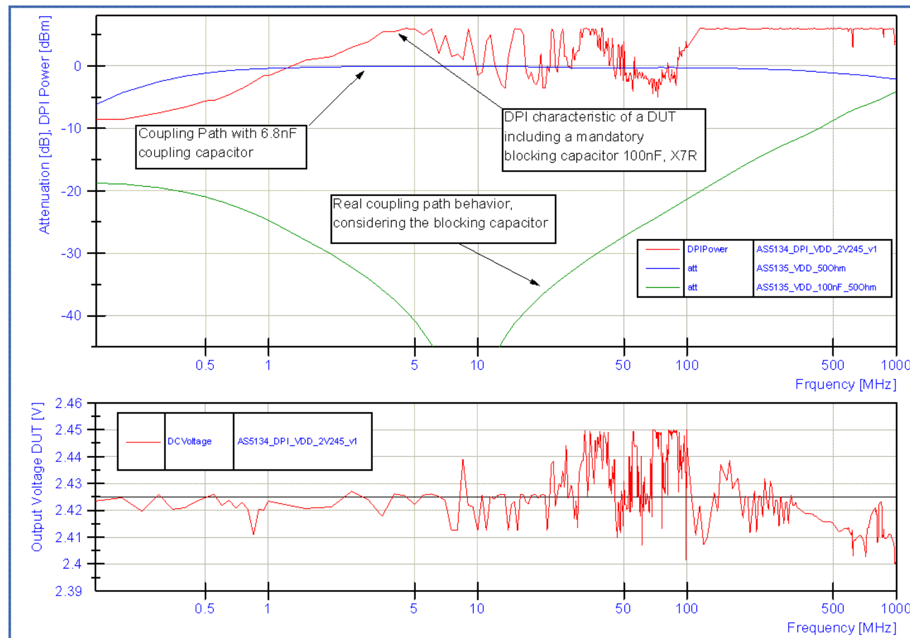

Figure 4.44: Coupling path characteristics of test PCB with and without a mandatory blocking capacitor for DUT functionality. The influence of the blocking capacitor to the test results can be seen in the frequency range up to 4 MHz. However, the lower immunity against EMI in the frequency range from 10 MHz - 100 MHz is not compensated by the blocking capacitor.

failure criteria of +/-1 LSB or +/-1.2 mV was used. The measurement was carried out at a disturbance power level of 37 dBm CW which is the maximal power level given in the IEC 62132-4.

Figure 4.51 shows the maximal disturbance power and the resulting output voltage after lowpass filtering of the PWM output signal with failure criteria of +/-16 LSB or +/-19 mV.

Figure 4.49 shows the maximal disturbance power and the resulting output voltage after lowpass filtering of PWM output signal. One detailed and one fast measurement (with higher or lower measurement sampling, respectively) was performend. The lowest EMC performance of the AS5145 is in the range from 210 MHz to 330 MHz.

Conclusion:

1. The AS5145 shows good EMI performance against conducted RF disturbances applied to the VDD5V pin if it is buffered with a 100 nF capacitance.

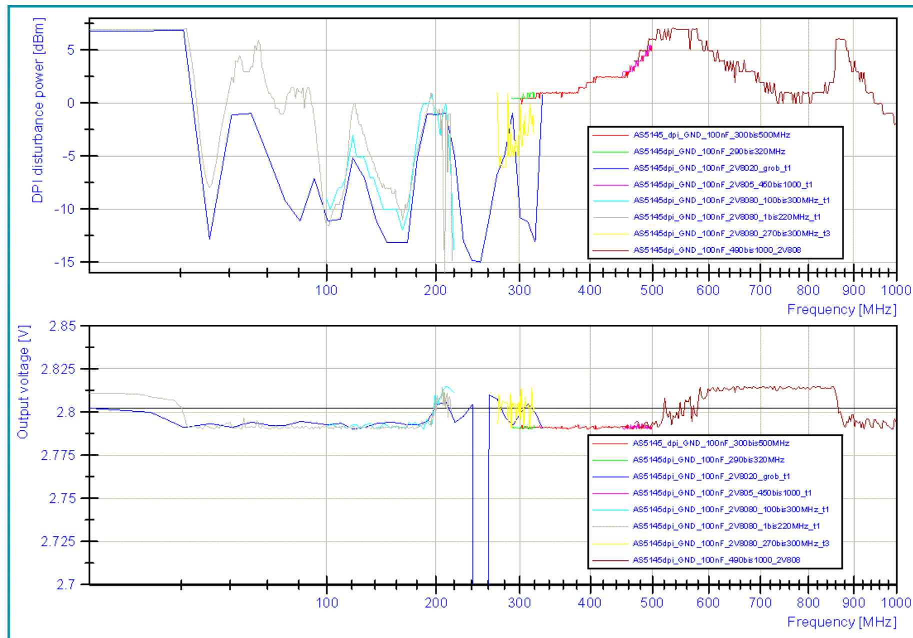

Figure 4.45: as5145 DPI measurement - disturbance coupling to VSS. The results are obtained by manual device reset and measurements in different frequency ranges.

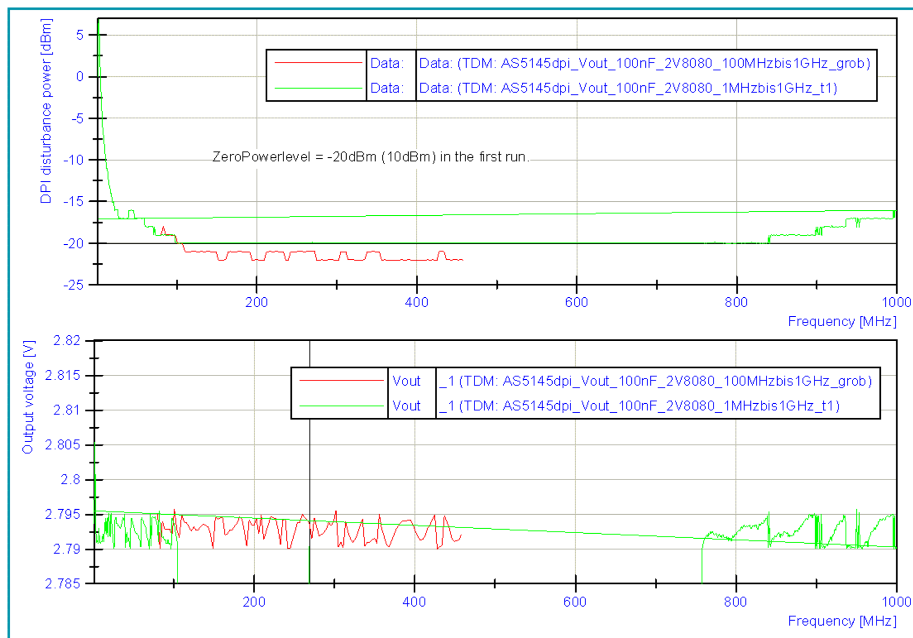

Figure 4.46: as5145 DPI measurement - disturbance coupling to OUT. The lowest power level was set to high. Thus the device fails, even at the lowest disturbance power.

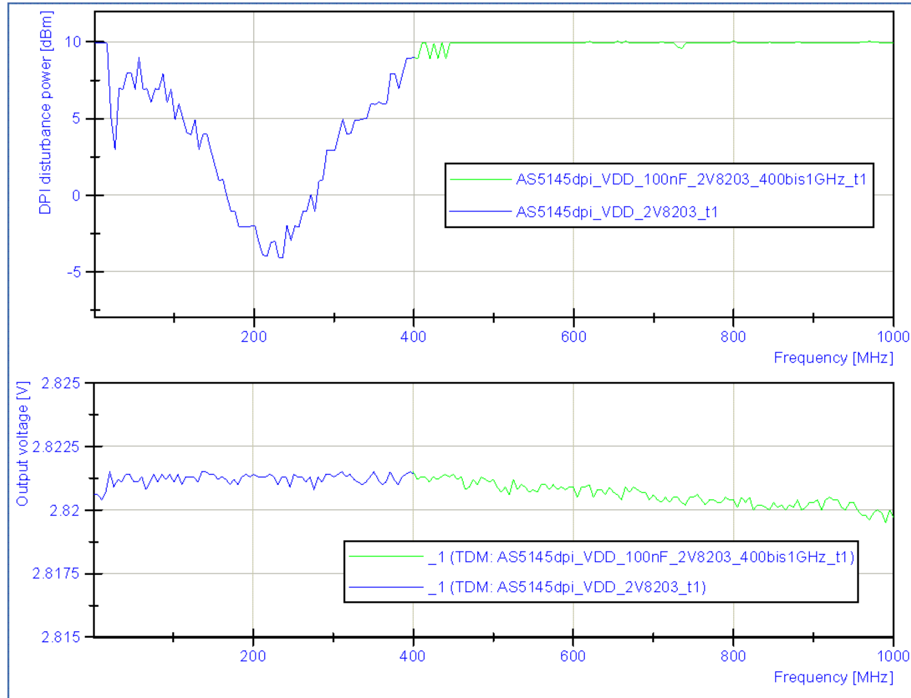

Figure 4.47: as5145 DPI measurement - disturbance coupling to VDD. The powerlevel of the disturbance power ist not corrected by the coupling factor of the directional coupler.

2. In the range from 210 MHz to 330 MHz the AS5145 has the lowest EMI performance.

The AS5135 is tested to its immunity against conducted disturbances at three pins. To detect a failure, the PWM output voltage after the lowpass filter was monitored by a digital multimeter. Also the PWM signal was monitored by a digital oscilloscope. Three different measurements are done:

- Direct power injection to pin VDD5V (Fig. 4.54)
- Direct power injection to pin PWM (Fig. 4.53)
- Direct power injection to pin VSS (including the lowpass filter) (Fig. 4.52)

Figure 4.54 shows the maximal disturbance power and the resulting output voltage after lowpass filtering of the PWM output signal. Failure criteria of +/-25 mV or +/-2 LSB were used. The measurement shows that the AS5134, buffered with a 100 nF capacitance, has a good EMI performance in the higher frequency range. According to the IEC 62132-4, a RF disturbance signal with 80% amplitude modulation and a maximum powerlevel of 33.1 dBm peak envelope power (PEP) (see Equation 4.2) which is equivalent

Figure 4.48: as5145 DPI measurement - disturbance coupling to VSS. The three results are obtained by the usage of three different power sources. The first measure (red) was done while using a Agilent E3631A. For the second measurement (green) a Weier Electronics W30 was used. The third mesurement (blue) was done using a lead-acid batterie and a linear voltage regulator (LM7805) to provide DC power to the DUT. The last measurement was done with less frequency steps.

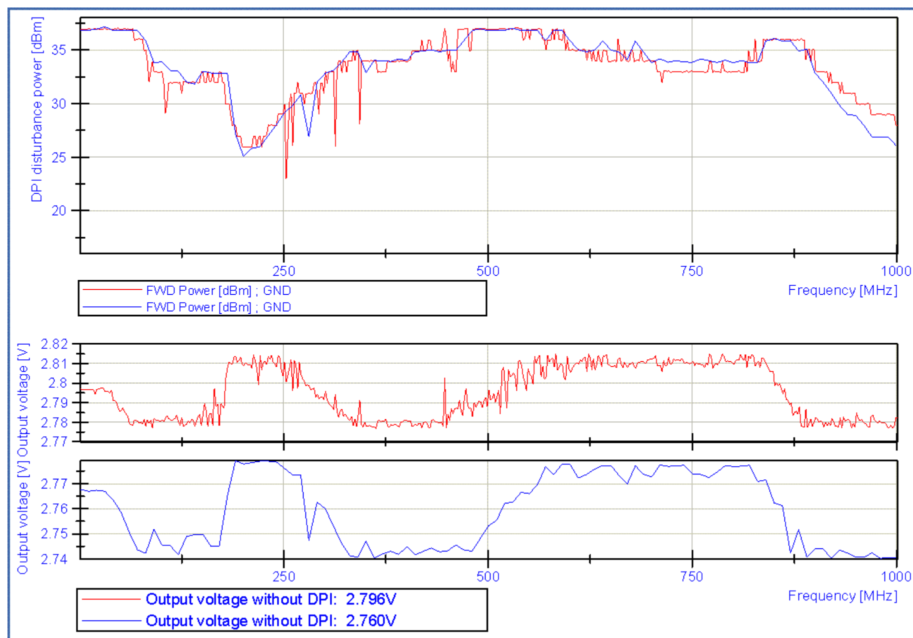

Figure 4.49: AS5145 DPI measurement - disturbance coupling to VSS.

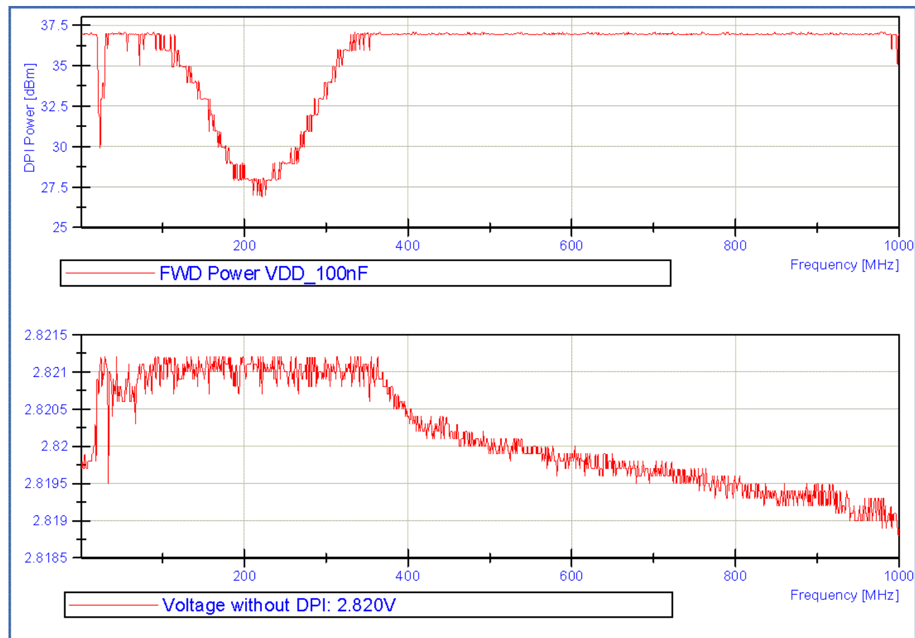

Figure 4.50: AS5145 DPI measurement - disturbance coupling to VDD5V.

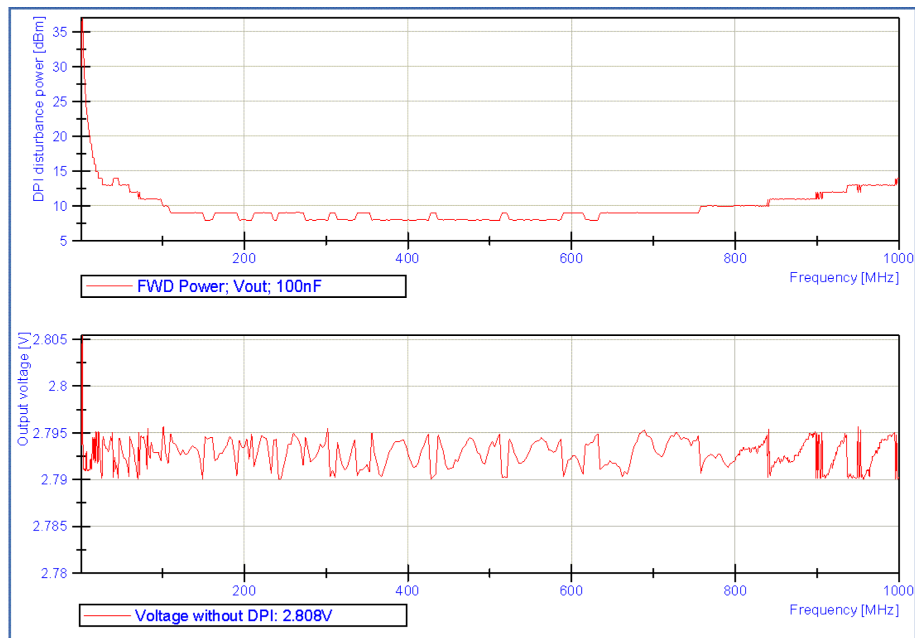

Figure 4.51: AS5145 DPI measurement - disturbance coupling to PWM output.

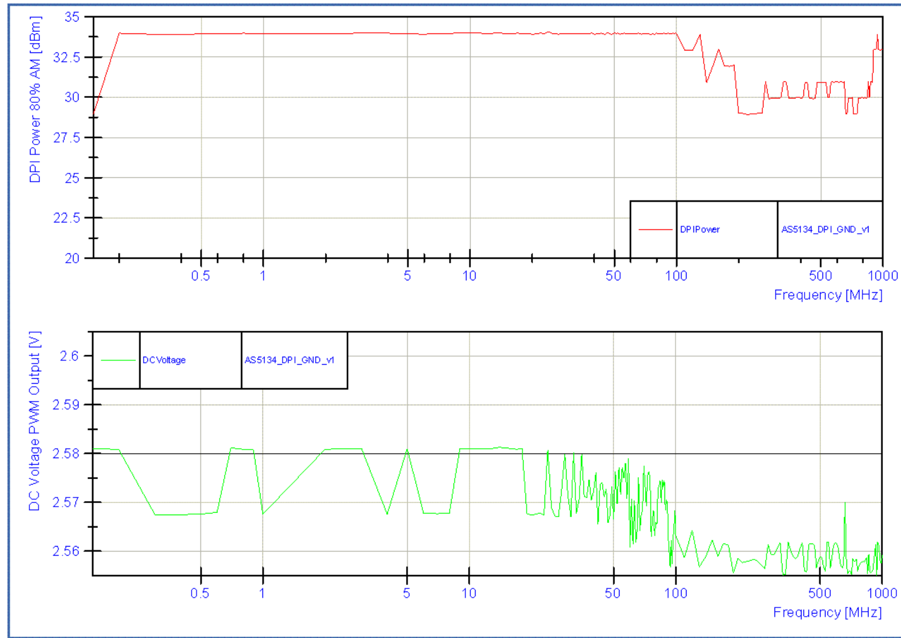

Figure 4.52: AS5134 DPI measurement - disturbance coupling to VSS (directly to pin).

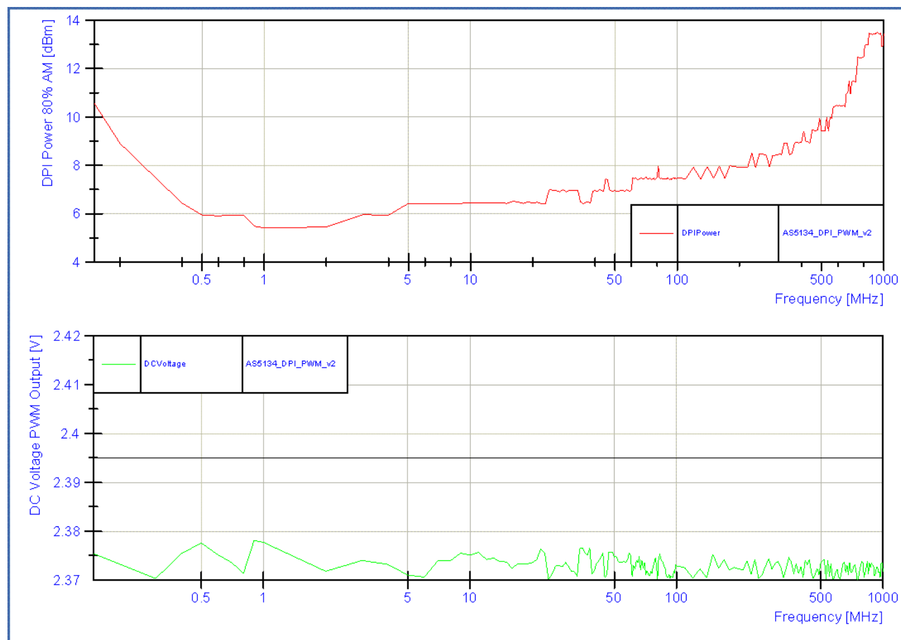

Figure 4.53: AS5134 DPI measurement - disturbance coupling to PWM output (directly to pin).

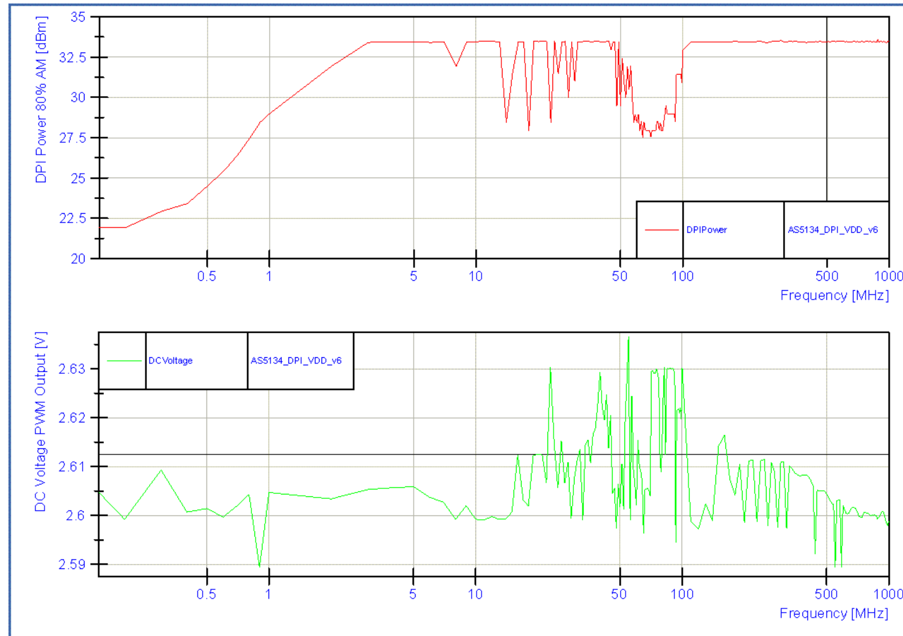

Figure 4.54: AS5134 DPI measurement - disturbance coupling to VDD5V (directly to pin).

to the 5 W or 37 dBm test signal power, was used in the DPI Setup.

Figure 4.53 shows the maximal disturbance power and the resulting output voltage after lowpass filtering of the PWM output signal with failure criteria of +/-25 mV or +/-2 LSB.

Figure 4.52 shows the maximal disturbance power and the resulting output voltage after lowpass filtering of the PWM output signal with failure criteria of +/-25 mV or +/-2 LSB.

Conclusion:

1. The AS5135 has a good EMI performance against conducted RF disturbances applied to the VDD5V pin if it is buffered with a 100 nF capacitance.
2. In the Range from 50 MHz to 100 MHz the AS5135 has its lowest EMI performance.

Chapter 5

Summary and Discussion

Contents

5.1 Summary 75
5.2 Discussion 76

In this work we have presented a measurement setup for electromagnetic immunity characterization of integrated circuits. Knowing about these characteristics is very important for system level and chip designers, because the clear trend to miniaturization is accompanied by increased sensitivity to electromagnetic interferences.

The task was to analyse and extend an existing measurement setup in order to perform `IC` characterization at chip level. We have investigated the direct power injection (`DPI`) method as described in the IEC standard 62132-4 and realized an automated measurement setup accordingly. The control software was extended to enable automated measurements and more extensive monitoring of the device under test (`DUT`).

5.1 Summary

In Chapter 2 we have subsumed the IEC standard 62132-4 and described the definition of the basic measurement setup as well as the injection process for single or multiple pins. Moreover, the test conditions (frequency range, power level and signal form) and the routines for the test procedure (equipment, setup and board) were summarized.

In Chapter 3 the realization of the attenuation measurement setup is described. It is composed of the `DUT` , the measurement devices (power meter, power splitter, signal generator, oscilloscope) and a controlling software developed in LabView. The control software has now the following functionalities: It can control a power meter, a signal

generator and a four-channel digital oscilloscope. With this setup, attenuation and signal characteristics can be measured, displayed and stored in a log file. The chapter contains details about the program structure and respective components. The resulting attenuation measurement setup is used for verification purposes in the subsequently following DPI measurement setup.

Chapter 4 is the core part of this work. It describes the measurement setup, which now allows to perform automated DPI measurements for a DUT , according to the IEC standard 62132-4. First, we discuss the workflow for general DPI measurement as well as shortcomings encountered in the current setup. Second, hardware adaptations regarding coupling and decoupling networks were introduced as suggested by the standard. Together with the hardware modification, we updated existing board layout libraries as used for the board design. Third, we revised the control software to comply with the frequency range recommendations of the standard. In addition, the software does now allow self-monitoring of the measurement process and performs automated restarting if necessary. Finally, we provide an evaluation of the established measurement setup on two rotary encoder IC . In our experiments, we found optimal behaviour of the measurement protocol execution when performed by the software in an automated way.

5.2 Discussion

DPI investigation methods can unveil device weaknesses, which may not be seen with other EMC evaluation methods. For instance, the given DUT of Section 4.6.1 did not show any noticable problems during TEM cell immunity testing up to 42 dBm or 500 V/m, while the DPI method exposed sensitivity to EMI as shown in Section 4.6.2. However, the test method allows only to identify a sensible IC pin but can not identify the affected area on the die. Another disadvantage of this method is its extended time consumption (which could be partially relaxed through automated measurements). Also, the influence of the test setup on the obtained results is questionable and should be investigated in a more detailed way. For evaluation and design improvements the real voltage levels at the DUT are subject of interest. Thus, simulations of a DPI test setup would be convenient to allow virtual EMC testing and further device improvements in future [4][1].

Even if the influence of the test setup on the results can be minimized and compliance to the standard can be achieved, there are still some remaining issues. The measurement intention should be, to apply the maximal stress to the DUT in order to detect unknown weaknesses. If the test method is used to reproduce EMC problems known from system

level, appropriate test power levels should be used.

The insertion loss of the SMA cable between the power splitter and the RF injection port at the test PCB should be mentioned. The measured forward power at the directional coupler differs from the power applied to the DUT by the amount of the insertion loss of the used connection cable and the coupling path.

Any mandatory additional parts, connected to a tested pin of the DUT , influence the behavior of the test signal. The position of a blocking capacitor in relation to the coupling capacitor, the decoupling network and the test pin of the DUT change the test conditions. The layout example (Fig. 2.6) would result in good conditions for the DUT as it shows a optimal placement of a filter capacitor at a supply pin [9]. The position of a mandatory blocking capacitance can influence the blocking capability. Differences up to 6 dB and more [15] are possible and should be mentioned (Fig. 4.44).

Appendix A

Acronyms and Symbols

List of Acronyms

AM	amplitude modulated
BCI	bulk current injection
CW	continuous waveform
DUT	device under test
DPI	direct power injection
EMC	electromagnetic compatibility
EME	electromagnetic emission
EMI	electromagnetic interference
GPIB	general purpose interface bus, IEEE-488
IC	integrated circuit
IO	input output
RF	radio frequency
RMS	root mean square
SMA	sub miniature version A
SWR	standing wave ratio
TEM	transverse electromagnetic mode
PEP	peak envelope power
PCB	printed circuit board
PkPk	peak to peak
VIs	virtual instruments

Bibliography

[1] A. Alaeldine, R. Perdriau, M. Ramdani and V. Veeragandham. Electrical model for power losses in direct power injection. *IET Sci. Meas. Technol., Vol. 1, No. 5, September 2007.*

[2] AeroflexMicroelectronicSolutions. *Power Splitters & Dividers Frequently Asked Questions about Power Splitters & Dividers.* Aeroflex Microelectronic Solutions, 5305 Spectrum Drive, Frederick, MD 21703-7362, April 2009.

[3] Inc. Agilent Technologies. *Differences in Application Between Power Dividers and Power Splitters.* Agilent Technologies, August 2007.

[4] Ali Alaeldine, Richard Perdriau, Mohamed Ramdani, JeanLuc Levant and Mhamed Drissi. A direct power injection model for immunity prediction in integrated circuits. *IEEE TRANSACTIONS ON ELECTROMAGNETIC COMPATIBILITY.*

[5] Bernd Deutschmann. Improving the Electromagnetic Compatibility of Integrated Circuits. *Technical University of Graz*, 2002.

[6] Bernd Deutschmann, Gunter Winkler, Timm Ostermann, Kurt Lamedschwandner. Electromagnetic Emissions: IC-Level versus System-Level. *IEEE International Symposium on Electromagnetic Compatibility*, 2004. ISBN: 0-7803-8443-1.

[7] Dieter Maier. Electrostatic Discharge Protection and Electromagnetic Compatibility of Microelectronic Devices. *Technical University of Graz*, 2009.

[8] Gunter Winkler, Bernd Deutschmann. Störfestigkeit integrierter Schaltungen gegenüber hochfrequenten leistungsgeführten Störgrößen. *4.EMV Fachtagung ARC Seibersdorf*, 2006. LV-Unterlagen, Evaluierung integrierter Schaltungen.

[9] Heinz Zenker, Alexander Gerfer, Bernhard Rall. Trilogie der Induktivitäten. *Würth Elektronik GmbH & Co.KG.*

[10] IEC. International Standard IEC 62132–1 Integrated circuits – Measurement of electromagnetic immunity 150 kHz to 1 Ghz – Part 1: General conditions and definitions. 2006.

[11] IEC. International Standard IEC 62132–2 Integrated circuits – Measurement of electromagnetic immunity 150 kHz to 1 Ghz – Part 2: Measurement of radiated immunity – TEM cell and wideband TEM cell method. 2006.

[12] IEC. International Standard IEC 62132–3 Integrated circuits – Measurement of electromagnetic immunity 150 kHz to 1 Ghz – Part 3: Bulk current injection (BCI) method. 2006.

[13] IEC. International Standard IEC 62132–4 Integrated circuits – Measurement of electromagnetic immunity 150 kHz to 1 Ghz – Part 4: Direct RF power injection (DPI) method. 2006.

[14] IEC. International Standard IEC 62132–5 Integrated circuits – Measurement of electromagnetic immunity 150 kHz to 1 Ghz – Part 5: Workbench Faraday cage method. 2006.

[15] Joachim Franz. EMV Störungssicherer Aufbau elektronischer Schaltungen. *VIEWEG+TEUBNER, 4.Auflage.*

[16] Roland Jungreithmair. Characterisation of Electromagnetic Emissions and Susceptibility of Integrated Circuits According to IEC 61967 and IEC 62132. Master's thesis, Technical University of Graz, 2002.

[17] LeCroy. *LeCroy Remote Control Manual*, WM-RCM-E Rev. D edition, 2005. http://cdn.lecroy.com/files/manuals/wm–rcm–e_rev_d.pdf.

[18] LeCroy. *HFP Series Active Probes*, HFPDS 29Sept06 edition, 2006. http://www.lecroy.com/germany/tm/products/probes/hfp/default.asp.

[19] Harald Pitsch. System- vs. Chiplevel EMC-Requirements. Master's thesis, Technical University of Graz, 2006.

[20] Rohde&Schwarz. *Dual-Channel Power Meter R&S NRVD*, NRVD_en edition, 2005. http://www2.rohde–schwarz.com/file/NRVD_en.pdf.

[21] Rohde&Schwarz. *Operating Manual Dual-Channel Power Meter R&S NRVD*, printed manual 857.8008.02 edition, 2005.

[22] Rohde&Schwarz. *Voltage and Power Measurement – Fundamentals, Definitions, Products – Brochure R&S NRVD*, printed manual 757.0835.23 edition, 2005.